JOURNAL OF PHYSICS OF THE EARTH

Volume VIII July 1960 Number 1

CONTENTS

PUBLISHED JOINTLY BY

THE SEISMOLOGICAL SOCIETY OF JAPAN
THE GEODETIC SOCIETY OF JAPAN
THE VOLCANOLOGICAL SOCIETY OF JAPAN

JOURNAL OF PHYSICS OF THE EARTH

The object of the publication of JOURNAL OF PHYSICS OF THE EARTH is to provide an international medium for the publication of original contributions in the field of geophysical science, more particularly concerning with physical properties and conditions of and phenomena occurring in the solid part of the earth.

The JOURNAL is open to any one who wishes to contribute his (or her) article. But the authors are, in principle, requested to pay page charges necessary for publishing their respective articles. The authors receive 100 copies of reprints free of charge.

In order to serve the purposes for which this JOURNAL is published, all contributions should be written in widely understandable languages, such as English, French and German, etc. Contributions should be sent to the Editor or to one of the Associate Editors.

For the time being, this JOURNAL will be issued at variable prices and at irregular intervals. The price of this issue is 200 yen inside Japan and $1.00 for foreign countries, the latter including postage.

Subscriptions may be made through Charles E. Tuttle Co., Booksellers and publishers; Rutland, Vermont, U.S.A. or 15, Edogawa-cho, Bunkyo-ku, Tokyo, Japan.

JOURNAL OF PHYSICS OF THE EARTH, VOL. 8, No. 1, 1960

Comparison of Block and Arc Tectonics in Japan with Those of Some Other Regions.

By

C. F. RICHTER

California Institute of Technology, Pasadena. On leave as Fulbright Research Scholar, Geophysical Institute, Tokyo University, 1959–1960

§ 1. Introduction

This paper is expanded from a mimeographed memorandum circulated, and presented for discussion, at the spring meeting of the Seismological Society of Japan, at Tokyo, May 12, 1960. The intention is not to offer any new material, but to bring together more or less well known results in a form suitable for critical comment.

During the remainder of his stay in Japan, the writer continued his study, reading, and discussion along the indicated lines. A few only of his personal indebtednesses are named in the section on Acknowledgments.

The writer's knowledge extends to only a small part of the vast body of seismological, geophysical, and geological data available in Japan. In spite of the great assistance he has received, he is certain that the paper still contains inexactitudes, and even downright mistakes. It is to be hoped that these are minor. Experienced workers will not be misled; but students are cautioned not to accept statements which they are inclined to question, without verifying them from the numerous publications which are more easily accessible to Japanese readers than to the present writer.

The point of view is that of the writer's text-book "Elementary Seismology"; the present paper is in effect a revision of the correspoding discussion in Chapter 30 of the book.

The presentation is with reference to the data of seismicity: accordingly, description and comparison refer to tectonic processes now going on, which in many areas differ significantly from those of the geological past. Moreover, present occurrence of earthquakes in a given small area may be due to special circumstances (either geographically localized, or temporary in terms of the geological time scale). Such local areas may present exceptions to the general tectonic pattern.

§ 2. Nature of block and arc tectonics

Most of the seismicity of the world is related to two principal environments–those of block and arc tectonics; the latter is found chiefly in the circum-Pacific and Alpide belts. The work of EWING and HEEZEN suggests that the seismicity of the Mid-Atlantic Ridge, and of other analogous oceanic ridges, may represent a third principal tectonic type.

From the viewpoint of historical geology, the distinction between regions of block tectonics and the active arc structures is usually not one of essential character, but of the present stage of development. The materials of most active block structures have been subjected to successive orogenies; at one or more earlier periods such areas presumably presented all the characteristic features now associated with active arcs, such as: (1) high seismicity including shallow, intermediate, and (in typical Pacific arc) deep earthquakes; (2) active volcanoes; (3) large gravity anomalies in narrow belts; (4) a pronounced foredeep. Block tectonics may be considered as a later stage which normally follows the folding and thrusting of a typical orogeny. This stage represents a lower degree of activity (especially when conditions at the greater depths are considered) than the arc stage. Although large shallow earthquakes occur, and some of them break the surface in faulting, intermediate earthquakes are rare and deep earthquakes absent (except when deep earthquakes

belonging to an adjacent active arc originate under the shallow block structure). Volcanoes are usually in a late stage of activity or extinct, while foredeeps and gravity anomalies are less pronounced than in active arcs. Such criteria have been used in the following discussion to distinguish the block tectonics of West Japan from the arc tectonics of adjacent areas. The distinction between block and arc tectonics is not perfectly exclusive; some seismic areas appear to be in a transitional condition, and others show characteristics of both kinds due to intersection or to complex geometrical relationship in three dimensions.

Stratigraphy and other geological evidence in some instances suggests, and in others clearly demonstrates, that a present active arc formerly passed through a stage of block tectonics.

This discussion has a definite relation to the concepts employed by the Soviet school of geologists and geophysicists. Active arcs are generally considered as representing active geosynclines. The major geosynclinal belts are marginal to the stable platform areas. The regions of active block tectonics, which occur in the geosynclinal belts in juxtaposition to the active arcs, are classifiable as former platform areas, now involved in the development of geosynclinal movements, and being broken up in consequence. If this process goes far enough, the block structure may be completely destroyed, and the material reconstructed into a typical active arc.

§ 3. Geographical subdivisions of Japan

The exceptional importance of Japan in comparative tectonics derives from the presence, in an accessible, civilized, and well-investigated region, of both block and arc structures, in such a geometrical and mechanical relationship as promises to shed light on the nature of both.

There are five evident subdivisions:

(1) West Japan, including the main islands west and southwest from the Fossa Magna; this is the major area of block tectonics, with only traces of arc features.

(2) Northeast Japan, including Honshu east of the Fossa Magna, and southwestern Hokkaido. This is part of a major Pacific arc. As in some other such arcs, there is block faulting in the interior; here it is chiefly in a belt adjacent to the Japan Sea.

(3) Northeastern Hokkaido, which is the terminus of the active arc of the Kurile (Chishima) Islands.

(4) The arc of the Ryukyu Islands, which extends into Kyushu, where it intersects and modifies the block structure. KOBAYASHI relates the structures of Korea centrally to this arc.

(5) The Shichito arc, extending southward to the Ogasawara (Bonin) Islands.

These divisions will now be discussed individually, pointing out some of the more interesting comparisons with other regions. Later sections will sketch the block and arc tectonics of several other distant areas, presenting tentative general correlations with the Japanese region.

In addition to the surface features of Japan, geophysical discussion must take into account the belts of deep and intermediate earthquakes discovered by WADATI, as well as the structure of the crust as derived from seismological and gravity data.

The study of most of the active Pacific arcs in hampered by their largely submarine character; often the accessible land area consists of a chain of small islands. This is true of the Shichito, Kurile, and Ryukyu arcs, except at their ends, where they intersect the other block and arc structures. Such areas of intersection are of special importance for investigation. There are three of them in Japan: one including the Fossa Magna and the western Kanto district, one in Kyushu, and one in Hokkaido. All three of these, Professor TSUBOI points out, are associated with large negative gravity anomalies. The next similar critical areas in opposite directions are in Kamchatka and Formosa (Taiwan); findings there should be compared with Japan so far as possible. KOBAYASHI describes the transition from the Ryukyu arc to Formosa rather as a sharp bend in the younger trends than as an intersection; whatever the interpretation, the contrast between adjacent block and arc structures is clear.

§ 4. West Japan

In comparing West Japan with other areas of active block structure, a further subdivision must be considered. The longitudinal separation, along the Median Tectonic Line, into an inner and an outer zone, is of very great importance in studying the geological past of West Japan; but it is not so significant in relation to present tectonic processes. On the other hand, there are important complications at the two ends of West Japan which do not appear in its central segment. At the west, although the block structures and the Median Line cross Kyushu, there is an evident intersection in three dimensions, where these shallow structures cross the Ryukyu arc. Among the known typical arc features are the clustering of shallow earthquakes, associated with negative gravity anomalies, along the Bungo channel, and the central line of active volcanoes followed by epicenters of intermediate earthquakes. Continued study of the deep crustal structure of Kyushu, combining data from earthquake records, explosion seismology, and gravity observations on land and off shore, should clarify the geometrical relation of the intersecting structures. It is highly important to learn how the Mohorovičić discontinuity behaves in such a region.

A somewhat similar three-dimensional relation exists in the North Island of New Zealand, but the trends of block and arc structures are more nearly parallel there than in Kyushu. In the North Island, as in Kyushu, there is a central trough, largely filled with volcanic material; the active volcanoes and the epicenters of intermediate earthquakes follow the trough in both cases. One hypocenter is known at a depth of over 500 kilometers below the central part of the North Island; under Kyushu a few earthquakes are known at depths between 300 and 400 kilometers.

In spite of some significant differences, the middle section of West Japan compares rather closely with other Pacific areas of dominant block tectonics, such as California and central New Zealand. The general level of small seismicity is not high; however, there are occasional very large earthquakes, especially off the southern coast. These earthquakes originate inshore from the Nankai Trench, which thus is comparable in position with the foredeeps of the active arcs. However, the Nankai Trench is much less well marked topographically than the typical foredeeps, such as the Nippon Trench. Middle West Japan has no intermediate earthquakes, and the deep earthquakes are those of the transverse belt, belonging to the Shichito arc structure. The volcanoes are extinct.

Analogy between Kyushu and the North Island of New Zealand would logically lead to comparing the outer zone of West Japan with the major part of the South Island. The principal belt of shallow earthquakes in New Zealand, associated with conspicuous surface faulting, follows the coast of the North Island; offshore is the southern end of the Kermadec Trench, belonging to the intersecting arc structure. The earthquake belt crosses Cook Strait and passes down the South Island near its center line, with gradually decreasing seismicity. On the Pacific side of this line is the depression, generally believed to be a geosyncline, underlying the Canterbury Plain; this depression is consequently the analogue of the Nankai Trench. On the opposite side of the earthquake belt are the New Zealand Alps, consisting largely of Mesozoic rocks of geosynclinal type; they are cut marginally by the Alpine Fault, beyond which Paleozoic rocks are found underlying the Tertiary and Cretaceous sedimentary blanket. This western and north-western part of the South Island might thus be compared with a portion of the inner zone of West Japan; the Alpine Fault is in approximately the same situation as the Median Tectonic Line. However, the Alpine Fault, like the San Andreas Fault of California, is primarily a strike-slip feature; in this respect it contrasts sharply with the Median Tectonic Line, which is described as primarily due to thrusting.

To complete the comparison, the wide eastern part of the South Island, including the Canterbury Plain, would correspond to an area south from the Nankai Trench; although

far off shore, this area has been suspected by several authors of being continental in character. The volcanoes of Banks Peninsula on the New Zealand coast are closely similar to typically Pacific structures like those of Hawaii, Tahiti, and Samoa; they probably have no close correlatives in the Japanese area.

The two principal orogenies of New Zealand, the post-Hokonui (Mesozoic) and the Kaikoura (late Tertiary) are comparable with those of California and of many other regions, particularly in that the Mesozoic orogeny has left many traces of thrusting and folding in the rocks, while the younger orogeny is chiefly responsible for the present block structure. While a similar remark applies to West Japan, it will not apply to East Japan, or indeed to any of the more active arc structures of the world.

The area of block faulting which includes California is larger than West Japan. Point-by-point comparisons between such widely separated areas are hazardous. California has no offshore trench, nor any clear evidence of the other arc features. However, the structures and seismicity of the Japanese outer zone are perhaps comparable with those of the California Coast Ranges. The Paleozoic and intrusive rocks of the Japanese inner zone are not greatly different from those of the Owens Valley region and the Sierra Nevada. The extinct volcanoes aligned parallel to the Inland Sea suggest comparison with the Pleistocene volcanism of the eastern Sierra Nevada, Owens Valley, and the Mono Basin.

The writer was at first inclined to correlate the Inland Sea with the alluviated geosyncline of the San Joaquin Valley; but it is at least as reasonable to suppose that the Japanese correlative of the San Joaquin Valley was compressed out of existence by the thrusting which established the Median Tectonic Line. Whereas the San Joaquin depression is a downwarp, the Inland Sea is a faulted depression, more strictly comparable with the graben of Owens Valley.

The Great Basin extends from the Sierra Nevada east to the Rocky Mountain structures, which are analogous to those of the mainland of Asia; but it would be rash to suppose that the Japan Sea covers a structure like that of the Great Basin.

There is no known feature in Japan closely resembling the San Andreas Fault of California, or the Alpine Fault of New Zealand. Both are primarily strike-slip features, with strikes generally along the major structural trends, which they occasionally cross at low angles. Those faults in Japan where there is predominant strike slip often are associated with topography like that found along the San Andreas fault; but their attitude toward the major trends, or their shorter extent, differentiate them from it.

In West Japan block faulting breaking the surface has chiefly been observed in the structural belt of the Akiyoshi orogeny, along the Japan Sea coast. This, like similar block faulting in other old structures in many parts of the world, is most readily interpreted as tectonic rejuvenation. Regional stresses of comparatively late geologic age are being relieved along old lines of weakness which were originally developed under a different stress distribution. This circumstance probably accounts in part for the tendency to complex surface faulting, with the development of multiple fault traces in a single event, here and elsewhere in the general region of Japan. Two distinct traces of nearly equal importance were developed in each of the earthquakes of 1896, 1927, and 1943 (and in Formosa, in 1906 and 1935).

The eastern segment of West Japan is anomalous. From Ise Bay eastward, the Median Line curves northward in approaching the Fossa Magna; the structures of the Outer Zone appear drawn out of position accordingly. This local distortion suggests that the crust is weak there, and the results of explosion seismology indicate a special structure. The western limit of the disturbed segment is in the vicinity of the faulting associated with the Mino-Owari earthquake of 1891. Geological maps suggest the Median Line is offset across Ise Bay.

The deviation of the Median Line as it approaches and crosses the Fossa Magna is one

of the major problems of field geology in Japan. Discussion revolves around points similar to those raised in California with reference of the deflection and possible breaking up of the San Andreas Fault, descending from the northwest to intersect the east-west structures of the Transverse Ranges (for details see the writer's "Elementary Seismology"). Another similar problem exists in New Zealand; the Alpine Fault is deflected eastward on approaching Cook Strait, and diverges into branches which have been variously correlated with the faults of the eastern North Island.

The zone of deflected trends is sharply limited on the east by the Fossa Magna, beyond which we should speak of fragmentation rather than of deflection. The western limit is in the narrowest part of Honshu. The faulting of 1891 is somewhat east of this limit; on the surface it is not a single fracture, but a complex of fractures with varying trends. In the field, the writer saw topographic features, west of the faulting of 1891, which strongly suggest geologically young displacements along known faults.

The presence, in the western part of the disturbed segment, of the epicenters of the transverse belt of deep-focus earthquakes, indicates a major transverse fracture belt, extending to great depth, but reaching the surface in a complicated and perhaps shifting series of breaks. This is essentially the interpretation of Ehara, in his paper on the geotectonics of central Honshu. With a wealth of geological detail, he represents the facts in terms of a relative northward displacement of the Shichito arc structures, with fracture at the surface indicated by the Fossa Magna, dipping westward as indicated by the belt of deep earthquakes.

The Fossa Magna is a structural boundary not obviously like any other known feature. There is every evidence of considerable difference in tectonic and geophysical conditions on opposite sides. However, this does not appear to be tectonic "contrast" in the sense used by Soviet geophysicists, since there is no clear indication of a sharp difference in the rate of displacements now going on. This agrees with the fact that the Fossa Magna is not a line of seismic activity.

§ 5. Northeast Japan

Northeast Japan is perhaps the most favorable region in the world for studying a Pacific-type active arc. It represents a different stage of development from that of West Japan. The distinguishing features of Northeast Japan are:

(1) Three-dimensional structure. Instead of block structure with vertical faults, we find the typical active surface of a Pacific arc, dipping from the offshore troughs under the land, and continuing downward and northwestward into the belts of deep-focus earthquakes. In reality this is not a thin surface, but an irregular thick sheet, of probably complicated structure. It is not active throughout, but (just as in block structures) seismicity is confined to limited regions and to belts traversing it. The dip is partly responsible for the circumstance noted by Tsuboi, that epicenters, even of the shallower earthquakes, do not align so clearly here as in West Japan, but show areal rather than linear distribution. Gravity anomalies, active volcanoes, and epicenters of intermediate earthquakes, are aligned longitudinally as in other arcs.

(1) In contrast with the relatively simple alignment of the volcanoes and the other principal arc features is the chaotic character of the surface geology. Studies by Kobayashi and others indicate that this was once a region continuous with and much like West Japan, crossed by the Median Tectonic Line; but in later geological time it has been displaced relatively east or southeast, breaking into blocks which did not all move simultaneously nor in the same direction. Consequently, the line between areas formerly on the inner and outer sides of the Median Line may be drawn differently if different criteria are used, particularly, if the data are of different age.

(3) Along the Japan Sea coast is a strip now associated with block faulting, which broke the surface in 1847 (Zenkoji earthquake), 1896 (Riku-U earthquake), and probably in 1894 (Shonai earthquake). The existence of this active tectonic belt was pointed out by Omori.

Shallow earthquakes and block faulting occur in the interior of some other active arcs, in both Pacific and Alpide belts.

(4) A difference in mechanism of strain accumulation and release is indicated by TSUBOI's finding that the proportion of small to large earthquakes is higher here than in West Japan. This may be interpreted as due to breaking into smaller units as in other regions where small earthquakes and earthquake swarms are relatively common.

(5) The high seismicity off the Pacific coast is cut by a belt of low activity, very clear in TSUBOI's mapping, which includes the epicenter of the great Sanriku earthquake of 1933. Probably this belt follows a resistant transverse structure, composed of relatively unfractured rocks which yield only occasionally, under strain sufficient to produce a great earthquake and numerous aftershocks. The block of the Kitakami Mountains appears to represent this structure on land.

(6) The Kanto district, extending west to the Fossa Magna, occupies the area of intersection of two arcs: the principal Honshu arc and the Shichito arc. The former accounts for relatively high seismicity in the Kanto district. In accordance with the three-dimensional arc structure, most of the numerous epicenters on land correspond to foci at depths of 40 km. or more. Hence, even when a great earthquake like that of 1923 occurs there, no evident main fracture reaches the surface. The many small faults formed in 1923 were incidental to the general surface distortion of the Kanto region, which was shown clearly by geodetic observations. This high degree of surface complexity recalls that of the great Indian earthquake of 1897, when faulting and complex warping of the surface took place over a wide area.

§ 6. Hokkaido

The intersection of two arcs in Hokkaido offers a promising field for geophysical investigation of crustal structure, provided that the difficulties of working in that terrain can be successfully overcome. There are interesting analogies with the North Island of New Zealand, even in geographical outline. The central tectonic division has suggestive similarity to the Auckland Peninsula. However, the active volcanism of southwest Hokkaido does not compare well with the Pleistocene volcano, Mt. Egmont, of New Zealand; and there is in Hokkaido no clear correlative of the coastal mountains of the North Island, with their active block faulting. In brief, the North Island is a region of intersection of block and arc structures, rather than of two arcs; it resembles Kyushu rather than Hokkaido.

§ 7. Branching

The two principal western branches of the circum-Pacific active belt diverge in central Honshu; they approach closely again between northern Celebes and Halmahera, then diverge again. West Japan may be assigned to the western branch; lying between the Honshu and Ryukyu arcs, its position is like that of the great region of dominant block faulting which includes California, between the Alaskan arc and the Mexican arc. The oceanic area between the two branches is of special interest; at the north it lies between the Shichito and Ryukyu arcs, although the deep arc structures of the former, extending into the transverse deep-focus belt, pass under it. This area includes the Nankai Trench; continental structure probably extends much further south, although the Mohorovičić discontinuity may be found to stand near the oceanic level.

§ 8. Comparison with the East Indies

If Indonesia could be investigated thoroughly by present geophysical and seismic methods, the results would probably go far toward clarifying the nature of both block and arc tectonics. The results reached by past investigators there must be considered carefully for correlation with work in Japan and in all active regions.

The belts of negative gravity anomaly, discovered by Vening MEINESZ, have commonly been held to indicate the location of contemporary active orogeny. The islands (such as Nias, Timor, Ceram) included in or traversed by these belts were involved in intense folding-

during the Miocene. Presumably the zone weakened at that time is now yielding under the general regional stress; this agrees with the fact that the Meinesz belts include the epicenters of many shallow earthquakes, some of them large. Shallow earthquakes elsewhere in Indonesia are mostly associated with block tectonics.

The principal Meinesz belt follows the Sunda arc, which is the least complex structure of the region; the arc extends from Sumatra and Java along the chain of the Sunda islands and round the Banda Sea. Broadly speaking, it is a typical active arc, with all the characteristic features; but some of these features are better developed in one part of the arc, and some in another. In certain respects the Sunda arc compares better with the arc of the Ryukyu Islands than with that of Honshu. Thus, the islands of the Sunda arc form a double chain; the inner arc, including Sumatra, Java, and smaller islands, is actively volcanic, but the islands of the outer arc, in the Meinesz belt, are non-volcanic. The Ryukyu arc has a similar double chain, but off the Pacific coast of Honshu there are no small islands in the belt of gravity anomalies.

The Honshu arc, in fact, is more closely comparable with the Java sector of the Sunda arc. Off Java there are no small islands in the Meinesz belt (although there is a submarine ridge); and the Java Trench, though not as significant as the Nippon Trench, is the principal foredeep feature of the Sunda arc. Large shallow earthquakes are not frequent in the Java sector; but active volcanoes, and epicenters of intermediate earthquakes, are numerous, and the corresponding deep earthquakes originate north of Java.

The relation between Sumatra and Java is somewhat like that between West and Northeast Japan; however, Sumatra is more comparable to an arc structure like that of the Ryukyu Islands. Sumatra has some definite characteristics of block tectonics, such as the high scarps along the southern coast, and the longitudinal internal rift, which the displacements in the earthquake of 1892 indicate is a right-hand strike-slip feature. (However, this rift is largely filled with volcanic products, and resembles the rifts in the North Island of New Zealand and in Kyushu).

North of the Sunda arc there is an important tectonic division, across a line passing through central Celebes. To the west and northwest is a large stable area, with relatively few earthquakes, except near the coasts of the Strait of Macassar, which is an internal fracture in the stable mass. All the earthquakes on this side of the division are shallow, except for deep earthquakes belonging to the Sunda arc. On the other side is the terminal section of the Sunda arc, in the Banda Sea; and another active arc descends from the northeast along the volcanic eastern peninsula of Celebes. Celebes, with its environment, presents a degree of complexity in three dimensions comparable with that of Honshu and its environment. Interpretation in this extremely interesting area is rendered particulary uncertain by the lack of precision attainable in the location of epicenters, as well as the absence of any direct geophysical data on the depth of the Mohorovičić discontinuity or on other details of crustal structure.

§ 9. West Indies

The Caribbean active arc has been much studied by geophysical means. Epicenter locations in this region have become reasonably accurate of late years; but general seismicity is only moderate, so that most of the important large earthquakes are known only from non-instrumental and historical records. The eastern front of the arc is double, with an outer non-volcanic island (Barbados) and an inner volcanic arc.

Negative gravity anomalies follow the outer arc, beyond which there is no deep trench. The northern limb of the arc is quite different; there is a very deep external trench, but there is no active volcanism, and the earthquakes are nearly all shallow. Both northern and southern limbs are classifiable as of block structure, and both are cut by important longitudinal strike-slip faults.

While the eastern front of the Caribbean arc may be compared with the Ryukyu and Shichito arcs, the remainder of the structures

differ so much from those of Japan that generalizations about arc tectonics derived from observations in the West Indies can be applied in Japan only with great caution.

§ 10. Himalayan arc

Northern India is potentially one of the most important regions in the world for the study of arc tectonics. The accessible geology has been well investigated, and gravity observations are plentiful. There is still much need for studies of crustal structure by the various seismic methods.

The Himalayan arc strongly resembles those of the Pacific system, except for its generally lower activity; in this it is typical of the system of Alpide arcs of Europe and Asia. The Ganges alluviated depression is a foredeep; along its northern margin is a belt of negative gravity anomalies, in which are located the epicenters of large shallow earthquakes. The proportion of large to small shocks is relatively high, which suggests comparison with regions of block structure. Volcanism is slight, intermediate earthquakes associated with the arc proper are few, and no correlated deep shocks are known.

The remarkable series of intermediate earthquakes under the Hindu Kush are not evidently related to the Himalayan arc. At the other end of the arc, the great earthquakes of Assam and Tibet are related to complicated structures which are still imperfectly known.

Nothing associated with the Himalayan arc suggests close correlation with the tectonics of Japan.

§ 11. Italian arc

Of the arcs of the Alpide system, the Italian arc most clearly shows relation to those of the Pacific. In "Elementary Seismology" it was pointed out that this parallelism is especially evident when referred to double arcs, like the Ryukyu and Sunda arcs. Epicenters of shallow earthquakes follow the chiefly nonvolcanic outer arc of the Apennines; the well-known active volcanoes of Italy are on an inner arc. Intermediate and deep earthquakes are known down to depths of 300 and even 450 kilometers. The depression of the Tyrrhenian Sea is correlative with such interior depressions as the Weber Deep in the Banda Sea interior to the Sunda arc.

§ 12. Correlation with tectonics of the Soviet Union

In section 2 reference was made to the classification of tectonics in terms of geosynclines and platforms. This classification has been applied in detail, and with excellent results, to the tectonic analysis of those parts of the Soviet Union which have been selected for intensive geophysical investigation in the past: the Crimea, the Caucasus, Turkmenia, and Central Asia (especially the region extending from the Tian Shan to the Pamir). The Soviet Union includes typical Pacific active arc structures, in Kamchatka and the Kurile Islands. These were subjected to intensive exploration during the IGY program, but results are only now beginning to be published, so that discussion is premature; the opportunity for comparison with Japan may be awaited with great interest.

Platform areas in the strict sense are lacking in Japan; they may be observed on the adjacent mainland of Asia, even though some deep earthquakes related to the Pacific active arcs originate under the platforms. The block and arc structures of Japan may be regarded as ancient platform material in different stages of being broken up and transformed by geosynclinal processes.

The geosynclinal zone along the southwestern border of the USSR is on the northern front of the Alpide structural belt. In the Black Sea, under the Caspian Sea, and in Turkmenia, there are tectonic downwarps, in which the Mohoroviĉić discontinuity descends to 40–50 km below the surface, and there are local areas from which the upper or "granitic" layer appears to be absent. Under the Caucasus the Mohorovičić discontinity, generally near 40 km deep, descends locally to a depth of 60 km.

In most of these areas typical arc features, and block tectonics fracturing the surface along active faults, are both absent. However, in Turkmenia the Transcaspian depression is in the position of a foredeep north of the

Kopet Dagh arc; and the epicenters of the Ashkhabad earthquake series were located between the mountains and the foredeep as in other arcs. No large gravity anomalies, no active volcanoes, and no intermediate or deep earthquakes are associated with this arc.

The area extending from the Tian Shan across the Garm district to the Pamir is at the southwestern end of the long Pamir-Baikal seismic belt, the trend of which diverges here from that of the series of Alpide arcs. The southern Tian Shan, especially, is a former platform region which in comparatively late geological time has been broken into blocks by the stresses associated with the Alpide geosynclinal movements of the Pamir. (Some recent evidence even suggests considerable strike-slip displacements in addition to vertical movements, in the Tian Shan). The tectonic character of the area is not unlike that of West Japan. Both northern Tian Shan ranges have "roots" represented by depression in the Moho; under the Pamir both the Moho and the intermediate ("Conrad") discontinuity descend.

The Pamir region presents some typical arc features, although volcanism is minor. However, there are large negative gravity anomalies. Intermediate earthquakes at depths of 100–150 km occur under the southern Tian Shan; if referred to the Pamir these seem anomalously placed. As already remarked, the numerous intermediate earthquakes under the Hindu Kush present a very special problem.

The Garm district, between the Tian Shan and the Pamir, is a region of relatively frequent small earthquakes at quite shallow depth. These are apparently connected with a local small-scale block structure; volcanism is not involved.

In "Seismicity of the Earth" it was suggested that the entire Pamir-Baikal seismic belt is at present subject primarily to block tectonics. This corresponds with the statistical result that the proportion of large to small shocks appears to be higher there than in the Pacific arcs.

§ 13. Concluding note

The statistical approach, noted in the preceding paragraph, is likely in future to become a valuable means of distinguishing between areas of different tectonic type. Tsuboi has already applied it with success to the distinction between West Japan and Northeast Japan, and to further more detailed subdivision. Naturally the method can be applied only in areas of high seismicity, or where there are plentiful historical data extending over many centuries.

The critical reader will have noted that there is no sharp distinction between block and arc regions, but rather a gradation. At one extreme are typical Pacific arcs in which the evidence of block faulting is lacking; at the other are regions like that of California in which most of the arc features are absent, and the block tectonics is characterised by large strike-slip faulting which tends to destroy the former alignments. Northeast Japan and West Japan are not quite at these two extremes; but their opposite characteristics are clear enough so that useful future results may be expected by comparing their features with those of arc and block tectonics respectively.

§ 14. Acknowledgments

It would be difficult, however pleasant, to acknowledge all my obligations in preparing this note. I am indebted to publications by many authors, and to personal discussions in Tokyo and elsewhere. Before coming to Japan I found much information and many useful suggestions in publications by Proffessor Kobayashi; since my arrival in Tokyo he has kindly made his publications available for further study, and has been very helpful personally. I have made almost incessant use of "Geology and Mineral Resources of Japan," with accompanying map, published by the Geological Survey in 1956.

For discussion of the preliminary draft of this paper, and the correction of various errors, I am particularly indebted to Professor H. Kuno and Professor T. Sakamoto.

Professor Ehara's valuable series of paper on the geotectonics of the Pacific have been extremely useful in the revision.

References

EHARA, S.:
1956 "Geotectonics of the Pacific with reference to Southwestern Japan, III. Geotectonics of Central Honshu". Jour. Geol. Soc. Japan, **62**, p. 289-301.
1960 "Geotectonics of the Pacific: Geotectonics of the Ryukyu arcuate islands", *ibid.* **66**, p. 229-241.

GUTENBERG, B., and RICHTER, C. F.:
1954 "Seismicity of the Earth". Princeton University Press, 2nd ed.

KOBAYASHI, T.:
1953 "The mountain structure of the Japanese island". Proc. 8th Pacific Science Congress, Vol. 2A, p. 743-751.
"The insular arc of Japan". *ibid.* p. 799-807,

MURAKOSHI, T., and HASHIMOTO, K. (editors):
1956 "Geology and Mineral Resources of Japan". Geological Survey of Japan.

RICHTER, C. F.:
1958 "Elementary Seismology". W. H. Freeman and Company, San Francisco.

CALIFORNIA INSTITUTE OF TECHNOLOGY, PASADENA, CALIFORNIA
(Division of the Geological Sciences, contribution No. 994)

DISASTER PREVENTION RESEARCH INSTITUTE
KYOTO UNIVERSITY
BULLETIONS

Bulletin No. 31 March, 1960

On the Possibility of the Metallic Transition of MgO Crystal at the Boundary of the Earth's Core

By

Tatsuhiko WADA

On the Possibility of the Metallic Transition of MgO Crystal at the Boundary of the Earth's Core

Tatsuhiko WADA

Abuyama Seismogical Observatory, Faculty of Science, Kyoto University
(Communicated by Prof. K. Sassa)

Ramsey's hypothesis on the origin of the Earth's core is applied to the model that the D-layer and the core are composed of the molecular and the metallic phase of MgO, respectively. The approximation of tight-binding method is employed to investigate the electronic band structure of MgO crystal. It is resulted that the pressure-induced transition of MgO to metallic phase occurs at a pressure of about 1.2×10^6 bars.

1. Introduction

The suggestion that the large increase of density at the boundary of the Earth's core is due to a pressure-induced transition from a molecular to a metallic phase, was first proposed by Ramsey (1948). He abondons the iron-core hypothesis and assumes that the mantle and the core have the same chemical composition, for example, such as olivine. Olivine, however, may not seem to compose the D-layer, since the ϕ ($=K/d$, where K and d denote incompressibility and density, respectively) of olivine is not compatible with that of the D-layer deduced from seismic data.

Recently Магницкий (1953) and Shimazu (1959) suggested the process $Mg_2SiO_4 \rightleftarrows 2MgO+SiO_2$ within the C-layer, which demands the D-layer composed mainly of MgO. In fact, it will be shown in the present paper that the elastic properties of MgO agree faily well with those of the D-layer deduced from seismic data.

Originally, Ramsey put forward his hypothesis to account for the density of the terrestrial planets. On his hypothesis the pressure at the boundary of the core should be characteristic of the chemical composition —— MgO in our model. Although it is important to determine whether the dimensions and masses of the terrestrial planets can or not show that this hypothesis is tenable, the possibility of the metallic transition of the constituent material at

the boundary of the Earth's core gives a determinable evidence to his hypothesis.

The critical pressure at which a metallic transition occurs depends upon the variation of the forbidden band (the energy gap between the conduction and the valence band) with pressure. It is desired that the electronic band structure of MgO crystal under a high pressure of about 10^6 bars is investigated. Since at present we can hardly expect to carry out it experimentally, although the recent development of shock-wave technique shoud be noted (Alder and Christian (1956)), the theoretical investigation is the only way to do so.

2. The electronic band structure of MgO crystal

MgO crystal consists of two kinds of ions, Mg^{2+} and O^{2-}, which have closed shell structures. We suppose that the uppermost valence bands of MgO crystal have 6N states, and they are completely filled with 6N electrons, since the crystal is an insulator. Then we may assume that the wave functions of these bands are approximately given by LCAO (linear combination of atomic orbitals) Bloch functions formed from suitable atomic orbitals which have the character of $2p$-orbitals of O^{2-} ion.

The foundamental problem in the determination of the electronic band structure of a crystal in the ordinary Hartree-Fock approximation is to find the eigenvalues of the equation.

$$F_{0p}(\boldsymbol{x}, \boldsymbol{k}) = \epsilon_p(\boldsymbol{k})\psi_p(\boldsymbol{x}, \boldsymbol{k}) \tag{1}$$

$\psi_p(\boldsymbol{x}, \boldsymbol{k})$ are the one-electron wave functions ($\boldsymbol{x}$ stands for both space and spin coordinates), $\boldsymbol{k}$ is a vector in the reciprocal latilce (body-centered cubic in the case of MgO) and the index p denotes the Brillouin zone number in $\boldsymbol{k}$-space. F_{0p} is the effective one-electron Hamiltonian operator in Fock's approximation. To obtain an approximate solution of Eq. (1), we suppose that the $\psi_p(\boldsymbol{x}, \boldsymbol{k})$ may be expressed as LCAO. For the valence band of MgO crystal containing N molecules, the atomic orbitals selected are the 12 free ion spin-orbitals consisting of 6N $2p$ spin-orbitals on the O^{2-} ions and 6N $2p$ spin-orbitals on the Mg^{2+} ions. These orbitals will be denoted by $\phi_p(\boldsymbol{x}, \boldsymbol{\alpha})$, where the vector $\boldsymbol{\alpha}$ specifies the position of the ions, and the index p goes over all spin-obitals associated with the ion at $\boldsymbol{\alpha}$. The radial parts of the orbitals used in present calculation are given by

$$P_0 = 0.07800\,\gamma \exp(-0.714\,\gamma) + 8.51793\,\gamma \exp(-3.412\,\gamma) + 1.6649\,\gamma \exp(-1.38\,\gamma) \tag{2}$$

for the $2p$ orbitals of O^{2-} (Watson (1958)) and

$$P_{Mg} = 7.360\,\gamma \exp(-2.7226\,\gamma) + 22.795\,\gamma \exp(4.808\,\gamma) + 21.348\,\gamma \exp(-7.9907\,\gamma) \tag{3}$$

for the $2p$ orbitals of Mg^{2+} (Löwdin (1953)), respectrively. For brevity, in what follows we condence our indices (p, α) and (p, k) into the single symbols α and k, and write

$$\boldsymbol{\phi} = \boldsymbol{\varphi} \boldsymbol{C}' \tag{4}$$

where $\boldsymbol{\phi}$ and $\boldsymbol{\varphi}$ are row matrices. $\boldsymbol{C}'$ is taken as a square $(6N \times 6N)$ matrix so that Eq. (2) defines a set of 6N crystal spin-orbitals. The row matrix $\boldsymbol{\varphi}$ is ordered such that the first 3N elements are the spin-orbitals on the O^{2-} ions, and the last 3N elements are those on the Mg ions. Let the indices μ, ν and λ denotes the orbitals on the O^{2-} ions, and l, m and n denotes the or bitals on the Mg^{2-} ions. The indices α, β, γ and δ will be used to denote any orbitals on the O^{2-} and the Mg^{2+} ions.

The set of orbitals $\boldsymbol{\varphi}$ are not all orthogonal at any finite lattice paramter. An orthonorml set $\boldsymbol{\Phi}$ are introduced by Löwdin transformation (for example, Löwdin (1956), Callaway (1958)). Thus

$$\boldsymbol{\Phi} = \boldsymbol{\varphi} \boldsymbol{L} \tag{5}$$

where

$$\left.\begin{aligned} \boldsymbol{L} &= (\boldsymbol{1} + \boldsymbol{S})^{-1/2} \\ S_{\alpha\beta} &= \int \phi_\alpha^*(\boldsymbol{x}) \phi_\beta(\boldsymbol{x})\, d\boldsymbol{x} - \delta_{\alpha\beta} \end{aligned}\right\} \tag{6}$$

Eq. (4) is expressed by the set $\boldsymbol{\Phi}$ as

$$\left.\begin{aligned} \boldsymbol{\phi} &= \boldsymbol{\Phi} \boldsymbol{C} \\ \boldsymbol{C}^\dagger \boldsymbol{C} &= \boldsymbol{C} \boldsymbol{C}^\dagger = \boldsymbol{1}. \end{aligned}\right\} \tag{7}$$

Using Eq. (7) in Eq. (1) our fundamental approximat'on is expressed as

$$\boldsymbol{C}^\dagger \boldsymbol{F} \boldsymbol{C} = \boldsymbol{\epsilon} \tag{8}$$

where $\boldsymbol{\epsilon}$ is a diagonal matrix, and the matrix $\boldsymbol{F}$ has element $F_{\alpha\beta}$ defined by

$$F_{\alpha\beta} = H_{\alpha\beta} + \sum_{k\gamma\delta} C_{k\gamma}^\dagger G_{\alpha\beta}{}^{\gamma\delta} C_{\delta k}, \tag{9}$$

where

$$\left.\begin{aligned} H_{\alpha\beta} &= \int \phi_\alpha^*(\boldsymbol{x}) H \phi_\beta(\boldsymbol{x})\, d\boldsymbol{x}, \\ G_{\alpha\beta}{}^{\gamma\delta} &= \int [\phi_\alpha^*(\boldsymbol{x}_1)\phi_\gamma^*(\boldsymbol{x}_2) G \phi_\beta(\boldsymbol{x}_1)\phi_\delta(\boldsymbol{x}_2) \\ &\quad - \phi_\alpha^*(\boldsymbol{x}_1)\phi_\gamma{}^+(\boldsymbol{x}_2) G \phi_\delta(\boldsymbol{x}_1)\phi_\beta(\boldsymbol{x}_2)]\, d\boldsymbol{x}_1 d\boldsymbol{x}_2 \end{aligned}\right\} \tag{10}$$

where $\boldsymbol{H}$ is the Hamiltonian operator for an electron moving in the field of the ion-cores, and $\boldsymbol{G} = (1/2)\, \boldsymbol{r}_1 - \boldsymbol{r}_2$.

Let $\boldsymbol{B}$ be a unitary matrix which transform $\boldsymbol{F}$, the matrix representation of all $F_{\alpha\beta}$, to a new matrix ϵ', where

$$\epsilon' = \boldsymbol{B}\dagger \boldsymbol{F} \boldsymbol{B}, \tag{11}$$

and $\boldsymbol{B}$ is chosen such that the submatrices $\epsilon'(\mu, m)$ and $\epsilon'(m, \mu)$ are null matrices. Then a set χ of orthonormal atomic spin-orbitals is introduced according to

$$\lambda = \Phi \boldsymbol{B}. \tag{12}$$

ϕ is expressed in terms of the set χ as

$$\phi = \chi \boldsymbol{V}, \tag{13}$$

where $\boldsymbol{V}$ is a unitary matrix, which reduces ϵ' to diagonal form with the eigenvalues $\epsilon_p(\boldsymbol{k})$ of Eq. (1) on the diagonal. Thus

$$\epsilon = \boldsymbol{V}\dagger \epsilon' \boldsymbol{V} \tag{14}$$

To find the eigenvalues we first construct the Bloch functions

$$\eta_p(\boldsymbol{r}, \boldsymbol{k}) = N^{1/2} \sum_{\mu} x_p(\boldsymbol{r}, \mu) \exp(2\pi i \mu \cdot \boldsymbol{k}) \tag{15}$$

Then

$$\psi_p(\boldsymbol{x}, \boldsymbol{k}) = N^{-1/2} \sum_{q} \eta_q(\boldsymbol{x}, \boldsymbol{k})\, U_{qp}(\boldsymbol{k}) \tag{16}$$

where

$$U_{qp}(\boldsymbol{k}) = N^{1/2} \exp(-2\pi i \boldsymbol{k} \cdot \mu)\, V_{qp}(\mu, \boldsymbol{k}) \tag{17}$$

Using Eq. (17) in Eq, (14), we arrive the secular equation

$$\det\ \varepsilon_{pq}(\boldsymbol{k}) - \delta_{pq} \epsilon(\boldsymbol{k}) | = 0 \tag{18}$$

for the eigenvalues $\epsilon_p(\boldsymbol{k})$. In Eq. (18)

$$\left.\begin{aligned} \varepsilon_{pq}(\boldsymbol{k}) &= \int \eta_p^*(\boldsymbol{x}, \boldsymbol{k}) F_{0p} \eta_q(\boldsymbol{x}, \boldsymbol{k})\, d\boldsymbol{x}, \\ &= \epsilon_{pq}{}'(\mu, \mu) + \sum_{\lambda} \varepsilon_{pq}(\mu, \mu + \boldsymbol{\lambda}) \exp(2\pi i \boldsymbol{\lambda} \cdot \boldsymbol{k}), \end{aligned}\right\} \tag{19}$$

where $\boldsymbol{\lambda}$ is a vectors which maps out the O^{2-} ion lattice from an arbitrary chosen O^{2-} ion at μ.

The ε' is obtained from Eq. (11) by treating all non-diagonal elements of F as first order small quantities and applying perturbation theory (Grimley (1958)). The results can be written in terms of the matrix elements defined in Eq. (10) and the matrix R with elements $R_{\alpha\beta}$ defined by

$$R_{\alpha\beta}=\sum_{\nu}B_{\alpha\nu}B_{\nu\beta}\dagger \tag{20}$$

For numerical calculation, it is more convenient to express Eq. (21) in terms of matrix elements formed with the given non-orthoganal spin-orbitals. A new matrix corresponding to $\bar{R}$ is defined by

$$\bar{R}_{\alpha\beta}=\sum_{\nu}B_{\alpha\nu}\bar{B}_{\nu\beta}\dagger \qquad \bar{B}_{\alpha\beta}=\sum_{\gamma}L_{\alpha\gamma}B_{\gamma\beta}$$

We can separate from $\bar{R}$ a new matrix $\bar{P}$ representing the contribution from the O-Mg interaction, i.e. $\bar{P}_{\mu\nu}=T_{\mu\nu}-\bar{R}_{\mu\nu}$, where $T=(1+S_1)^{-1}$, and S_1 is the submatrix of S consisting of all elements of the form $S_{\mu\nu}$. In terms of these quantities we obtain

$$\begin{aligned}\epsilon_{\mu\nu}'=\bar{H}_{\mu\nu}&-2G_{\mu\nu}{}^{\nu\mu}\bar{P}_{\mu\nu}-2\sum_{m}\bar{G}_{\mu\nu}{}^{m\mu}\bar{P}_{\mu m}-2\sum_{m}\bar{G}_{\mu\nu}{}^{\nu m}\bar{P}_{m\nu}\\&+\sum_{m}P_{\mu m}\bar{P}_{m\nu}(H_{\mu\mu}-H_{mm})+H_{\mu\mu}\sum_{\lambda}S_{\mu\lambda}S_{\lambda\mu}-\sum_{\lambda}S_{\mu\lambda}H_{\mu\lambda}\end{aligned} \tag{22}$$

where $\bar{H}_{\alpha\beta}$ and $\bar{G}_{\alpha\beta}{}^{\gamma\delta}$ stand matrix elements like $H_{\alpha\beta}$ and $G_{\alpha\beta}{}^{\gamma\delta}$ in Eq. (10) but with the set φ replacing the set Φ.

We can express all non-vanishing elements $\epsilon_{pq}'(\mu,\mu+\lambda)$ as fallows:

$$\begin{aligned}&\epsilon'_{xx}(\mu,\mu)=\epsilon'_{yy}(\mu,\mu)=\epsilon'_{zz}(\mu,\mu)=A_0\\&\epsilon'_{xx}(\mu,\mu+\lambda)=\epsilon'_{yy}(\mu,\mu+\lambda)=A_1 \qquad \lambda=(r,r,0)\\&\epsilon'_{zz}(\mu,\mu+\lambda)=A_1' \qquad \lambda=(r,r,0)\\&\epsilon'_{xy}(\mu,\mu+\lambda)=A_1'' \qquad \lambda=(r,r,0)\\&\epsilon'_{xx}(\mu,\mu+\lambda)=A_2 \qquad \lambda=(2r,0,0)\\&\cdots\cdots\cdots\qquad\cdots\cdots\cdots\end{aligned} \tag{23}$$

Here r is the cation-anion distance. The numerical calculation are carried out for three values of r=2.10, 2.00, 1.80 A. These are tabulated in Table 1.

Table 1 The values of ϵ'_{pq} in three cases of γ (see Eq. (23)).

ϵ'_{pq}	γ=2.10Å	γ=2.00Å	γ=1.80Å
A_0	0.205605	0.179944	0.100703
A_1	0.001162	0.009200	0.010147
A_1'	−0.009746	−0.013314	−0.025088
A_1''	0.017948	0.028438	0.041487
A_2	0.001628	0.005233	0.006604

Using Eq. (23) in Eq. (18) we now have

$$\left.\begin{aligned}\varepsilon_{xx}(\boldsymbol{k}) &= A_0+4A_1(\cos 2\pi rR_x \cos 2\pi rR_y+\cos 2\pi rk_x \cos 2\pi rk_z)\\ &\quad +4A_1\cos 2\pi rk_y \cos 2\pi rk_z+2A_2 \cos 4\pi rk_x\\ \varepsilon_{xy}(\boldsymbol{k}) &= -4A_1{}''\sin 2\pi rk_x \sin 2\pi rk\end{aligned}\right\} \quad (24)$$

and the other elements follow from (24) by interchanging x, y and z. The secular equation (18) is easily solved for several prominent directions in k-space, i. e., (k, O, O), (k, k, O) and (k, k, k). The final results are showed in Fig. 1.

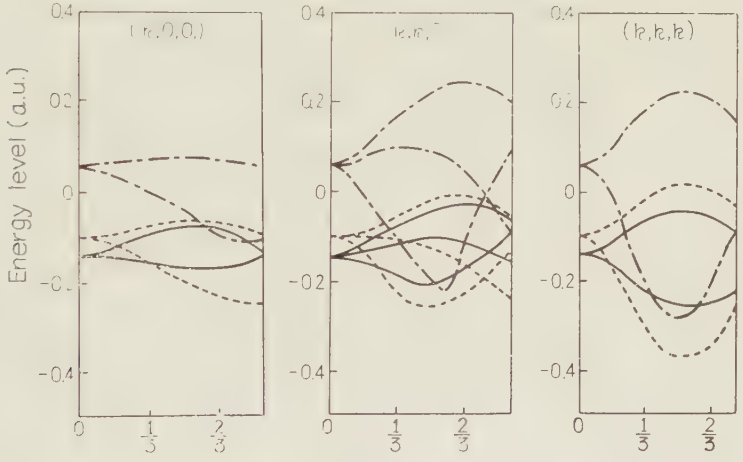

Fig. 1. Band structure of MgO in three cases of r along three directions in k-space. (····· ; 2.10Å, —— ; 2.00Å, -•-•- ; 1.80Å)

To obtain the transition point, one may proceed in the following : start with MgO crystal in the ionic state and determine when the energy gap disappears. The maximum and the minimum energy values of the valnece band are plotted against r in Fig. 2., which shows the broadening of the band with r. Since the evaluation of the conduction band of MgO crystal can hardly be made by the approximation of tight-binding, we assume that the conduction band braodens within the forbidden band as much as the valence band. At the ordinary lattice parameter $r=2.10$ Å, it is found by using optical method that the energy gap is about 9 e. v.. With the assumption above cited, thus it is found that the energy gap disappears at $r=1.87$ Å

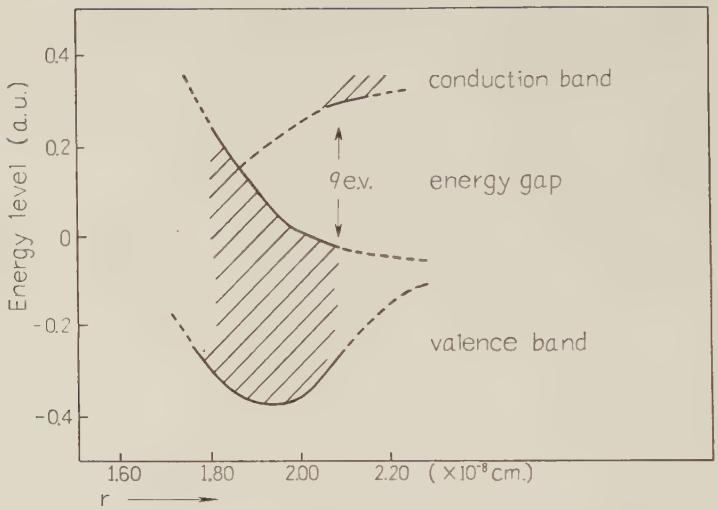

Fig. 2. The electronic band structure of MgO as a function of Conduction band and valence band are crossing at =1.87Å.

3. An equation of state of MgO crystal

To obtaine the pressure of MgO crystal corresponding to the transition point, we must express the lattice energy of MgO crystal as a function of r. According to Born and Mayer's expression, the lattice energy E_r is shown by

$$E_r = -(a_M z^2 e^2/r) + b\left[MC_{12}e^{(r_1+r_2-r)/\rho} + M'/2)(C_{11}e^{2r_1/\rho} + C_{22}e^{2r_2/\rho})e^{-a'r/\rho}\right] \qquad (25)$$

per molecule, where a_M is Madelung's constant (1.7476 for the NaCl type in MgO), M and M' are the numbers of unlike and like neighbours of each ion, respectively (6 and 12 for the NaCl type), a' is the ratio of the distance between like neighbours to that between unlike neighbours ($\sqrt{2}$ for the NaCl type), b is arbitrary constant chosen to have the value 10^{-12} erg, r_1 and r_2 are what shall be termed the radii of the ion 1 and 2, C_{ij} is a factor calculated by Pauling and is expresed as $C_{ij}=[1+(z_i/n_i)+(z_j/n_i)]$ where z_i is the valence of i-ion, and n_i the numbers of valences electrons in the outer shell of i-ion.

Acoording to Huggins and Mayer's method (1933), the unknown parameters r_1, r_2 and ρ in Eq. (23) are dertermined by using some experimental values of MgO. The final resultsis expreseed as

$$E_r = -76.76605/(r/r_0) + 1385,24705\ exp\ (-4.8837(r/r_0)) + 3660.44466\ exp\ (-6.9066(r/r_0)) \qquad (26)$$

By differentiating Eq. (26) once and twice we obtaine pressure p, and incompressibility K_T as the functions of (r/r_0). And the relation between

(r/r)	p(.10 dynes/cm)	K_T (.10 dynes/cm)	d (gr/cm)
1.00	0.000	1.64	3.60
0.99	0.052	1.81	3.71
0.98	0.109	1.98	3.82
0.97	0.174	2.19	3.94
0.96	0.245	2.42	4.08
0.95	0.324	2.66	4.20
0.94	0.413	2.92	4.33
0.93	0.511	3.21	4.48
0.92	0.623	3.52	4.62
0.91	0.741	3.85	4.78
0.90	0.887	4.24	4.94
0.89	1.033	4.61	5.10
0.88	1.194	5.08	5.28
0.87	1.376	5.63	5.47

Table 2. Variation of density d, incompressidility K_T and pressuse p of MgO versus change (r/r_0).

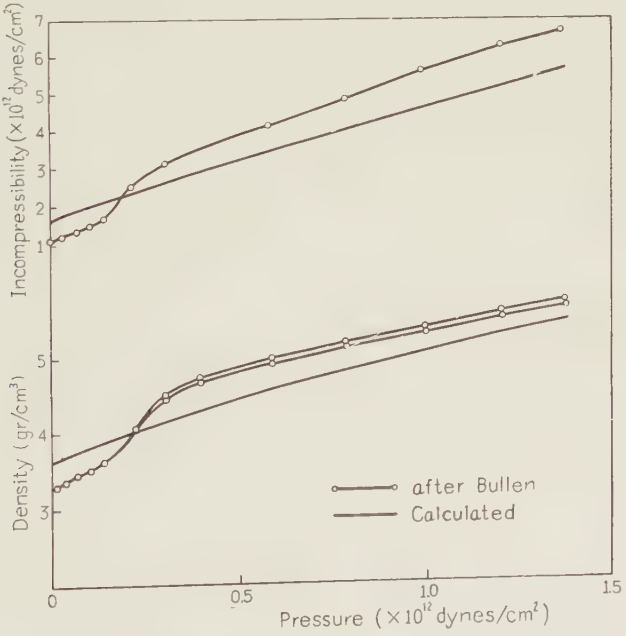

Fig. 3. Distribution of density (lower curve) and incompressibility (upper curve) within the Mantie.

density d and (r/r_0) is obtained by using the atomic weights of Mg and O. These values are given in Table 2. To examine the model that the D-layer is composed of MgO, these calculated values and Bullen's values (1953) are shown in Fig. 3, where we find that the maximum discrepancy between both values ϕ $(=K_T/d)$ is about 20%. We must note that the accuracy of Eq. (26) decreases as the pressure increases (Wada (1959)) and the calculated values show the isothermal and, on the other hand, Bullen's values the adiabatic. At any rate, we may conclude that Eq. (26) will be enough good approximation to estimate the transition point, since the process in evaluating the electronic band structure is not so accurate that the discrepancy above cited playes a heavy roll.

4. Pressure-induced transition of MgO crystal to metallic phase

From sec. 2 and sec. 3 we find that the pressure corresponding to the transition point ($r=1.87$ Å) is about 1.2×10^6 bars, which is the pressure of the depth of about 2600 km in the interior of the Earth, as shown in Bullen's table. The result obtained, in the other word, shows that the energy gap between the conduction band and the valence band of MgO crystal disappears at $r=1.87$ Å. In this situation the valence electrons in ordinary ionic state are made free, and the electronic band structure becomes metallic. We must note that this transition point is not such as suggested by Ramsey. In the former no density-jump occurs, while in the latter density increases discontinuously. To estimate the latter type of transition, we must obtain the lattice energy curve of the metallic phase. Of course we may expect that the minimum point of the energy curve ot the metallic phase could be near the transition point given in the present calculation. It is, however, not necessary that both transition occur at asame pressure. This case that the transition with density-jump at a high pressure than the transition without density-jump, is very interesting. In this case the electronic conductivity increases abruptly at an certain depth in the deeper part of the D-layer and the density increases discontinuously at the boundary of the Earth's core. The suggestion that the electric conductivity will increase abruptly in the case of the transttion to metallic phase, is made by Mott (1956). Mott's opinion is as follows : if an electron is removed from valence band to

conduction band, a mobile positive hole is formed. The minimum energy necessary to form a free electron and positive hole will decraase as the lattice parameter comes closer, but cannot tend to zero. since an electron and a positive hole attract each other with a foree of which the potential energy for large r is of Coluomb's type. Thus small number of free carriers of positive sign is impossible in the ground state, since the free earriers of positive and negative sign are bounded to form pairs. On the other hand, when there is a large number of free carriers any pair of charged particles may be expected to attract each other with a force derivative from a screened potential, which does not necessary lead to a bound state. Thus the transition to a state showing metallic conductivity will be sharp.

5. Conclusion

It is found that the valence band of MgO crystal broadens rapidly as lattice parameter decreases, and the energy gap will disappear at $r=1.87$ Å corresponding to pressure of about 1.2×10^6 bars which is deduced from an equation of state of MgO. We may expect that the pressure-induced transtion of MgO crystal to metallic phase could occur at the boundary of the Earth's core. A new model that the electric conductivity increases abruptly in the deeper part of the D-layer and the transition from molecular (or ionic) phase to metallic one occurs at the boundary of the Earth's core with a large density-jump, is also suggested.

6. Acknowledgement

The writer is indebted to Prof. K. Sassa of Kyoto University and Prof. H. Miki of Kyoto University for their invaluable advices and encouragement. Further the writer wishes to express his thanks to Dr. Y. Shimazu of Nagoya University for his constant gaidance in the course of the work and his advice.

Reference

1) Alder, B. J., and Christine, R. H., Pressure-induced metallic transition in insulators, Discus. Farady Soc., 22, 44–46, 1956.
2) Bullen, K. E., An introduction to the theory of seismology, 2nd Ed., Cambridge Univ. Press, Cambridge. 1953.
3) Callaway, J., Electronic energy bands in solids, Solid State Physics, (Ed. by Seitz,

F., and Turnbull, D.,) 7, 643–646, 1958.
4) Grimley, T. B., The electronic structure of crystals having the sodium chloride of lattice, Proc. Phys. Soc., A–71, 749–757, 1958.
5) Huggins, M. L., and Mayer, J. E., Interatomic distances in crystals of the alkali halides., J. Chem. Phys., 1, 643–646, 1933.
6) Löwdin, P. O., Studies of atomic self-consistent fields. I. Calculation of Slater functions, Phys. Rev., 58, 120–125, 1953.
7) Löwdin, P. O., Quantum theory of cohesive properties of solids, Advance in Physics, 5, 1–172, 1956.
8) Магницкий, В. А., Основы физики земли, геодезиздат, москва. 1953.
9) Mott, N. F., Conduction in the impurity band, Report of the Meeting on Semiconductors, British Thompson-Houton LTD, Rugbey, 5–13, 1956.
10) Shimazu, Y., A chemical phase transition hypothesis if the origin of the C-layer within the mantle of the earth, J. Earth Sci. Nagoya Univ., 6, 12–30, 1958.
11) Wada, T., An equation of state of periclase (MgO) and the D-layer, (in Japanese) Zisin Ser. 2, 12, 171–181, 1959.
12) Watson, R. E., Analytic Hartree-Fock solutions for O^{2-}, Phys. Rev., 90, 120–125, 1958.

DISASTER PREVENTION RESEARCH INSTITUTE
KYOTO UNIVERSITY
BULLETIN

Bulletin No. 32 March, 1960

Variation of the Elastic wave Velocities of Rocks in the Process of Deformation and Fracture under High Pressure

By

Shogo MATSUSHIMA

Variation of the Elastic wave Velocities of Rocks in the Process of Deformation and Fracture under High Pressure

By

Shogo MATSUSHIMA

Geophysical Institute, Faculty of Science, Kyoto University

(Communicated by Prof. K. Sassa)

Abstract

Variation of the ultrasonic velocities of granite in the process of deformation and fracture caused by the axial compressional stresses was observed under high confining pressure up to 5,000 atmospheres. At the initial stage of deformation, the velocities increased with the overlapped stresses, then reached the constant value in cases of both the axial direction and the transverse of it. In the facture range, however, the velocities of waves passing through in the direction transverse to the axis remarkably decreased with the progression of facture, while such change of velocities was scarcely observed in the axial direction.

The tendency of the velocity change as stated above decayed rapidly with elevating pressure. Then, these phenomena can be explained with the assumptions of pores, closed initially and extended by pressures or stresses at the fracture stage, the same as the increase of strength with that of pressure and the extraordinary stress-strain relation reported in the previous papers.

Introduction

In our previous experiments[1] on the mechanism of deformation and fracture of igneous rocks, we researched that the rocks had the extraordinary values of Poisson's ratio in the fracture range caused by the axial compressional stresses. That is, the lateral strain increases abruptly with the increase of the stress in this range, and the ratio of the lateral strain to the long-

itudinal is far beyond 0.5, suggesting that the volume of the specimen increases with development of fracture, because the longitudinal strain varies almost linearly. Under elevating confining pressure these phenomena gradually disappear with the increase of pressure, and over two or three thousands atmospheres they are scarcely observed.

On the other hand, the strength of rocks increses rapidly with the increase of pressure, but the rate of the rise of the strength has the same decreasing tendency as of the variation of Poisson's ratio in the fracture range.

These properties will be the characteristic of igneous rocks, and can be elucidated by a large number of pores contained in the rock specimen which may act like "the Griffith's cracks" in case of fracturing. The volume-increase at fracturing can be interpreted with the assumption that the progression of such pores or cracks produces the accumulation of a bulk of cavity. The increase of strength with that of pressure can be explained by closing of the pores.

It has been clearly explained from the experimental results by F. Birch[2] and D. S. Hughes[3] that such cavities originally contained in the rocks have a remarkable effect upon the elastic wave velocities of them under pressure. The influence is stronger under a lower pressure. On the other hand, it has been reported[4] that the variation of elastic wave velocities of metals caused by the plastic deformation is within the limit of only one per cent.

Then it is expected that at the fracturing under a relatively low pressure, the velocities of rocks decrease appreciably, for they have also the considerable bulk of cavities produced in themselves. Yet, from the experiments of the strain measurements, it is supposed that this decrease must be remarkable in the direction transverse to the applied axial stress, though the velocities of the axial one may scarcely change.

F. Birch has also suggested that the factors having influence on the seismic wave velocity in the crust are pressure, temperature and the mineral composition of it. The rise of pressure increases velocity, that of temperature decreases it, and the increase of the composition of the basic minerals strongly increases the velocity in general.

However, under the pressure which can not perfectly close the pores of rocks, the applied differential stresses overlapped to the hydrostatic pressure will be able to affect upon the wave velocities, for they can close the pores too.

From the above viewpoint, we studied the variation of the elastic wave velocities of granite in the process of deformation and fracture caused by the axial compressional stresses under moderate confining pressures up to 5,000 atmospheres.

Experimental Methods

Fig. 1 shows schematically the methods of ultrasonic measurements of rocks under the axial compressional stress combined with high confining pressure both a) in the direction of the axis and b) transverse to the axis. The high pressure equipment and the full sketch of the triaxial cylinder for this experiment were shown in the previous paper.

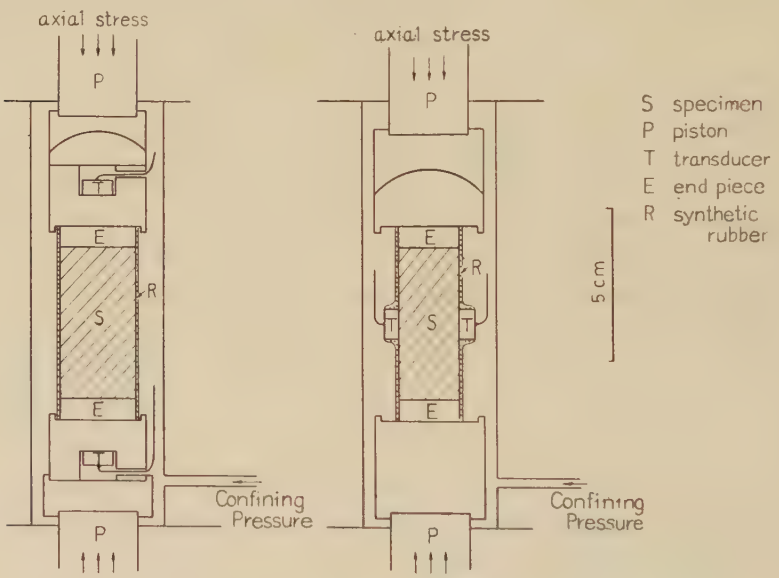

Fig. 1. The schematic representation of the methods for the measurements of the ultrasonic wave velocities under axial compressional stress combined with high confining pressure, a) in the axial direction, and b) in the direction transverse to the axis.

Specimens used for the measurements of the axial direction shown in Fig. 1, a) are the long columns of Kitashirakawa biotite granite 50 m/m long and 25 m/m in diameter, and that of the transverse direction in b) are the square pillars of the same location, 50 m/m height and 20 m/m in the base.

All specimens are covered with synthetic adhesive rubber. The barium

titanate crystals are used as the ultrasonic transducer which generates dilatational waves of frequency of 500 k.c..

Experimental Results

In Fig. 2 and Fig. 3, the variation of the dilatational wave velocities with stress respectively in the axial and the transverse direction under various confining pressures is shown. In each case, the velocities show the increase with the increasing of the axial stress, and reach the nearly constant value. This will mean that the pores of the specimen have not yet been perfectly closed under these pressures, and that the overlapped forces close gradually such residual cavities. Under higher pressure, the additional stresses scarcely affect on the variation of velocity, for the pores are fully closed. The ultimate values of velocities are nearly constant for each specimen without regard to the measured directions and the confining pressures.

In the fracture stages, however, the tendency of the velocity change is quite different in each observed direction. The velocities of the transverse direction abruptly decrease with the progress of the internal failure which is caused by the increase of stress and with the lapse of time, though that of

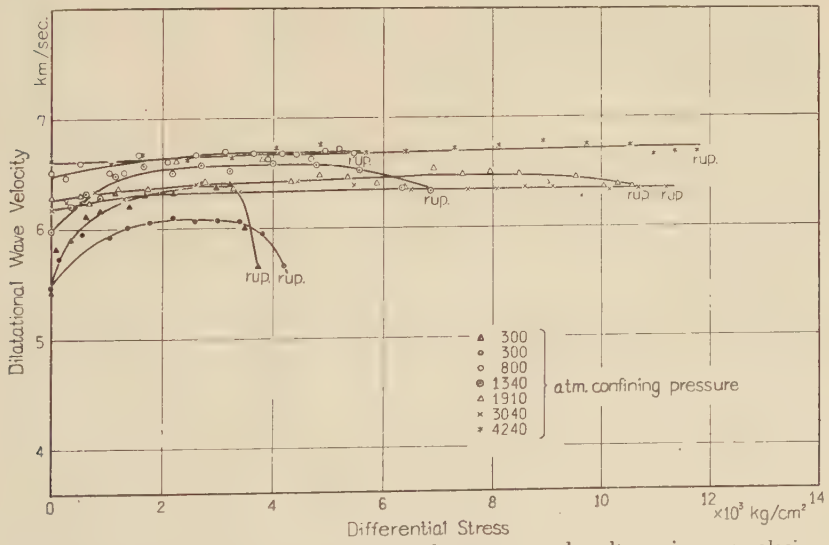

Fig. 2. Effect of the axial compressional stresses on the ultrasonic wave velocities passing through the specimen in the axial direction under various confining pressures.

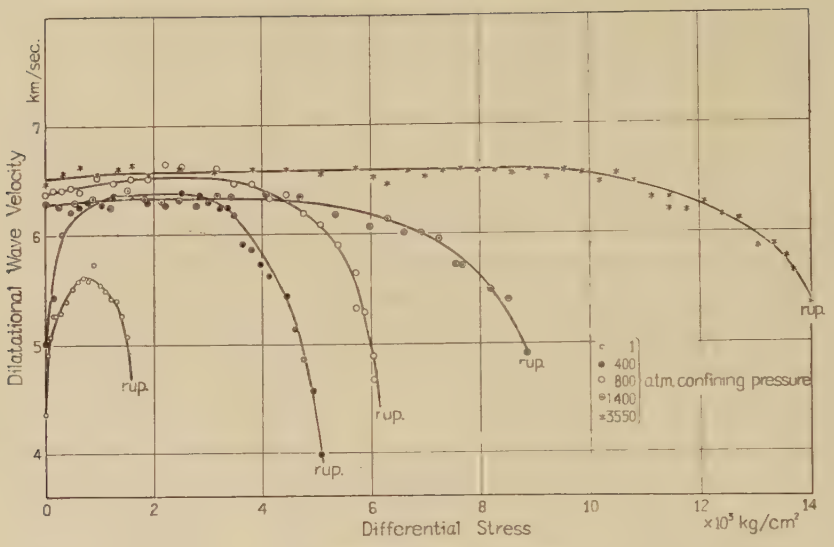

Fig. 3. Effect of the axial compressional stresses on the ultrasonic wave velocities passing through the specimen in the direction transverse to the axis under various confining pressures.

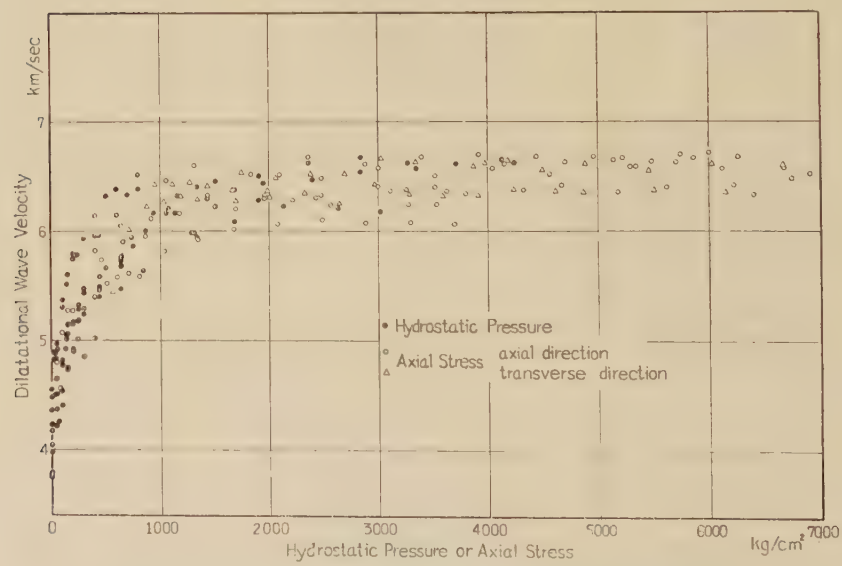

Fig. 4. Variation of the ultrasonic wave velocities with pressures and overlapped differential stresses.

the axial one are approximately constant up to the rupture moment. The change of length of specimens is negligible to this tendency, for this effect is in the limit of the observed error. The above phenomena will show that the considerable apertures are produced in the lateral direction with the progress of fracture. This tendency gradually decays under higher pressure, it is the same tendency as observed at the strain measurements.

As expected before, it is shown in Fig. 4 that the elastic wave velocities of rocks increase with the increasing of the applied axial compressional stresses overlapped to the confining pressure as well as with that of the hydrostatic pressure. The rates of the increase by the hydrostatic pressure and the axial stress are the same order of the magnitude, though the numbers of the observed values are insufficient to assert it. Then it may be said that the overlapped forces have nearly the same effect upon the wave velocity as hydrostatic pressure.

Conclusion

It will be supposed, though it may be very impudent, that the seismic wave passing through the relatively shallow region in the crust, where the composed rocks are highly stressed by a overlapped force and being fractured, decreases its velocity in the direction transverse to the applied force. In the deeper part of the crust, these effects may not be observed, because the confining pressure is strong enough here to be brought no change of velocity by the overlapped force.

If the above argument is possible on the earth's crust, the variation of the seismic wave velocity can be observed in the progress of the shallow focus earthquakes, or even of the somewhat deeper earthquakes, fo which the region extends to the part near the surface, such as accompanied by the surface faulting.

It will be possible to explain the velocity distribution, considering the stress distribution in the crust.

Acknowledgements

The writer wishes to express his sincere thanks to Professor K. Sassa for his continual encouragements.

The present study has been performed by the aid of the resarch funds

of the Ministry of Education for this Institute.

References

1) S. Matsushima, "On the flow and fracture of igneous rocks.", J. Phys. of the Earth., (In Press)
——, "On the deformation and fracture of granite under high confining pressure.", J. Phys. of the Earth., (In Press)

2) F. Birch, "Seismic structure of the crust.", Contributions in Geophysics, vol. 1, 158–70 (1958)

3) D. S. Hughes, C. Maurette, "Elastic wave velocities in granites.", Geophysics, vol. 21, 277–84 (1956)
——, ——, "Variation of elastic wave velocities in basic igneous rocks with pressure and temperature.", Geophysics, vol. 22, 23–31 (1957)

4) R. S. Bergman, R. A. Shahbender, " Effect of statistically applied stresses on the velocity of propagation of ultrasonic waves.", J. Appl. Phys., 1736–38 (1958)

DISASTER PREVENTION RESEARCH INSTITUTE
KYOTO UNIVERSITY
BULLETIN

Bulletin No. 34 June, 1960

Volcanic Micro-tremors at the Volcano Aso

By

Michiyasu SHIMA

Geophysical Institute, Faculty of Science, Kyoto University
(Communicated by Prof. K. Sassa)

Volcanic Micro-tremors at the Volcano Aso

By

Michiyasu SHIMA

Geophysical Institute, Faculty of Science, Kyoto University
(Communicated by Prof. K. Sassa)

Abstract

We investigate the variations and other properties of the micro-tremors at the Volcano Aso observed by the Wichert seismographs in the Volcanological Laboratory since 1950. In this paper, we treat the first kind and the second kind of the micro-tremors of the four kinds which have been classified by K. Sassa. He studied in decade of 1930 the phenomenon that the micro-tremors stop rapidly before eruptions and again increased after them. This time, we perceive the same phenomenon in the eruptions of Apr., 1953, Dec., 1957, and June, 1958. Next, we can perceive that the values of NS-component/EW-component of amplitudes of the second kind increase from 0 to 1 at the eruptions. It is found that this disposition occured also in the violent eruptions of 1933. Thus, on the assumption that the crack parallel to the row of the present craters, which has been infered from the mode of vibration at the eruption-earthquake by K. Sassa, vibrates after the eruption, being accompanied with the magmatic reservoir, we calculate the azimuthal distributions of amplitudes and indicate that the transversal component is the same order as the longitudinal component in the direction of the Volcanological Laboratory.

1. Introduction

The jets of lava and volcanic ashes and gas, the deformation of the earth's surface near the craters, the volcanic earthquake and micro-tremors, and the volcanic geomagnetic variations have been studied by many investigators. With respect to the Volcano Aso, many geophysical facts were revealed by K. Sassa in decade of 1930[1)2)]. Particularly, he studied in detail

the volcanic micro-tremors which appeared remarkably at the Volcano Aso, and pointed out that the volcanic eruption could be foretell by investigating the variations of the micro-tremors which came before the eruption. It is already revealed that not only the period but also the mode of oscillation distinguish the first kind of micro-tremors from the second and that from the detailed investigations during the comparatively silent time, the mode of the first kind is a Love wave type and that of the second kind is a Rayleigh wave type[1]. This time, we will further reveal these points by investigating the latest volcanic actions. In the following we describe only the results of the analysis of recordings of the first kind and the second kind of micro-tremors by Wichert horizontal and vertical component seismographs. For, although there appear the micro-tremors of the shorter period than that of the above waves and they are observed by S. Yoshikawa[3] near the craters, those which have the amplitudes of the same order as the first kind of micro-tremors at the origin damp so perfectly as to be unable to be observed at the Volcanological Laboratory, owing to the short period.

Fig. 1. Positions of Volcanological Laboratory and craters.

2. The micro-tremors and the eruptions between Apr. aud June of 1953.

The center of the eruption shifted from the fourth crater to the first and the second since Sep., 1932 and after the comparatively silent period between 1934~1950, we had a violent eruption of the first crater at 11^h32^m on Sep. 27th, 1953. Namely, after the small eruption on May, 1951, we had the silent time of two years and then the seismographs recorded the

regular waves of the first and the second kinds of the amplitudes of 0.5 μ and 1.5 μ since Apr. 14th and on 25th they interrupted rapidly and after calm state of three hours, we had a violent eruption of the first crater and abundant quantities of lava blocks of diameter of two feet were ejected, some of them being thrown 600 m. The amplitude of the first and the second kinds of micro-tremors which were recorded by Wichert seismographs at the Volcanological Laboratory during the active period, are shown in Fig. 2. The arrows indicate the eruption times when the lava blocks

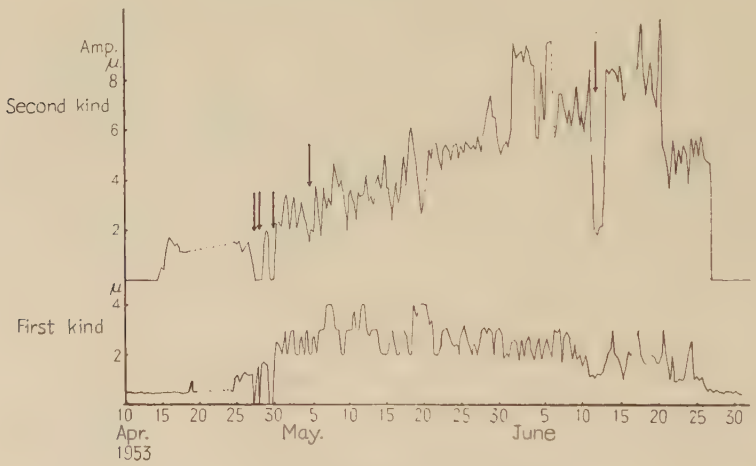

Fig. 2. Mean amplitude of micro-tremors.

were emitted. As known from this figure, the first crater exploded also at Apr. 28th, 29th and May 4th. The mean amplitude of the micro-tremors of the first kind which was 1 μ, and that of the second which was 1.5 μ increased 2.5 μ and 3~7 μ after the eruption, particularly, the second kind remarkably increased. Such a interruption of the micro-tremor just before the eruption is a character of that in April, and this fact gives the powerfull clue for the foretell. We see the same disposition also in decade of 1930.

3. The micro-tremors and the eruptions from July to Sep. of 1955.

The micro-tremors of the first kind which have been silent since July,

1953 increased on July 19th and the second increased on 24th. The second which had been the regular wave gradually became the continuous and irregular wave on July 25th and the amplitude increased to 3 μ, but, this time, the phenomenon that the micro-tremors interrupted just before the eruption was not clear and we could asertain only a irregularity in the wave form. Namely, we had the eruptions a few times on July 25th, particularly, the eruption at 10^h13^m was considerably strong, many lava blocks being ejected, and then the small eruptions were repeated on July 28th and 29th. The amplitudes of the first and second kinds of micro-tremors in this period are shown in Fig. 3.

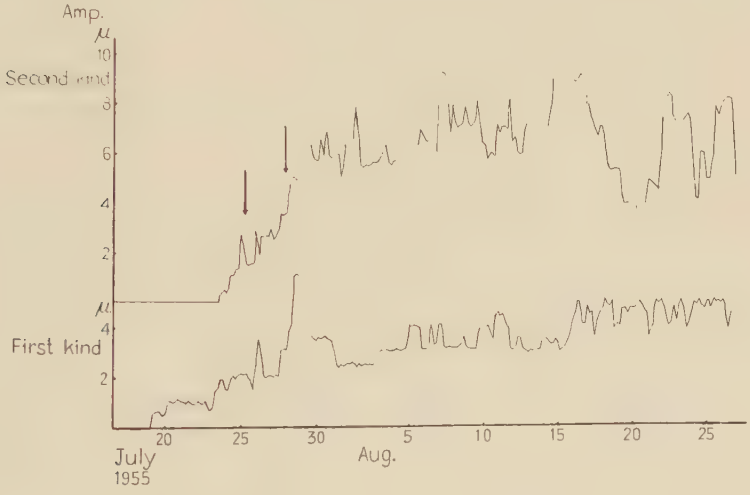

Fig. 3. Mean amplitude of micro-tremors.

Also, this time, the amplitudes after the eruption were larger than that before it. The micro-tremors of ca. 3 μ continued during Sep. and then damped gradually.

4. The micro-tremors and the euptions from Nov., 1957 to Jan., 1958.

After two years repose, on Nov. 17th, 1957, the micro-tremors of the first kind and the second kind began to increase gradually both in frequency of occurence and in amplitude. The first kind interrupted on Nov. 18th the second on Nov. 28th and the eruption occured at 19^h on Dec. 1st. The

micro-tremors for this time are shown in Fig. 4.

After this eruption, while the amplitude of the first kind was ca. 2 μ, the state of the second kind continued to rest, and the eruption occured at 1^h on Dec. 3rd, and then, the micro-tremors of the both kinds were slightly stronger than that before the eruption, continued in Dec. and damped gradually to April.

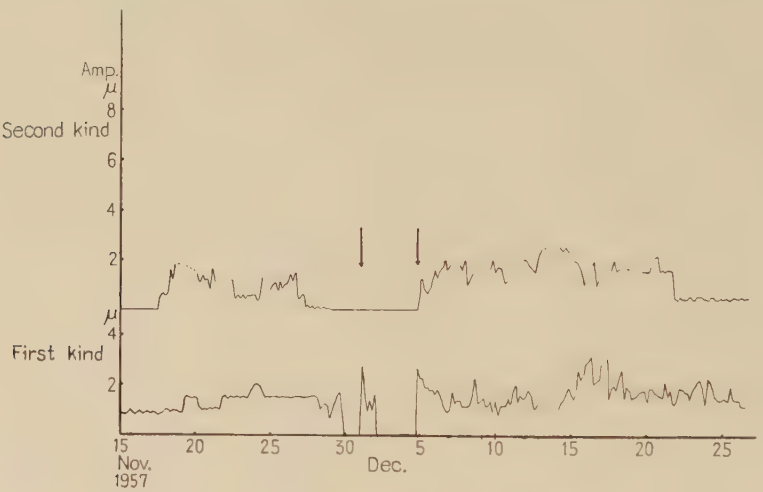

Fig. 4. Mean amplitude of micro-tremors.

5. The micro-tremors and the eruptions during June, 1958.

The smallness of the amplitudes of micro-tremors was a character of the eruption on June 24th, 1958, in comparison with the scale of the eruption, that is, the Wichert seismographs in the Volcanological Laboratory recorded only the micro-tremors of ca. 0.2~0.5 μ for a few days. However, the continuous micro-tremors of ca. 1 μ were recorded for some days before the eruption by the short period seismographs of very high magnifications in the Hondo's Observatory near the crater and interrupted two hours before the eruption and increased after it.

6. The characters of the variations of micro-tremors.

From the variation of the amplitudes of micro-tremors of the both kinds which occured between 1953~1958, we can summarize the following.

1) The micro-tremors of the both kinds occur several ten days before the eruption, the amplitudes larger than 1 μ at the Volcanological Laboratory continue and the micro-tremors which reach a maximum in amplitude and frequency of occurence often stop rapidly several hours or several days before the eruption. However, this disposition was not evident only in the eruption on July, 1957.

2) After the micro-tremors of the first kind of the amplitude of ca. 1 μ continue to be recorded within the limits of several days or several ten days, the state of them often return to rest without the eruption. For example, the end of June, 1954, the beginning of Jan., 1955, about the middle of Jan., 1957, and etc.. These are distinguished from the disposition of the micro-tremors before the eruption, by being accompanied with the second kind, and by the gradual stop of the first kind before it. However, to foretell the eruption, there are many points to study yet.

7. The variations of the mode of vibration of micro-tremor of the second kind

Irrespective of the activity of volcano, there occur the volcanic microtremors which have been called the second kind by K. Sassa, and the period of which is 3.5~8.0 sec.. The mode of oscillation was investigated by means of the simultaneous observations with the Galitzin type seismographs, which were set two points on Oct., 1932, and which were set six points on Aug., 1933.

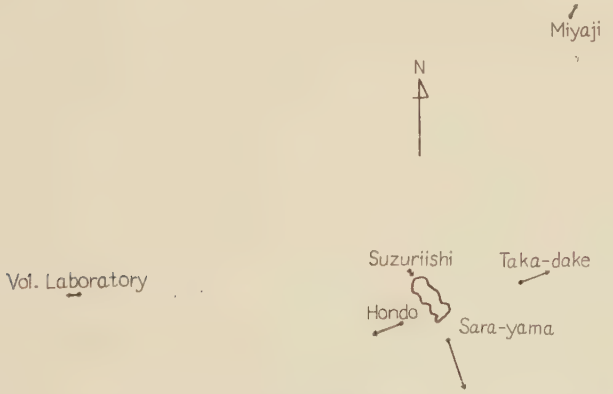

Fig. 5. Direction of horizontal displacements of micro-tremors of the second kind (after Sassa).

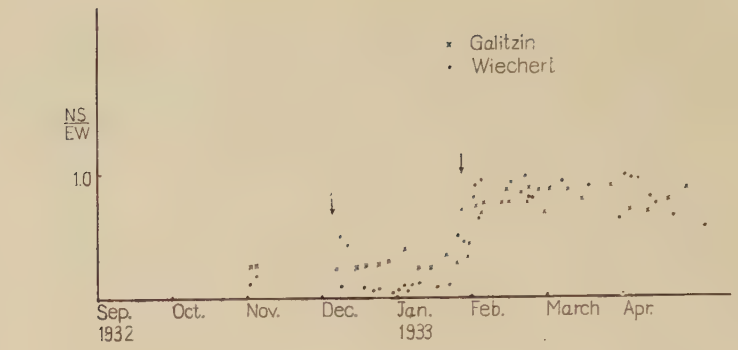

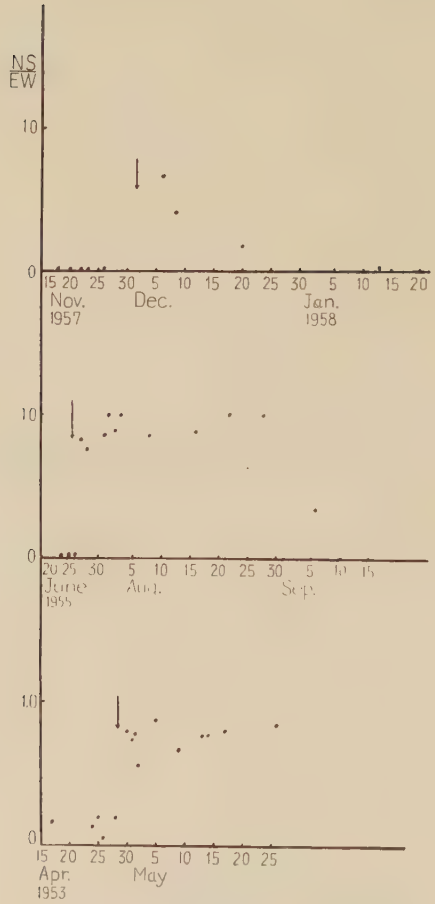

Fig. 6. Ratio of NS-component to EW-component of amplitude of micro-tremors of the second kind.

These results are shown in Fig. 5.

Namely, the second kind seems to be a kind of longitudinal wave from the fact that the direction of the horizontal component is that of the propagation. The vertical componont is the same order as the horizontal component or less than that, and then they may be a kind of Rayleigh type, but not the ordinary one. That is, the horizontal longitudinal vibrations virtually coincide in phase with the vertical, which are not in accord with the theory of ordinary Rayleigh waves. These results were obtained during the silent period when a series of eruptions of 1932~1933 drew to a close, and the amplitude was small, e.i. 1 μ and at the Volcanological Laboratory only the EW-component was recorded.

And also in the case of the eruption of Oct., 1932, they were about the same. These waves which occured towards the close of volcanic active period seem to be created from the magmatic reservoir of the considerable dimensions which is under the crater. We investigate the variations at eruption of the mode of vibration of the second kind of the period of ca. 3~4 sec., because the micro-tremors of the period larger than 5 sec. were not recorded. That is, the daily mean values of NS-component/EW-component of the second kind in Apr., 1953, July, 1955 and Dec., 1957 are read. The results are as follows.

The values increase from 0.2 to 0.8~0.9 at the volcanic eruptions.

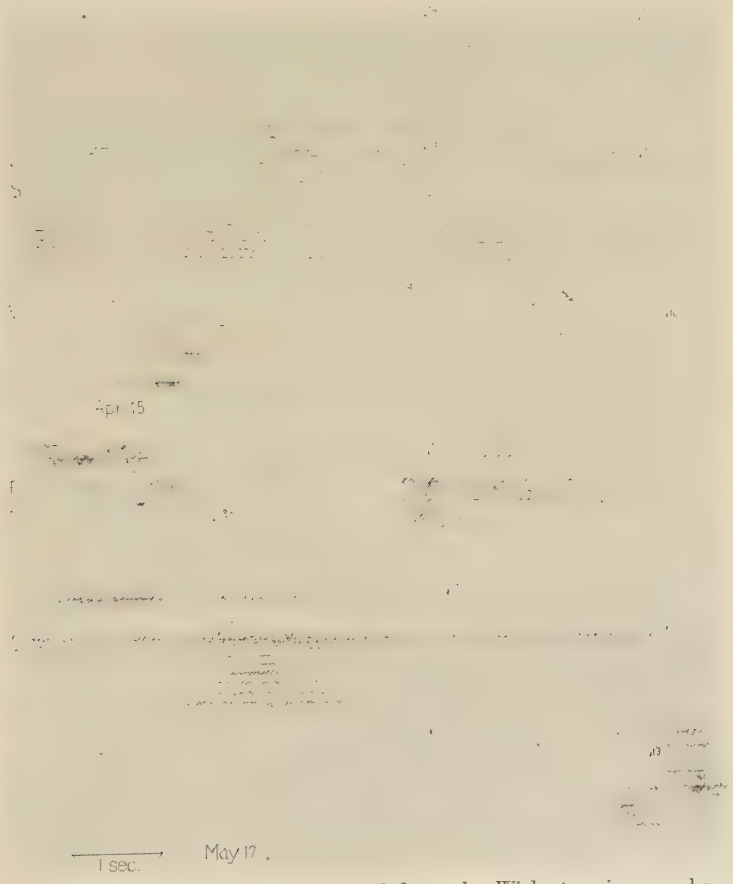

Fig. 7. Portions of records obtained from the Wicherts seismographs on Apr., 15, 1953 and May 17, 1953 at Vol. Lab.

Namely, the NS-component which do not occur yet before the eruption occurs after it. Also the mean values for the eruptions of 1933 are read, as shown in Fig. 6. As known in this figure it is evident that the same phenomena took place also in them. This fact suggests that a wave generates from the vibrational origin other than the magmatic reservoir, being accompanied with the vibration of it. Next, NS-component/V-component observed at the Volcanological Laboratory are plotted in Fig. 8. We obtain the result corresponding to the case of NS-component/EW-component. That is, while the vertical component of the same order as the EW-component both before and after the eruption, NS-component occur only after it.

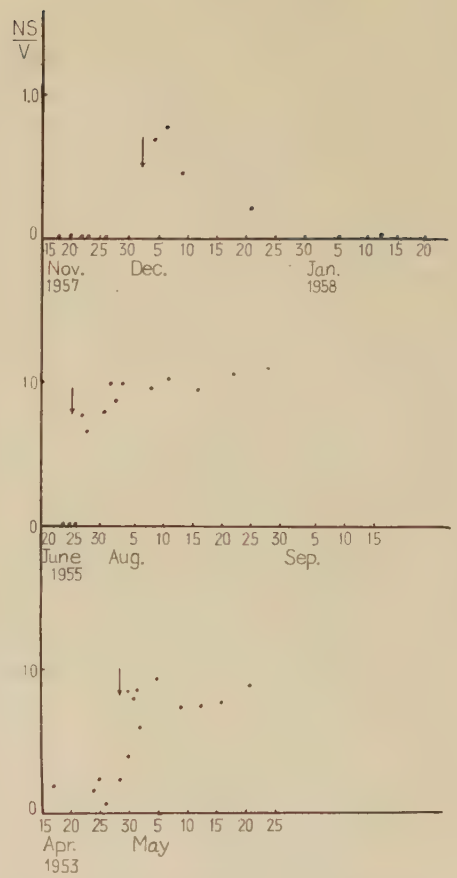

Fig. 8. Ratio of NS-component to V-component of amplitude of micro-tremors of the second kind.

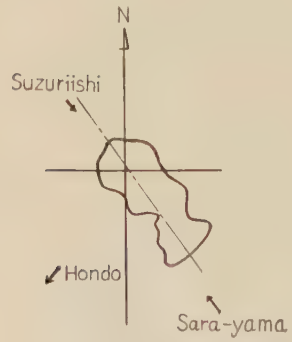

Fig. 9. Distribution of initial motions of eruption-earthquake of the First Crater in Aug. 1933 (after Sassa).

Previously, K. Sassa studied the mode of vibration near the crater of the small eruptive earthquake on July, 1933. The primary shocks are shown in Fig. 9.

It was indicated that the observed fact of the eruption earthquake could be fairly well explained by the vibration of crack parallel to the row of the present active craters.

After the considerable eruption, the ground will loosen near the reservoir and then the above vertical crack will become to be able to move perpendicular to the crack plane, being accompanied with the vibration of reservoir. Then the remarkable variations after the eruption of the mode of vibration of the second kind seem to be due to the waves generated from the above movements. In order that we examine if there occur the transversal component of the same order as that of the longitudinal component in the direction of the Volcanological Laboratory, we calculate the vibrational modes of the waves round the crater generated from the movements of crack of ca 1 km., which continues to the reservoir and is parallel to the row of craters.

8. The distributions of amplitude.

There lie the above crack of finite dimension, a certain depth under the surface, however, the complete treatment of such a problem would be so difficult to solve that we neglect the effect of the free surface and assume for simplicity that the length of the vertical direction is infinite, that is, the problem is reduced to two dimensional one. As we calculate the horizontal propagation of wave in the above problem, it seem to be valid. Using the elliptic coordinate, the wave equations are written as follows

$$\left.\begin{aligned} \rho\frac{\partial^2 \Delta}{\partial t^2} &= \frac{\lambda+2\mu}{c^2(\cosh^2\xi-\cos^2\eta)}\left(\frac{\partial^2\Delta}{\partial\xi^2}+\frac{\partial^2\Delta}{\partial\eta^2}\right) \\ \rho\frac{\partial^2\omega}{\partial t^2} &= \frac{\mu}{c^2(\cosh^2\xi-\cos^2\eta)}\left(\frac{\partial^2\omega}{\partial\xi^2}+\frac{\partial^2\omega}{\partial\eta^2}\right) \end{aligned}\right\} \quad \cdots\cdots\cdots\cdots (1)$$

$$x = c\cosh\xi\cdot\cos\eta$$

$$y = c\sinh\xi\cdot\sin\eta$$

$$\Delta = h_1^2\left\{\frac{\partial}{\partial\xi}\left(\frac{u}{h_1}\right)+\frac{\partial}{\partial\eta}\left(\frac{v}{h_1}\right)\right\}$$

$$2\omega = h_1^2\left\{\frac{\partial}{\partial\xi}\left(\frac{v}{h_1}\right)+\frac{\partial}{\partial\eta}\left(\frac{u}{h_1}\right)\right\}$$

$$\frac{1}{h_1^2} = c^2(\cosh^2\xi-\cos^2\eta),$$

where

u, v = components of displacement refered to curvilinear coordinates,

ρ = density of isotropic solid,

λ, μ = Lames elastic constants.

According to K. Sezawa,[6][7] the solutions of these equations are expressed as follows

$$\left.\begin{aligned} \Delta &= \sum_{n=0}^{\infty} B_n H_n(\xi, q) G_n(\eta, q) e^{ipt} \\ 2\omega &= \sum_{n=0}^{\infty} C_n H_n(\xi, q') G_n(\eta, q') e^{ipt}, \end{aligned}\right\} \quad \cdots\cdots(2)$$

where

$$q = \frac{h^2 c^2}{32}, \quad q' = \frac{k^2 c^2}{32}, \quad \frac{\rho p^2}{\lambda + 2\mu} = h^2, \quad \frac{\rho p^2}{\mu} = k^2.$$

$G_n(\eta, q)$, $G_n(\eta, q')$ are Mathiues functions and $H_n(\xi, q)$, $H_n(\xi, q')$ are the solutions of the following equations

$$\left.\begin{aligned} \frac{d^2 H_n(\xi, q)}{d\xi^2} + (h^2 c^2 \cosh^2 \xi - n^2) H_n(\xi, q) = 0 \\ \frac{d^2 H_n(\xi, q')}{d\xi^2} + (k^2 c^2 \cosh^2 \xi - n^2) H_n(\xi, q') = 0. \end{aligned}\right\} \quad \cdots\cdots(3)$$

u_1, v_1 the components of displacements of the dilational wave and v_2, v_2 those of the distortional wave are given by

$$\left.\begin{aligned} u_1 &= -\sum_{n=0}^{\infty} \frac{h_1 B_n}{h^2} \frac{\partial H_n}{\partial \xi}(\xi, q) G_n(\eta, q) e^{ipt} \\ v_1 &= -\sum_{n=1}^{\infty} \frac{h_1 B_n}{h^2} H_n(\xi, q) \frac{\partial G_n}{\partial \eta}(\eta, q) e^{ipt} \\ u_2 &= -\sum_{n=1}^{\infty} \frac{h_1 C_n}{k^2} H_n(\xi, q') \frac{\partial G_n}{\partial \eta}(\eta, q') e^{ipt} \\ v_2 &= -\sum_{n=1}^{\infty} \frac{h_1 C_n}{k^2} \frac{\partial H_n}{\partial \xi}(\xi, q') G_n(\eta, q') e^{ipt}. \end{aligned}\right\} \quad \cdots\cdots(4)$$

In this case, as the gas rich magma seem to press only vertically the surface of crack, the boundary conditions are given by

$$\left.\begin{aligned} \text{normal stress} &= \left\{ \lambda \Delta + 2\mu \left\{ h_1 \frac{\partial (u_1 + u_2)}{\partial \xi} + h_1^2 (v_1 + v_2) \frac{\partial (1/h_1)}{\partial \eta} \right\} \right\}_{\xi_0 = 0} = S e^{ipt} \\ \text{tangential stress} &= \mu \left\{ \frac{\partial h_1 (v_1 + v_2)}{\partial \xi} + \frac{\partial h_1 (u_1 + u_2)}{\partial \eta} \right\}_{\xi_0 = 0} = 0. \end{aligned}\right\} \quad \cdots(5)$$

When ξ approaches 0, asymptotic relations are known such as

$$H_n(\xi, q) \to 1 \qquad \frac{\partial H_n(\xi, q)}{\partial \xi} \to -i\sqrt{h^2 c^2 - n^2}$$

$$H_n(\xi, q') \to 1 \qquad \frac{\partial H_n(\xi, q')}{\partial \xi} \to -i\sqrt{k^2 c^2 - n^2}.$$

Taking the physical conditions into consideration, Mathieu function for the dilatational component is even with respect to η, while that for the distortional component is odd. Then, the boundary conditions (5) are reduced into the following expressions

$$S=\mu\Big[\sum_{n=1}^{\infty}B_nG_n(\eta,q)+\frac{1}{\sin^2\eta}\Big\{-\sum_{n=1}^{\infty}\alpha_nB_nG_n(\eta,q)+\sum_{n=1}^{\infty}i\beta_nC_n\frac{\partial G_n(\eta,q')}{\partial\eta}\Big\}$$
$$-\frac{\cos\eta}{\sin^3\eta}\Big\{\sum_{n=1}^{\infty}\gamma B_n\frac{\partial G_n(\eta,q)}{\partial\eta}+\sum_{n=1}^{\infty}i\beta_nC_nG_n(\eta,q')\Big\}\Big]$$
$$0=\mu\Big[-\frac{\alpha_0'B_0}{\sin^2\eta}\frac{\partial G_0(\eta,q)}{\partial\eta}-2\sum_{n=1}^{\infty}\frac{\alpha_n'B_n}{\sin^2\eta}\frac{\partial G_n(\eta,q)}{\partial\eta}+\sum_{n=0}^{\infty}\frac{\alpha_n'B_n\sin 2\eta}{\sin^4\eta}G_n(\eta,q)$$
$$-\sum_{n=1}^{\infty}\frac{i\beta_n'C_n}{\sin^2\eta}G_n(\eta,q')+\sum_{n=1}^{\infty}\Big\{-\frac{\gamma'C_n\sin 2\eta}{\sin^4\eta}\frac{\partial G_n(\eta,q')}{\partial\eta}+\frac{\gamma'C_n}{\sin^2\eta}\frac{\partial^2G_n(\eta,q')}{\partial\eta^2}\Big\}\Big] \quad \cdots\cdots(6)$$

where

$$\alpha_n=2\Big(\frac{n^2}{h^2c^2}-1\Big),\quad \beta_n=\frac{-2i\sqrt{h^2c^2-n^2}}{h^2c^2},\quad \gamma=\frac{2}{h^2c^2},$$
$$\alpha_n'=\frac{-i\sqrt{h^2c^2-n^2}}{h^2c^2},\quad \beta_n'=\frac{n^2-k^2c^2}{k^2c^2},\quad \gamma'=\frac{1}{k^2c^2}.$$

In order to solve the problem approximatelly, we use Mathieu functions of 0th to 6th orders, and neglect the higher terms in q. The Mathieu functions are given by

$$ce_0=1+4q\cos 2\eta,\qquad ce_1=\cos\eta+q\cos 3\eta,$$
$$ce_2=\cos 2\eta+q\Big(\frac{2}{3}\cos 4\eta-2\Big),\qquad ce_3=\cos 3\eta+q\Big(-\cos\eta+\frac{1}{2}\cos 5\eta\Big),$$
$$ce_4=\cos 4\eta+q\Big(-\frac{2}{3}\cos 2\eta+\frac{2}{5}\cos 6\eta\Big),$$
$$se_1=\sin\eta+q\sin 3\eta,\qquad se_2=\sin 2\eta+\frac{2}{3}q\sin 4\eta,$$
$$se_3=\sin 3\eta+q\Big(-\sin\eta+\frac{1}{2}\sin 5\eta\Big),\quad se_4=\sin 4\eta+q\Big(-\frac{2}{3}\sin 4\eta+\frac{2}{5}\sin 6\eta\Big). \quad \cdots\cdots(7)$$

Using these functions, the normal stress and the tangential stress at the crack plane are expressed by

$$S_0+\sum_{n=1}^{\infty}S_n\cos n\eta$$
$$=\mu\Big[S_{11}B_0+S_{12}B_2+S_{13}B_4+S_{14}C_2+S_{15}C_4+\cdots\cdots$$

$$+(S_{21}B_0+S_{22}B_2+S_{23}B_4+S_{24}C_2+S_{25}C_4+\cdots\cdots)\frac{1}{\sin^2\eta}$$
$$+(S_{31}B_0+S_{32}B_2+S_{33}B_4+S_{34}C_2+S_{35}C_4+\cdots\cdots)\cos 2\eta$$
$$+(S_{41}B_0+S_{42}B_2+S_{43}B_4+S_{44}C_2+S_{45}C_4+\cdots\cdots)\cos 4\eta$$
$$+\cdots\cdots\Big\} \quad \cdots\cdots(8)$$

$$\sum_{n=1}^{\infty} S_n' \sin n\eta$$
$$=\mu\Big\{(S_{11}'B_0+S_{12}'B_2+S_{13}'B_4+S_{14}'C_2+S_{15}'C_4+\cdots\cdots)\frac{\cos\eta}{\sin^3\eta}$$
$$+(S_{21}'B_0+S_{22}'B_2+S_{23}'B_4+S_{24}'C_2+S_{25}'C_4+\cdots\cdots)\sin 2\eta$$
$$+\cdots\cdots\Big\},$$

where

$$S_{11}=1+8q\alpha_0$$
$$S_{12}=-2q+2\alpha_2+\frac{8}{3}q\alpha_2-4\gamma-\frac{64}{3}q\gamma$$
$$S_{13}=\frac{16}{15}q\alpha_4+4\alpha_4-32\gamma-\frac{608}{15}q\gamma$$
$$S_{14}=-2\beta_2-\frac{16}{3}q'\beta_2$$
$$S_{15}=-8\beta_4-\frac{88}{15}q'\beta_4$$
$$S_{21}=-\alpha_0-4q\alpha_0$$
$$S_{22}=-\alpha_2+\frac{4}{3}q\alpha_2+4\gamma+\frac{32}{3}q\gamma$$
$$S_{23}=-\alpha_4+16\gamma+\frac{4}{15}q\alpha_4+\frac{176}{15}q\gamma$$
$$S_{24}=0$$
$$S_{25}=0$$
$$S_{31}=4q$$
$$S_{32}=1+\frac{8}{3}q\alpha_2-\frac{32}{3}q\gamma$$
$$S_{33}=-\frac{2}{3}q+4\alpha_4+\frac{16}{5}q\alpha_4-16\gamma-\frac{192}{5}q\gamma$$
$$S_{34}=-8q'\beta_2 \quad \cdots\cdots(9)$$
$$S_{35}=-12\beta_4-\frac{64}{5}q'\beta_4$$
$$S_{41}=0$$

$$
\left.\begin{aligned}
&S_{12}=\frac{2}{3}\,q\\
&S_{13}=1+\frac{8}{5}\,qa_4-\frac{48}{5}\,q\gamma\\
&S_{14}=0\\
&S_{15}=-8q'\beta_4\\
&S_{11}'=2a_0'+8qa_0'\\
&S_{12}'=2a_2'-\frac{8}{3}\,qa_2'\\
&S_{13}'=2a_4'-\frac{8}{15}\,qa_4'\\
&S_{14}'=-4\gamma'-\frac{16}{3}\,q'\gamma'\\
&S_{15}'=-8\gamma'-\frac{32}{15}\,q'\gamma'
\end{aligned}\right\}
$$

Now we consider the case that uniform pressure changes periodically with time, and the tangential stress is zero. Moreover, we may put for symmetry,

$$B_1\equiv B_3\equiv C_1\equiv C_3\equiv 0.$$

Then, we obtain the following simultanious equations

$$
\left.\begin{aligned}
&S_{11}B_0+S_{12}B_2+S_{13}B_4+S_{14}C_2+S_{15}C_4=S_0/\mu\\
&S_{21}B_0+S_{22}B_2+S_{23}B_4+S_{24}C_2+S_{25}C_4=0\\
&S_{31}B_0+S_{32}B_2+S_{33}B_4+S_{34}C_2+S_{35}C_4=0\\
&S_{41}B_0+S_{42}B_2+S_{43}B_4+S_{44}C_2+S_{45}C_4=0\\
&S_{11}'B_0+S_{12}'B_2+S_{13}'B_4+S_{14}'C_2+S_{15}'C_4=0.
\end{aligned}\right\}\quad\cdots\cdots\cdots\cdots(10)
$$

We obtain B_0, B_2, B_4, C_2, C_4 from these equations.

When ξ is large, the asymptotic expressions for $H_n(\xi, q)$, $H_n(\xi, q')$ are obtained in the following form.

$$
\left.\begin{aligned}
&H_n(\xi,q)\to\frac{e^{-ihc\sinh\xi}}{\sqrt{hc\sinh\xi}}\\
&H_n(\xi,q')\to\frac{e^{-ikc\sinh\xi}}{\sqrt{kc\sinh\xi}}.
\end{aligned}\right\}\quad\cdots\cdots\cdots\cdots(11)
$$

Thus, the radial component of the dilational wave u_1 and the tangential component of the distortional wave v_2 at a distant are given on insertion of (11) into (4) by

$$\frac{ta}{\lambda}$$

$$u_1 = -\sum_{n=0}^{\infty} \frac{B_n}{k^2 c\sqrt{\cosh^2\xi - \cos^2\eta}} \frac{\partial H_n(\xi, q)}{\partial \xi} ce_n(\eta, q) e^{ipt}$$

$$= -\sum_{n=0}^{\infty} \frac{1}{k^{3/2} R^{1/2}} \left\{ a_n ce_n(\eta, q)\sin(pt - kR) + b_n ce_n(\eta, q)\cos(pt - kR) \right\}$$

$$v_2 = -\sum_{n=1}^{\infty} \frac{C_n}{k^2 c\sqrt{\cosh^2\xi - \cos^2\eta}} \frac{\partial H_n(\xi, q')}{\partial \xi} se_n(\eta, q') e^{ipt}$$

$$= -\sum_{n=1}^{\infty} \frac{1}{k^{3/2} R^{1/2}} \left\{ c_n se_n(\eta, q')\sin(pt - kR) + d_n se_n(\eta, q')\cos(pt - kR) \right\}, \quad \cdots\cdots(12)$$

where

$$B_n = a_n + ib_n, \quad C_n = c_n + id_n$$

R = the distance from the origin.

Now we put

$$T = 4 \text{ sec.}$$

$$2c/v_s = 1.32,$$

where $2c$ = length of crack.

On results of calculations of a_n, b_n, c_n, d_n, we obtain

$$\left.\begin{array}{lll} a_0 = 0.02346, & a_2 = -0.01584, & a_4 = -0.001562, \\ b_0 = -0.09339, & b_2 = 0.08791, & b_4 = -0.0008799, \\ d_2 = 0.1214, & d_4 = 0.001355, & \\ c_2 = -0.1645, & c_4 = -0.001651. & \end{array}\right\} \quad \cdots\cdots(13)$$

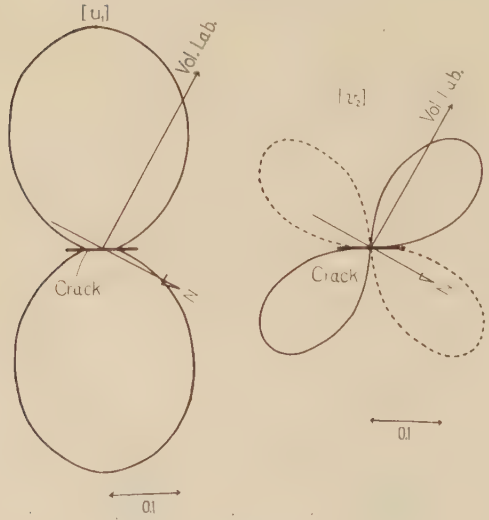

Fig. 10. Azimuthal distributions of displacements, u_1 and v_2, at a distant point.

The azimuthal distribution of u_1, v_2 in this case is shown in Fig. 10.

We thought previously that the gas riched magma in the reservoir which was infered to exist under the craters frequently exploded in the active period of the Volcano Aso and being accompanied with it, there occured the micro-tremors of the second kind, and then indicated that the dimensions of the reservoir

corresponding to the period of the second kind is the order of 1 km, on the assumption that the form of the reservoir is a sphere[4)5)]. As a result of the above investigation, we find that a transversal wave propagates simultaneously with a longitudinal wave during the short period after the considerable eruption. The above calculations indicate that when there exist the crack of the order of 1 km which connect with the reservoir and after the eruption it operates as the origin of waves with reservoir, the transversal wave of the same order as the longitudinal wave propagates in the direction of the Volcanological Laboratory. Therefore, it is infered from the appearance of the transversal component only during the short period after the eruption that there occur the rapid changes in the ground around the reservoir and in the distribution of the gas riched magma and that they restore to the state before the eruption with the decrease of the volcanic activity. As we did not observe at many points for the long period, we cannot bring the unambiguous conclusions, however, the above mechanism of the wave generation near the crater can explains the observed results.

The writer wishes to express his hearty thanks to Prof. K. Sassa for his instructions.

Reference

1) K. Sassa : Volcanic Micro-tremors and Eruption Earthquakes (I) ; Memoirs of the College of Science Kyoto Imperial University Series A, Vol. XVIII, 1935, 255～293.

2) K. Sassa : Micro-seismometric Study on Eruptions of the Volcano Aso (II) ; ibid. Vol. XIX, 1936, 11～56.

3) S. Yoshikawa : On the Micro-tremors of Short Period at the Volcano Aso ; Bull. Volc. Soc. Japan., Vol. III, 1959, 147～153.

4) M. Shima : On the Second Volcanic Micro-tremor at the Volcano Aso ; Disaster Prevention Institute Bull. No. 22, 1958.

5) M. Shima : On the Thermoelasticity in the Semi-infinite Elastic Solid ; ibid. No. 25.

6) K. Sezawa : Bull. Earth. Res. Inst. Vol. 5, 59, 1928.

7) W. Inoue : ibid. Vol. 15, 674～685, 1937.

Journal of Physics of the Earth, Vol. 8, No. 2, 1960

On Processes of Heat Transfer in the Earth's Mantle.

By

H. A. Lubimova

Institute for Earth's Physics, Academy of Science, USSR.

§ 1. Introduction

The accumulation of data of the physics of semi-conductors and dielectrics created new possibilities of studying the thermal regime and the thermal history of the earth. For instance the role of the radiative thermal conductivity was investigated (Clark 1956, Preston 1956) which in addition to the lattice thermal conductivity must lead to an intensive heat transfer in the deep interior of the earth.

The investigation of the pattern of the lattice part of the thermal conductivity led to a conclusion about the presence of the resultant thermal conductivity minimum at 50 to 100 km depths of the mantle. This is of a decisive importance for the study of the earth's thermal regime. The low thermal conductivity of the earth's upper layers hinders an intensive loss of heat and provides for the accumulation of heat and for heating of the deep interior of the earth but not its cooling. Due to the minimum of the thermal conductivity the temperature gradient has an increased value which is sufficient to explain the observed lowering of the velocities of seismic waves at these depths (Lubimova, H. A., 1958, 1959).

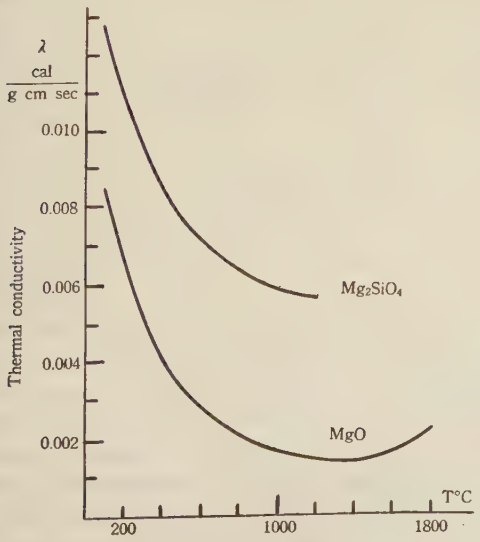

Fig. 1a

The new data about the properties of ionic semi-conductors and non-metallic materials in the range of high temperatures indicate the existence of one more process of energy transfer by the excited states of atoms or excitons. The possibility of the existence of exciton states in a given material is established by the absorption spectra of the material.

Compounds MgO and Mg_2SiO_4 are the main components of the typical earth rocks and meteorites. Kingery (1954) measured the thermal conductivity of these materials at high temperatures. Fig. 1a shows that at $T>$ 1000°C the thermal conductivity passes through its minimum and begins to grow with the increase of T. The deviation from the lattice thermal conductivity law $\frac{1}{T}$ or $\frac{1}{T^{5/4}}$ increases with the increase of temperature (Fig. 1b). Let us compare these data with the data concerning the absorption spectra of these materials.

The absorption spectrum of olivine was studied by Clark (1957), special attention being paid to the existence of the transparency interval providing for the radiative energy transfer. The presence of several absorption peaks in the transparency interval remained unexplained although a hypothesis about their possible exciton origin was assumed by Clark and Jamieson and Lawson (1958).

Reiling and Hensley (1958) found strong and weak absorption peaks in the spectrum MgO at $T=-170°$, $+25°$ and $+150°$ and ascribed them solely to excition state. Exciton peaks are found in the spectra of a number of other substances, such as KI, KBr, InSb, Cu_2O, PbI_2, TeBr, Ge and others (Haken, 1959).

In atomic semi-conductors these lines can be observed only at low temperatures when the background absorption is weakened, whereas in ionic crystals the exciton absorption is so strong that it can be observed even at high temperatures (MARTIENSSEN, 1959). CLARK's observations are made at room temperatures.

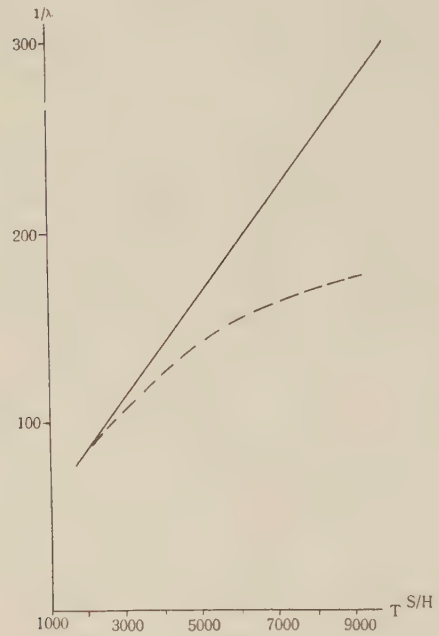

Fig. 1b

The distinguishing of exciton lines is facilitated by the fact that a definite type of excitons—non-localized excitons—gives lines narrow in their spectra with the frequencies satisfying a hydrogen-like law:

$$\nu_n = \nu_\infty - \frac{R_{ex}}{n^2} . \qquad (1)$$

We found that several narrow lines in the absorption spectrum of olivine can be identified with the exciton state of a definite quantum number $n=1, 2, 3$ assuming that $\nu_\infty = 29000\,\mathrm{cm}^{-1}$, $R_{ex}=25800\,\mathrm{cm}^{-1}$. These are lines with frequencies 3200, 22600, 25200, 29100 cm^{-1}. The condensation of lines occurs in the direction of the ultra-violet absorption, the interface frequency of the series coincided with the edge frequency of this band which is equal to 29100 cm^{-1}.

The value of the constant $R_{ex}=25800$ yields a correct value for the given mass of exciton

$$M_{ex}^* = \frac{R_{ex} n_0^4 m}{R} \sim 2\,m$$

where $R=1{,}097 \cdot 10^5\,\mathrm{cm}^{-1}$ is the RYDBERG's constant in wave numbers, $m=9.11 \cdot 10^{-28}$ g is the electron mass, and n_0 is the refractive index. The diameters of excitons can be calculated:

$$d_e = 2\frac{h^2}{M^* e^2} n_0^2 h^2 .$$

For instance for $n=2$ and 5, we obtain $d_2=6$Å and $d_5=150$Å.

These numbers do not contradict with the diameter values established for other semiconductors. The considerations mentioned above permit us to believe it plausible that in olivine exciton states exist with the energy of excitation:

$E_1=0{\cdot}4$ e.V., $E_2=2{\cdot}8$ e.V., $E_3=3{\cdot}12$ e.V.

There is a difficulty as Dr. CLARK said to me. It is difficult to fix exactly the interface frequency. As usual the data are scanty. One must make new experiments in this direction.

In the light of the above stated the energy $E=1.19$ has no relation to excitons as was erroneously assumed by JAMIESON and LAWSON (1958). It is associated with a wide absorption band at frequency $\nu=10{,}000\,\mathrm{cm}^{-1}$ which is due to the presence of Fe ions. All the excitons should make a contribution to the thermal conductivity, therefore

$$\lambda_{ex} = \lambda_1(E_1) + \lambda_2(E_2) + \lambda_3(E_3) + \cdots$$

where

$$\lambda_i = \frac{16\pi}{3}\left(\frac{K}{h}\right)^3 \mu^* T^2 l \exp\left[-\frac{Ei}{KT}\left\{\left(\frac{Ei}{KT}+2\right)^2+2\right\}\right],$$

$l=l_0/T$ being the length of the free path of excitons. In normal conditions practically only the first number λ_1 with the lowest excitation energy plays the main role. With the increase of temperature exciton peaks shift in the direction of longer waves and lower energies (MARTIENSSEN, 1959). Therefore at high temperatures the contribution from the subsequent terms must increase and

the role of the exciton thermal conductivity must increase. The rate of the peaks' movements with the increase of T in the direction of greater energies in MgO is -5.10^{-4}e.V./°K (Reiling and Hensley, 1958).

The contrary effect on the parameters of the radiative thermal conductivity $\lambda_r = 16\sigma n_0^2 T^3/3\varepsilon$ is caused by temperature. The absorption coefficient ε of the radiative energy depends on T and ν in a complicated way. At different frequencies different absorption mechanisms exist but they all lead to an increase of absorption with the increase of temperature and pressure and the dying away of the radiative heat transfer at great depth.

In the transparency interval of olivine $(0.3\sim 11)\mu$ the absorption is due to free carriers, excitons and split of the energy levels of the unfilled electron shells of iron Fe^{++}. The formula for ε can be written as

$$\varepsilon = \varepsilon_0 + \varepsilon_1 \frac{\exp\left(-\frac{E_g}{KT}\right)}{\nu^2} + \sum_i \varepsilon^i{}_2 \exp\left\{-a_i \frac{h(\nu_i - \nu)}{KT}\right\} + \varepsilon_3 \frac{\nu^3 max}{\Delta\nu} \quad (2)$$

where ε_0 is the absorption due to the scattering processes. E_g is the energy of the activation of the carriers, ν_i is the frequency of the i-th exciton absorption peak, ν_{max} is the frequency of the maximum absorption by ion Fe^{++}, $\Delta\nu$ is the width of the absorption band due to Fe^{++}.

Such complicated dependence of ε on ν and T is rather difficult to be used. For the sake of simplicity the Rossland averaging formula can be used, then the average value $\bar{\varepsilon}$ of the spectrum must be calculated for the given temperature T and the pressure P from the formula

$$\frac{1}{\varepsilon} = \frac{15}{4\pi^4} \int_0^\infty \frac{1}{\varepsilon_u} \frac{u^4 e^{-u}}{(1-e^{-u})^2} du$$

where $u = h\nu/KT$, h is the Planck's constant. Formula (2) for ε includes the value E_g the energy of the activation of the current carriers. The energy of the activation of the ionic electrical conductivity predominant in the upper layers of the earth is studied in a number of papers (see Review of Prof. Tozer, 1959). The dependence of the activation energy of the intrinsic electron conductivity predominant in the lower layers of the mantle on T and P can be written as

$$E_g = E^0{}_g + P\frac{\partial E_g}{\partial P} - \alpha KT\frac{\partial E_g}{\partial P} - \beta T \quad (3)$$

where α is the coefficient of the thermal expansion; K is the incompressibility, $E^0{}_g$ is the width of the energy gap at normal pressure and temperature. The second term allows for the effect of the pressure on the width of the zone. According to the data of Balchan, A.S., and Drickaneer, H.G., (1959), $\frac{\partial E_g}{\partial P} = -2.5 \cdot 10^{-6} \frac{\text{e. V.}}{\text{dyne cm}^2}$. The third term allows for the effect of temperature on E_g due to the thermal expansion of the crystal and the fourth term allows for the effect of the interaction of electrons with the thermal vibrations of atoms (phonons). Irrespective of the crystal structure the interaction of electrons with phonons always leads to contraction of the width of the energy gap and to an increase of the electron conductivity. The value of the coefficient β is $\beta = \beta_0/\rho^{2/3}(u)^2$ (u is the sound velocity). The results of the calculations of the valus E_g (P, T) and the distribution of the intrinsic electron conductivity $\sigma = \sigma_0 \exp(-E_g/KT)$ are given in Table I, our former results about the distribution of temperature in the earth having been used.

Table I

km	σ observed from geomagnetic variations	T	E_g	σ Theoretical
750	2.10^{-2}	2920	2.6	2.10^{-2}
1500	4.10^{-1}	3960	2.0	2.10^{-1}
2000	7.10^{-1}	4160	1.5	5.10^{-1}
2900	2.2	4300	0.6	2.1

We can see a satisfactory coincidence of the calculated values of σ for the lower part of the mantle with the data of the value σ according to McDonald (1957), obtained by means of geomagnetic variations. This indicates the plausibility of our initial assump-

tion about the predominant role of the intrinsic electron conductivity in the lower layers of the mantle and confirms also that our former temperature calculations are in agreement with geomagnetic data.

Applying the above mentioned considerations we calculated the absorption coefficient of olivine at $T=1500°K$ and obtained that $\bar{\varepsilon}=500\,cm^{-1}$. The curve of the thermal conductivity of olivine against temperature can be best explained if it is assumed that besides lattice (phonon) thermal conductivity the radiative transfer and exciton thermal conductivity are present, the absorption coefficient varying from $\bar{\varepsilon}=20\,cm^{-1}$ at room temperatures to $\bar{\varepsilon}=500\,cm^{-1}$ at $T=1500°K$ and the length of the free path of excitons being $l=10^{-6}$ cm at $T=300°K$ as it is the case for a number of other semi-conductors (DEVYATKOVA 1957).

The theory of the lattice (phonon) part of the thermal conductivity of dielectrics in the range of high temperatures was dealt with in a number of papers. Most of them are based on the allowance for the anharmonicity of the thermal vibrations of the crystal lattice. The ultimate formulas differ somewhat from one another but it can be shown (LAWSON 1957) that they are equivalent and are reduced to the unique expression:

$$\lambda_{ph}=\lambda_0/3\gamma^2 TX^{3/2}\rho^{1/2} \qquad (4)$$

where X is the compressibility, γ is the GRÜNEISEN coefficient. Special place is occupied by the formula of POMERANCHUK (1943) who besides the anharmonicity took into account the dispersion of the thermal vibrations of the lattice. It cannot be reduced to expression (4) and is written as follows:

$$\lambda_{ph}=\lambda_0\rho^{2/3}\frac{u^3u^{1/2}}{T^{5/4}}\,. \qquad (5)$$

Since the temperature of the matter of the earth's mantle is very high, close to the temperature of melting T_m, we can use the relations existing at such temperatures, such as LINDEMANN relation. Inserting the compressibility value from the LINDEMANN relation instead of X into (4) we obtain the following relation between λph and T_m (KEYES, R.W., 1959).

$$\lambda phT=B_0T_m^{3/2}\rho^{2/3}A^{7/6} \qquad (6)$$

where $B_0=R^{3/2}/3\gamma^2\mathcal{E}^2N_0^{1/3}$

is the average atomic weight, $\mathcal{E}$ is the amplitude of the thermal vibrations at melting point, N_0 is the AVOGADRO number. The value B_0 can be considered constant to a rough approximation. The validity of this relation is tested by KEYES for more than thirty dielectric crystals. A similar transformation can be made with the POMERANCHUK formula and we can obtain:

$$\lambda phT^{5/4}=B_1\rho^{2/3}T_m^2/A^2\,. \qquad (7)$$

Inserting the values typical for the mantle of the earth into formula (6) we shall find that the values of T_m in the mantle will be less than those estimated by R.I. UFFEN (1952) and JHARKOV (1959) and given by MCDONALD (1959). A better approximation is obtained if relation (7) is used which is derived from the POMERANCHUK formula (5), and increase the average atomic weight of the material in the lower part of the mantle believing it to consist of the orthosilicates of iron.

We must not overestimate the accuracy of these semi-empirical relations. But since our knowledge about the behaviour of the material in the deep interior of the earth is very scanty it is sometimes very important to establish that various values do not contradict with one another. An example of it is the above consideration as well as the comparison of the electrical-conductivity pattern with the distribution of temperature.

A comparative distribution of the three components of the thermal conductivity in the earth's mantle is represented in Fig. 2. The temperature distribution for the present moment was taken from our paper (1958) for the calculation of the curves. We see that the minimum of the thermal conductivity in the upper layers of the mantle becomes sharper than it was earlier without the allowance for the exciton component. The thermal conductivity at the base of the mantle exceeds its value at the suface by almost two orders. However this does not practically change the inferences about the process of the thermal history of the earth made earlier without taking

into account the exciton component on the assumption that the absorption coefficient of the radiative energy $\varepsilon = 10\,\mathrm{cm}^{-1}$.

Let us consider now the case of the infinitely great thermal conductivity in the layer of the mantle lying below the level of the minimum thermal conductivity. Our former calculations as well as the calculations made by McDonald (1959) showed that at the depth of 100 to 700km the temperature was close to T_m and in this region conditions seem to have been favourable for convection. The moment of the appearance of such a layer refers to the time of $2 \cdot 10^9$ years ago. Together with Van Zin Di we calculated the temperature distribution and the heat flow which could have existed in such an extreme case where the thermal conductivity is infinitely great in the indicated layer. The calculations were made by Lykyanov's hydrointegrator by the method described in our paper (1958). The infinitely great thermal conductivity was reached by a complete removing of the corresponding hydraulic resistances. Figs. 3 and 4 respresent the results of the calculations of the heat flow and temperature distributions for different moments of time. We can see that the earth began cooling 1.5×10^9 years ago. However the heat flow at this period exceeds its modern observed value by 5 to 8 times. This indicates the unreality of the initial assumption about the existence of an intensive transfer of heat by convection in the mantle up till now and shows that such convection embracing a continuous belt in the earth must have stopped by the present time. With the end of such convection the earth's interior must have begun heating anew. This calculation can be believed as an ultimate proof of the absence of convection with the global scale in the earth's

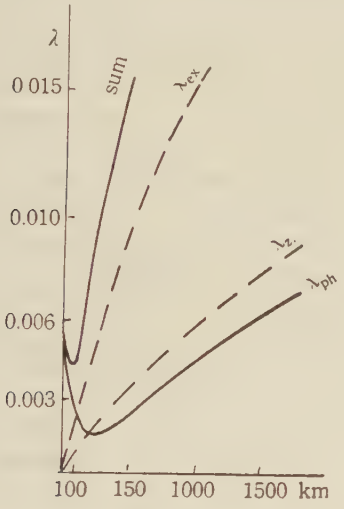

Fig. 2

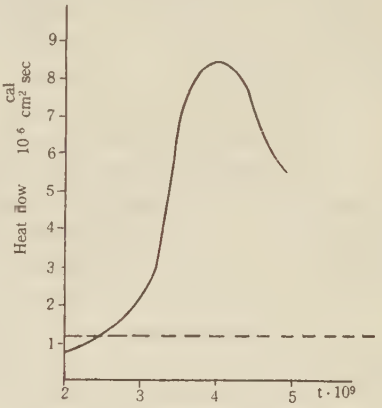

Fig. 3

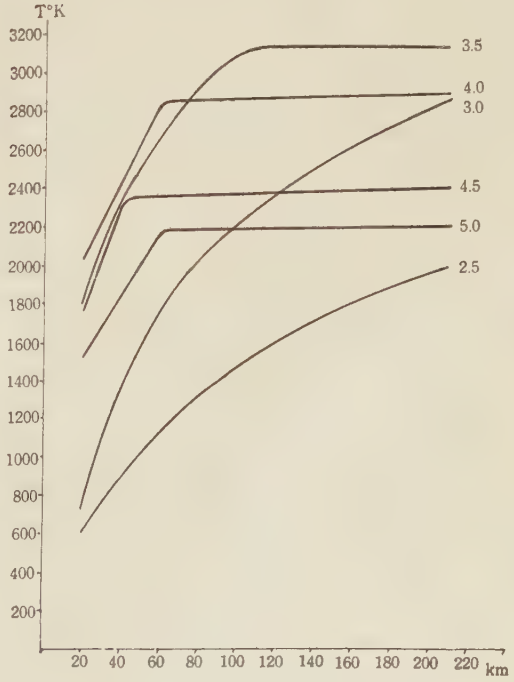

Fig. 4

interior. The convection could have occurred slower. It is essential that in this case according to our calculations a less intensive convection cannot have led the globe to the state of great cooling.

We cannot deny a convective transfer of heat in the earth's mantle. It was rather of a local character in the form of carrying out of heat when the sialic material was transferred from the mantle to the surface in the process of the crust formation. In this case the heat flow could have passed through its maximum several times in local areas of the earth (LUBIMOVA, 1960).

Acknowledgments

It is a pleasure to thank Prof. R.J. UFFEN, J.A. JACOBS, SYDNEY P. CLARK, D.C. TOZER for helpful discussions of this manuscript at the XII General Assembly of IUGG in Helsinki.

References

BALCHAN, A. S., and DRICKANEER, H. C.:
1959 Effect of pressure on the spectra of Olivine and Garnet. J. App. Phys. **30**, 9.

CLARK, S. P.:
1956 Effect of radiative transfer on temperatures in the earth. Bull. Geol. Soc. Am., **67**, 1123.
1957 Absorption spectra of some silicates in the visible and near infrared. Am., Mineral, **42**.

DEVYATKOVA, E. D :
1957 J. T. F., **27**, No. 3.

HAKEN H.:
1958 Die theorie des Exzitonts in festen Körper, Fortschritte der Physik, **6**, 271–334.

JAMIESON, I. C., and LAWSON, B. W.:
1958 Heat transfer in the earth. J. Geol. **66**, No. 5.

JHARKOV, V. N.:
1959 Melting points of the earth and iron at high pressures. Izvestiya AN SSSR, ser. geophys., No. 1.

KEYES, R. W.:
1959 High temperature thermal conductivity of insulating crystals: Relationship to the melting point. Phys. Rev., **115**, No. 3, 564.

KINGERY:
1954 The variation of conductivity with temperature for some silicates. J. Am. Cer. Soc., **37**, No. 2.

LAWSON A. W.:
1957 On the high temperature heat conductivity of insulators. J. Phys. Chem. Soc., **3**, No. 1/2.

LUBIMOVA, H. A.:
1958 Thermal history of the earth with consideration of the variable thermal conductivity. Geoph. J. Roy. Astr. Soc., No. 1, 2.
1959 On temperature gradients in earth's upper layers and possibility of explanation of low velocities. Izvestiya AN SSSR, ser. geophys. No. 12.
1960 On conditions of magmatism origin and the role of volcanic activity in the thermal regime of earth's crust. Bull. Volcanologique (in press).

MARTIENSSEN, W.:
1959 The optical absorption edge in ionic crystals. J. Phys. Chem. Soc., **8**, 264.

McDONALD, G. I.:
1959 Calculations on the thermal history of the earth. J. Geoph. Res. **64**, No. 11.

McDONALD, K. L.:
1957 Penetration of the geomagnetic secular field through a mantle with variable conductivity. J. Geophys. Res. **62**, No. 1.

POMERANCHUK, J.:
1943 Heat conductivity of dielectrics at high temperatures. J. Phys. USSR, **7**, 5.

PRESTON, F. W.:
1956 Thermal conductivity in the depth of the earth. Am. J. Sci., **254**, 754.

REILING, G. H., and HENSLEY, E. B.
1958 Fundamental optical absorption in magnesium oxide. Phys. Rev., **112**, No. **4**, 1106.

TOZER, D. C.:
1959 The electrical properties of the earth's interior. Physics and Chemistry of the Earth, **3**, Pergamon Press L.N.L.

UFFEN, R. Y.:
1952 A method of estimating the melting point gradient in the earth's mantle. Trans. Am. Geophys. Un., **33**, No. 6.

JOURNAL OF PHYSICS OF THE EARTH, VOL. 8, No. 2, 1960

On Conditions of Magmatism Origin and Role of Volcanic Activity in the Thermal Regime of Earth's Crust.

By

H. A. LUBIMOVA

Institute of Earth's Physics, Academy of Science, USSR

The origin of magmatism is closely connected with the general development of the earth, particularly with its thermal history. At present a number of papers (LUBIMOVA H. A., 1952–1958, JACOBS and ALLAN 1954–1956, MCDONALD 1959) dealing with several variants of the earth's thermal history in detail are available. Despite some differences as to the initial assumptions these papers lead to a general conclusion about the secular accumulation of the radiogenic heat inside the earth and the slow heating of its interior. The formation of the earth by means of the accumulation of interplanetary particles is now considered as the most probable initial state of the earth. In this case as it was first shown in papers of O. Y. SCHMIDT and his followers (1955–1958) the heating of the planet in the process of its formation could not cause its entire melting.

The use of data of physics of solids casts new light on the thermal state of the earth and permits in particular to study the thermal conductivity distribution in the earth's mantle. It was established that in the upper mantle (50 to 100km) the thermal conductivity decreases to its minimum and at great depths it rapidly increases with the increase of temperature (LUBIMOVA 1958). This minimum of the thermal conductivity hindered the intensive loss of heat through the surface. Our calculations showed that the conditions for the cooling of the whole earth and for the contraction of the earth did not exist.

The greatest temperature gradient was in the upper mantle approximately up to 100 km deep. This caused the temperature at the depth from 50–200 to 500–700 km to amount to the temperature of melting at 2 to 3 billion years after the formation of the earth (Fig. 1). In the upper part of the earth's mantle a belt was formed within which the conditions were favourable for magmatism to originate and the matter started differentiation (LUBIMOVA 1956, 1958). The age of magmatism should be counted off since that moment. Before $3 \cdot 10^9$ years ago magmatism did not exist.

Approximately at the same time inner parts of the earth's core at the boundary of which the transformations into the metallic state takes place must have melted. The recent computations of MCDONALD (1959) made by an electronic computer confirm in the main these conclusions.

The melting belt was not continuous. Within the accuracy of the available data we can speak about the approximation of the temperature curve to the melting curve. The excess over the melting temperature is small. Moreover taking the heat losses due to the latent heat into consideration we can speak only about the local melting pockets in points with sharply weakened pressure, for instance along the line of deep breakings. The local decrease of the melting temperature caused by the weakening of pressure facilitates the formation of magmatic pockets (UFFEN, 1959).

Many geophysical facts can be interpreted in terms of such belt that will be called the "differentiation belt." For instance it is known that the deep earthquakes are not observed at depths greater than 600 to 700 km. Below this depth a zone of relative stability begins. The lower boundary of our "differentiation belt" is just at this depth. The magmatic foci of the volcanoes can be considered as the remains of melting that have lasted up till now as separate cases. Actually according to the seismic determinations of G. S. GORSHKOV (1956), the hearth of Klyuchev-

sky volcano lies under the earth's curst in the upper mantle of the earth, which coincides with the location of the upper boundary of the "differentiation belt." At last at depths of 600 to 900 km the so-called C-layer with high seismic velocities and a sharp jump of electrical conductivity is known to exit and at the depth of about 150 km a layer with low velocity of seismic waves, the so-called low-velocity layer, is observed. These facts may also be explained as the traces of once existed molten layer that underwent the differentiation which resulted in the lifting of more acid rocks to the top and the lowering of the material more rich in iron to its base. The re-distribution of the radioactive elements caused an increase of temperature gradient in the so-called low velocity layer and a decrease of it at the base of the "differentiation belt" which coincides with the location of the C-layer. Calculations show that the gradients are just such which are necessary for the observed change of the velocities of seismic waves (LUBIMOVA, 1959). Thus we can explain the physical nature of the low velocity and C-layers from a new point of view.

In accordance with the discussed theory the volcanic and intrusive activities were the main processes due to which easily fused and volatile fractions were brought to the earth's surface.

Our considerations of the thermal evolution of the earth leads to a conclusion that the volcanic and tectonic activities as well as the process of the formation of the earth's crust in general must be due to deep activity extending to the upper layers of the mantle, i. e. the "differentiation belt" mentioned above.

Temperature distribution with account of the variation of thermal conductivity.

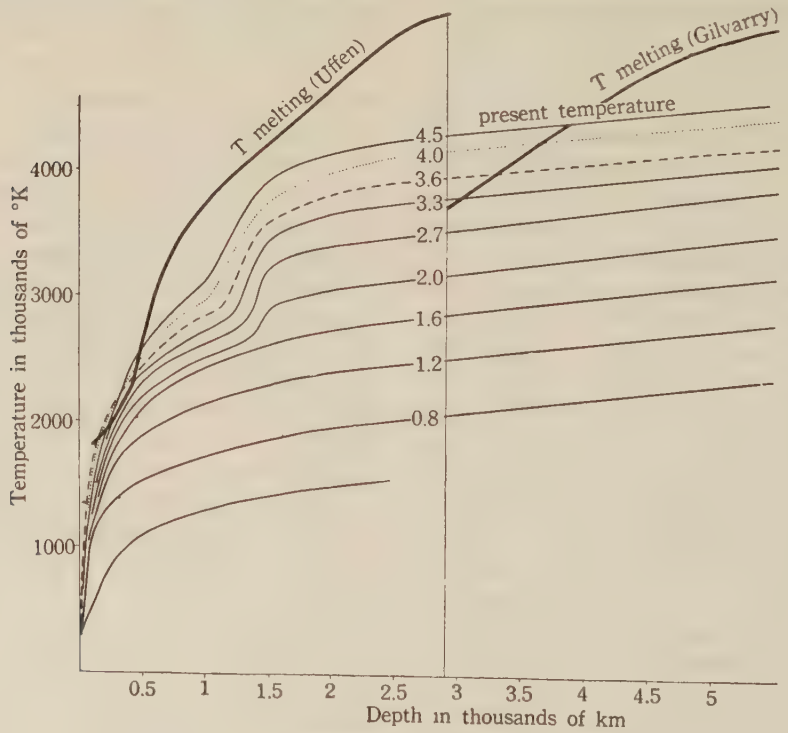

Fig. 1. The distribution of temperature with depth for different time, since the moment of the origin of the earth.

An independent consideration of the chemical evolution of the earth recently made by Academician VINOGRADOV (1959) draws to the same conclusion. VINOGRADOV conducted an interesting comparison of the content of H_2O,

CO_2(C), F, Cl and other gases in the atmosphere and ocean with their content in the material of the earth's mantle of dunite of meteorite structure. He showed that only the matter of the mantle could provide for the appearance of all the amount of volatile substances to the surface of the earth. He gave many convincing facts that the source of these steams and gases must be a persistent volcanic or intrusive activity. Vinogradov calculated that layers to the depth of 800 to 900 km must take part in the formation of volatile substance. The experiments of the zone of melting of the chondrite "Saratov" showed that the result of the melting of the meteorite matter would be the formation of basaltic lava on one hand and of dunite on the other. It can be expected that as a result of such melting the maximum quantity of the molten light fraction would be about 6 per cent. This well accounts for the fact that the earth's crust is rather thin and it is only 1 per cent of the total thickness of the mantle and that the matter of the mantle must transform into the matter of dunite type in the process of the evolution of the earth.

Since the moment of the origin of magmatism the volcanic activity and the thermal regime of the upper layers of the earth must have been closely connected with each other. The theory of geotectonic history given by Prof. V. V. Beloussov (1960) emphasizes the significance of the carrying of heat from the interior of the earth in the process of the easily melting fraction to the surface.

Earlier we considered the influence of the transfer of heat sources into the earth's crust on temperature assuming that this transfer occurred $3 \cdot 10^9$ years ago (the age of the earth's crust) practically instantaneously. This case is suitable for the description of the regime of ancient crustal regions whose formation ended long ago. These are ancient shields, possibly platforms. For this case the distribution of temperature is shown by solid lines in

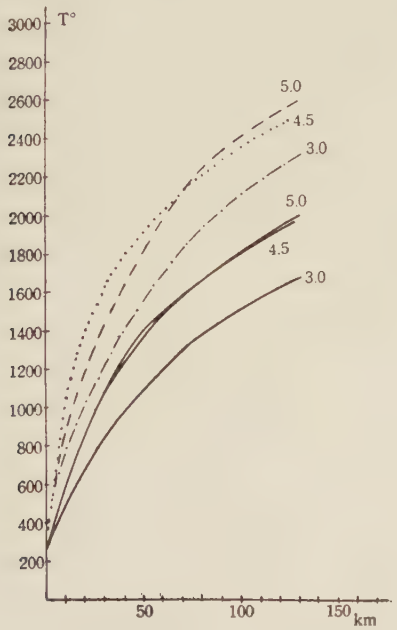

Fig. 2. The distribution of temperature in the upper layers of the earth for the continental type of the crust for the case of quick differentiation of the matter ended $3 \cdot 10^9$ years ago (solid curves) and for the case of continuous differentiation (dotted curves) for the moment of time ($t = 3 \cdot 0$; $4 \cdot 5$; $5 \cdot 10^9$ years from the beginning of the existence of the earth.

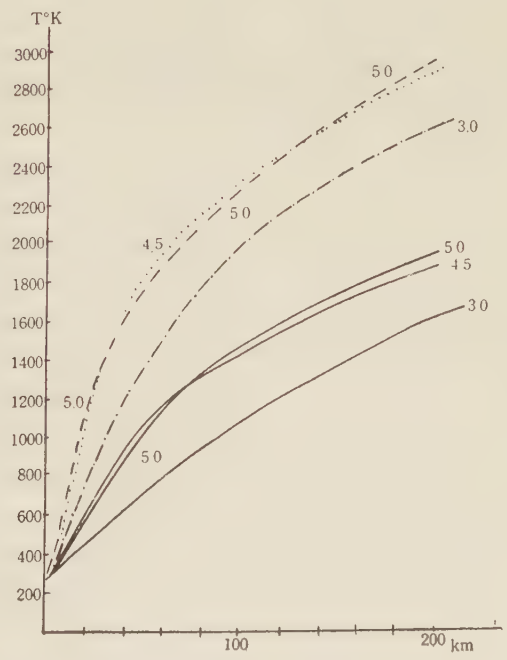

Fig. 3. Same as Fig. 2 for the oceanic type of the crust.

Fig. 2 for the case of the continental crust and in Fig. 3 for the case of the 10 km oceanic crust.

Another extreme case would be that the increase of the concentration of sources in the earth's crust occurred during the last $3 \cdot 10^9$ years uniterruptedly by equal rate. In the case the generation of heat in granitic and basaltic layers of the earth increased with time, as is shown in Fig. 4. The heat generation in the mantle respectively decreased. This case was theoretically discussed by the author (LUBIMOVA 1959). Numerical calculations were performed by means of hydrointegrator together with VAN

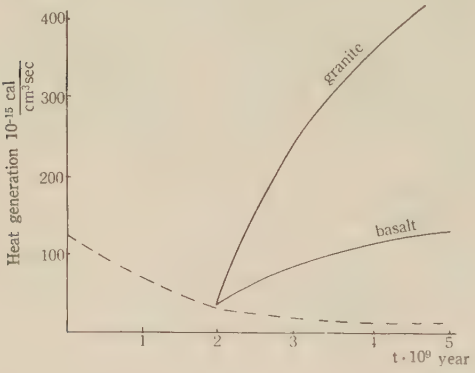

Fig. 4. Heat generation in the granitic and basaltic layers in the case of continuous carriage of the heat sources into the earth's crust during the last $3 \cdot 10^9$ years.

ZIN DI in 1959. The continuous differentiation of the matter of the earth's mantle was discussed also by LEVIN and MAEVA (1960). However they did not take into account that the transfer of heat to the surface part was carried out also by the masses of the matter heated inside the mantle. They considered the earth's crust to be homogeneous as to its structure and its thermal conductivity equal to that of dunite and did not take into account the exciton component of the thermal conductivity. All these factors being taken into account we obtained temperature curves denoted by dashed lines in Figs. 2 and 3 for the case of continuous defferentiation. The amount of heat Q carried out by the matter that formed the earth's crust is estimated by us on the assumption that all the matter of the crust is tranferred from the depths where the temperature was by $\Delta T = 1000 \sim 3000$°C greater than in the crust. Then $Q = V_k \rho_k C_k \Delta T$ where V_k is the volume of the crust and ρ_k and C_k are density and heat capacity of crustal rocks. For the period of time Δt this makes a contribution $\Delta q = Q/s\Delta t$ to the surface heat flow where s is the area of the earth's surface. Thus for the 30 km thick crust at $\Delta t = 3 \cdot 10^9$ years and $\Delta T = 1000$°C or 3000°C, the heat flow $\Delta q = 0.11$ or 0.4×10^{-6} cal/cm² sec should be added to the heat flow due only to the heat generation in the crust. This gives the value of the total heat flow $(1.8 \sim 2.1) \cdot 10^{-6}$ cal/cm² sec for the present time.

The temperature decrease δT in the mantle from where the material is carried must be $\delta T = \left(\frac{V_k}{V}\right) \Delta T$ where V is the volume of the mantle. This gives $\delta T = 150$ to 300°C if we assume that the material is carried uniformly from all the depths up to 1000 km. This case is represented in Figs. 2 and 3 for the continental and oceanic crust. In reality the degree of the differentiation was not uniform at all the depths. In lower layers it should have been less active than in the upper ones. If we assume that the maximum carriage of the

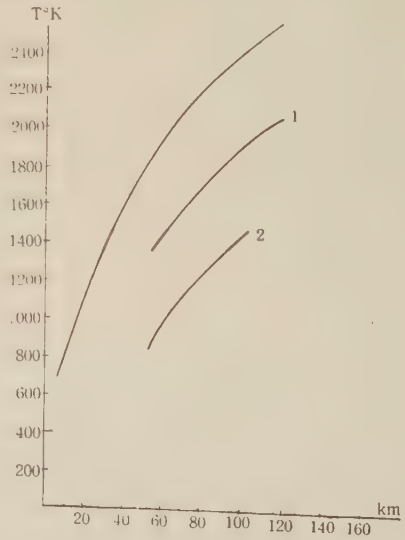

Fig. 5. The decrease of temperature in the upper layers of the mantle in the process of the carriage of heat sources from the depths up to 200 km (curve 1) and up to 100 km (curve 2).

material was from the upper 100 to 200 km the total temperature decrease for the time interval in question would be already a considerable value i. e. $\delta T=1000°$ to 500°C respectively. In Fig. 5 curves designate those temperatures which would be observed in this case.

We can see that in the upper layers of the earth a tendency of cooling exists while in the deep interior, below the level of 1000 km, continuous heating is under way.

Geological data imply (Beloussov, 1960) that the formation of the earth's crust was not uniform in space and time.

At one and the same moment of time different areas of the earth's crust were at different stages of the development. Therefore the discussed example of the gradual lifting of the materials to the upper layers of the earth that occurred uniformly during the last 3 billion years cannot be considered typical and characteristic for the earth's crust on the whole. It is true in some particular case.

In reality the geological periods connected with the lifting of the material from the mantle corresponded to some intervals of time $<3\cdot10^9$ years alternating with the states of relative rest.

If the process of the material lifting is concentrated for instance say at the interval of $\Delta t=1\cdot10^8$ years then $\Delta q=(4\sim10)\cdot10^{-6}$, if $\Delta T=$ 1000 to 3000°. This can explain the anomalously great value of the heat flow observed on young sea ridges in the Atlantic ocean. If there were 2 or 3 such periods Δt of the material carriage then Δq must have been equal to $(2\sim5)\cdot10^{-6}$ or $(1\sim3)\cdot10^{-6}$ each time. Then the heat flow must have amounted to its maximum several times during the history of the earth.

This case seems to be the most probable and typical. The position of the flow maximum in time depends on the concrete history of a given geological region. In different areas of the earth's crust the maximum of the heat flow could have been reached at different times. In the light of all that was said above it now seems more reasonable to put the problem on to the thermal regime of local areas of the earth's crust instead of the regime of the crust as a whole. This regime is different in different areas. Such consideration will depend completely on the geological history of the region, its past and present volcanic activity.

References

Beloussov, V. V.:

1960 The evolution of the globe and tectogenesis. Soviet Geology **6**.

Gorshkov, G. S.:

1958 On some theoretical problems of volcanology. Bull. Volcanologique, Ser. II, 19.

Jacobs, J. A. and Allan, W.:

1954 Temperature and heat flow within the earth. Trans. Roy. Soc. Canada, **48**, Ser. III.

Lubimova, H. A.:

1952 On the influence of radioactive decay upon the thermal regime of the earth. Bull. Acad. Sci. URSS. Geophys. Ser. 2.

1956 On the influence of radioactive element redistribution upon the thermal history of the earth. Bull. Acad. Sci. URSS, Geophys. Ser. 10.

1958 Thermal history of the earth with consideration of the variable thermal conductivity of its mantle. Geophy. Journ. R. A. S., **1**, 2.

1959 On temperature gradient in the upper layers of the earth.

MacDonald, G.:

1959 Calculations of the thermal history of the earth. J. Geophy. Res., **64**, N11.

Schmidt, O. Y.:

1957 Four lectures on the theory of the origin of the earth. 3rd. ed. Moscow, Acad. Sci.

Uffen, R. J.:

1959 On the origin of rock magma. J. Geophy. Res., **64**, N1.

Vinogradov, A. P.:

1959 The chemical evolution of the earth. Ac. Sci. USSR, Moscow.

DISASTER PREVENTION RESEARCH INSTITUTE
KYOTO UNIVERSITY
BULLETINS

Bulletin No. 36 August, 1960

On the Deformation and Fracture of Granite under High Confining Pressure

By

Shogo MATSUSHIMA

Geophysical Institute, Faculty of Science, Kyoto University, Kyoto

On the Deformation and Fracture of Granite under High Confining Pressure

By

Shogo MATSUSHIMA

Geophysical Institute, Faculty of Science, Kyoto University, Kyoto.

(Communicated by Prof. K. Sassa)

Abstract

The stress-strain relations for granite under various high confining pressures were observed experimentally. Mean Young's modulus is numerically constant independent of increasing pressure. The volume increase in the fracture range, observed characteristically at an atmospheric pressure, decays with pressure. The empirical formula of pressure-strength relationship is given by

$$P^* = P_0^*(kP_H+1)^{1/2}.$$

It seems that the phenomena above mentioned have the close connection with compressibility (i.e. porosity). The pressure-strength relation was calculated with use of Griffith's crack (pore) theory, putting the reasonable (or convenient) assumptions into calculation. This calculated relation, deduced from the empirical equation of compressibility with pressure, gives the same formula as above mentioned empirical one.

1. In recent years, a large number of experimental results on the deformation and fracture of rocks have been reported, but most of them were carried out for carbonate rocks such as marble and limestone (Griggs, et al., 1951, Turner, et al., 1954, Robertson, 1955, Paterson, 1958). These rocks exhibit the rheological properties the same as igneous rocks at an atmospheric pressure and room temperature. Under high pressure, however, these rocks flow plastically showing the distinct yielding zone, while the igneous rocks have scarcely the sign of plastic deformation up to the considerablly high pressure, at room temperature. The mechanism of the deformation and fracture of igneous rocks is much complicated as is observed about brittle substances in general. As the igneous rocks, however, have

the close connection with the rheological behavior in the deeper part of the crust, it must be made throughly clear how these rocks deform and fracture under high pressure.

In the previous paper, the experimental results of the deformation and fracture for granite under an atmospheric pressure have been reported (Matsushima, 1960). Here, we report the experimental results under high confining pressure, then express a brief consideration upon the mechanism of the fracture phenomena.

Of course, in order to obtain the definite knowledges on the earth's interior, we must take into consideration the physical and the chemical states of the earth's interior such as temperature, its gradient and time-fluctuation, heat-flow and -generation, states of the internal stresses and their dependence on time, and the constituent substances. But we shall neglect all these effects and confine ourselves into the studies of deformation and fracture of granite.

2. The apparatus used for this experiment is the conventional triaxial testing cylinder as shown in Fig. 1. The shape and the size of specimen give the considerable affection upon the aspect of deformation and the strenghth. Especially as to the crystalline aggregate constructed with a large size of grains, such as granite, these effects may be strikingly large. Then the capacity of pressure vessel was taken as large as possible to be able to contain the large size of specimen. Therefore, the durability against pressure of this vessel was sacrificed inevitably. This vessel can endure up to 5,000 atm., and axial stress can be produced by the 300 ton press. All the specimens were enclosed to prevent the confining liquid penetrating into the specimens. Synthetic adhesive rubber was used as covering material, for its good insulating character and flexibility. The strain was measured by the strain gauges of electric resistance type, same as in the previous

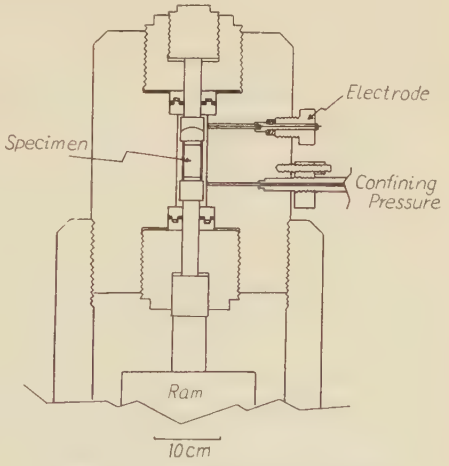

Fig. 1. Triaxial Testing Cylinder.

experiments. Accuracy of the measurement was within 50 atm. as to the confining pressure, 100 kg/cm^2 as to the axial compressional stress and 10^{-5} as to the strain.

3. The relations between the axial compressional stress and the strain under various confining pressures are shown in Fig. 2. The strains were measured in the axial direction and along the circular arc of the cylindrical specimen. The long columns of Kitashirakawa biotite granite, 30 mm. in diameter and 60 mm. long were used up to 1800 atm. confining pressure, 25 mm. in diameter 50 mm. long up to 3800 atm., and 20 mm. in diameter 50 mm. long above 3800 atm.. The slender specimen has a tendency to bend, and the stumpy one may deform into barrel shape. In these experiments, it was scarecely observed that the specimens deform in barrel shape within the elastic range. Near the rupture point, however, the plastic flow was observed, though it was not considerable, and a slight barrel shape deformation was recognized.

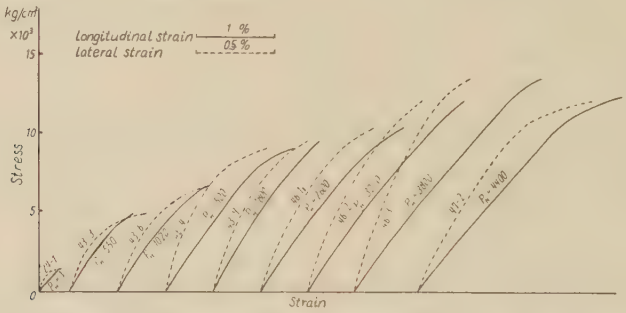

Fig. 2. Stress-Strain Curves from Axial Compression Tests for Kitashirakawa Granite.
Each full line denotes the longitudinal direction and broken line the lateral direction.

The stress-strain curves in the longitudinal direction have the approximately constant slope, independently of confining pressure, as shown in Fig. 2. That is, it can be said that the mean Young's modulus of this rock is constant at any confining pressure. In the fracture range under enough high pressure, however, as above mentioned, the curves have the tendency to be concave toward the strain axis and show the indistinct yielding zone, producing the appreciable plastic flow.

In Fg. 3, the relations between the stress and preudo-Poisson's ratio under various confining pressures are shown. Where percentage stress is

used as abscissa, the percentage stress is defined as a hundred times of the ratio of stress to the rupture strength. The stress and Poisson's ratio relations under various pressures can be clearly shown by the use of percentage stress. With the increase of the confining pressur, the unusual lowness of pseudo-Poisson's ratio at the first stage of loading is gradually lost and the volume increasing effect in the fracture range, observed characteristically at the ordinally pressure (Bridgman, 1949), decays rapidly.

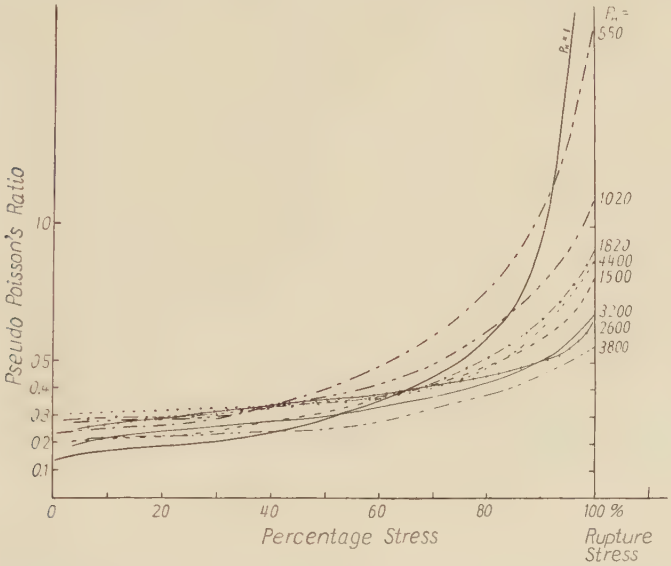

Fig. 3. Pseudo-Poisson's Ratio (ratio of lateral strain to longitudinal strain) vs. Percentage Stress under Various Confining Pressures.

Rupture strength (approximately equal to yield strength) increases strikingly with the increase of pressure. The increment of strength, however, was not so considerable at fairly high pressure. The observed values of strength at various pressures are shown in Fig. 4(a). Blanc circles express the values for the specimens in the ratio of length to diameter, 2 : 1, and full circle, 2.5 : 1.

The empirical formula which expresses the pressure-strength relation is,

$$P^* = P_0^* (kP_H + 1)^{1/2},$$

where P^* is the strength, k is the constant and P_H is the confining pressure.

The important numerical results are listed in the following Table.

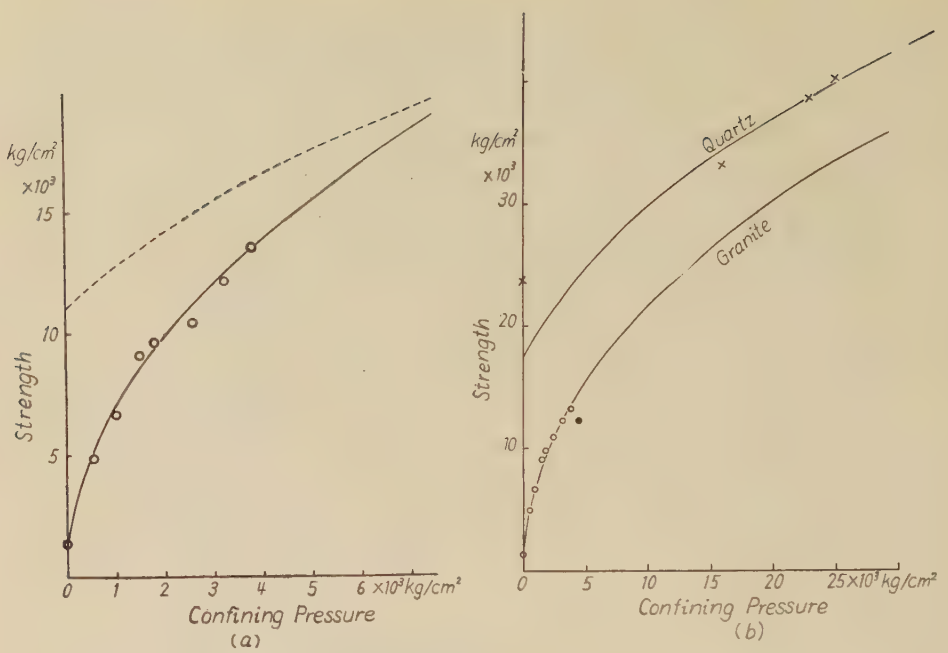

Fig. 4. Strength vs. Confining Pressure.

(a) Observed values and empirical curve (full line) of strength for Kitashirakawa granite, and assumed strength (broken line) as the pores are perfectly closed.

(b) Extended figure of (a), and strength of quartz.

Table. Mean Young's Modulus, Rupture Strength, and Indistinct Yielding Point.

Confining Pressure atm.	Mean Young's Modulus		Rupture Strength kg/cm²	Yielding Point (indistinct) kg/cm²
	$E\times10^{-11}$ dyne/cm²	Stress Range kg/cm²		
1	5.4	0– 1250	1380	—
550	6.9	– 3960	4860	4200
1020	6.25	– 5940	6660	6000
1500	6.7	– 7800	9100	8300
1800	7.5	– 8530	9160	—
2600	6.5	– 8580	10400	8600
3250	6.25	–11600	12110	—
3800	6.2	–12500	13520	12500
4400	6.0	–10100	12150	10900

On the other hand, the strength of quartz measured by Bridgman (1952) is shown by mark X in Fig. 4(b). The strength of this substance is relatively little affected by the pressure and only slightly increases as pressure does. The pressure-strength relation of granite at considerably high pressure seems to become the same as that of quartz by the reason after Griffith's theory (1924). Therefore, the assumed P^*-P_H curve can be obtained by extrapolating the above relation toward the lower pressure. This curve is shown by the broken line in Fig. 4(a).

We regard the difference between the assumed curve and the observed value as "the strength lowering" $P^{*\prime}$, considering that the strength is lowered by a certain cause characteristic of granite.

Now, we compare the change of "the strength lowering" and the volume increase in the fracture stage with the decrease of compressibility (Adams, 1951). As shown in Fig. 5, there is a close connection among these phenomena. As the compressibility decrement with the increase of pressure may be caused by the closing of pores, it is reasonably considered that the strength may be strongly affected by the existence of pores. In Fig. 5, the volume increment S in the fracture range show the area of the part where the pseudo-Poisson's ratio goes over 0.5 in Fig. 3 as the index.

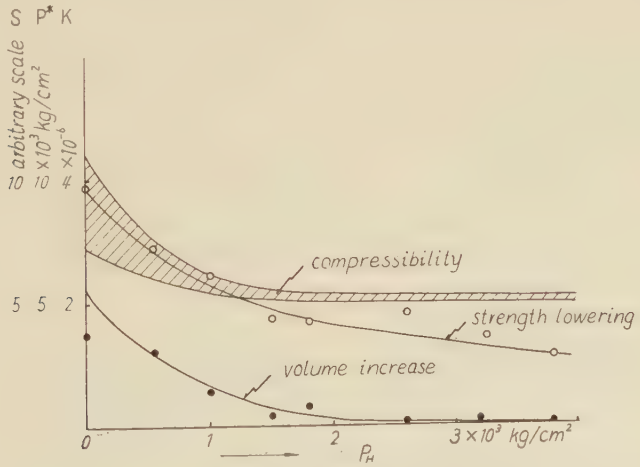

Fig. 5. Comparison of "Strength Lowering", Volume Change in the Fracture Range and Compressibility, for Granite under Various Pressures.

4. We will introduce one representation with respect to the relationship between the strength and the prosity of granite under various confin-

ing pressures, it will be considered that these two have a close connection with each other.

We assume that the pressure is able to affect to the porosity alone, but not to its strength. Then the rupture can be directly produced only by the differential stress acting on the porous specimen. Of course, the pressure exerts the indirect effect upon the strength, changing the shape of the pores.

Compressibility κ is given as follows,

$$\kappa = -\frac{1}{V}\frac{dV_1}{dP_H} - \frac{1}{V}\frac{dV_2}{dP_H} = \kappa_1 + \kappa_{por}, \quad V_1 \gg V_2, \quad \cdots\cdots(1)$$

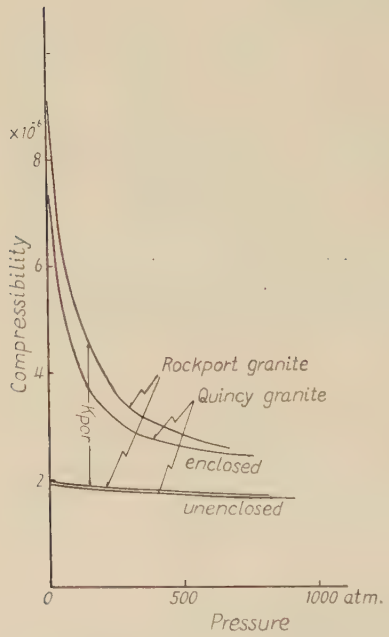

Fig. 6. Compressibility of Enclosed and Unenclosed Specimens of Granite under Various Pressures (Zisman, 1933).

where V, V_1, V_2, the total volume of specimen and the volume of substantial and empty part respectively, κ_1 denotes the compressibility of material and κ_{por} the effective value with respect to the pores.

Put N the number of the pores contained in this specimen, and v_1, v_2,$\cdots\cdots v_N$ the volumes of the respective pores, then

$$\kappa_{por} = -\frac{1}{V}\frac{d}{dP_H}\left(\sum_{i=1}^{N} v_i\right). \quad \cdots\cdots(2)$$

The empirical formula of κ_{por} is given as follows

$$\kappa_{por} = \frac{1}{(mP_H+n)^2} = \frac{1}{n^2(kP_H+1)^2},$$

$$k = \frac{m}{n}, \quad \cdots\cdots(3)$$

from the experiment on the measurements of the compressibility by Zisman (1933), considering the difference between the compressibility of the covered specimen and the uncovered one.

Now, we assume that the contraction of the respective pores with pressure has the similar tendency, then the effective compressibility of i-th pore in this specimen is given by

$$\left.\begin{aligned} \kappa^{i}{}_{por} &= \frac{1}{(m_i P_H + n_i)^2} = \frac{1}{n_i^2 (kP_H+1)^2}, \\ k_i &= \frac{m_i}{n_i} = k, \quad \sum_{i=1}^{N} \frac{1}{n_i^2} = \frac{1}{n^2}. \end{aligned}\right\} \qquad \cdots\cdots(4)$$

This formula (4) corresponds to the i-th term of formula (2), then

$$-\frac{1}{V}\frac{dv_i}{dP_H} = \frac{1}{n_i^2}\frac{1}{(kP_H+1)^2} \qquad \cdots\cdots(5)$$

Integrating and put the condition $P_H \to \infty$, $v_i \to 0$ into account,

$$v_i = \frac{V}{m_i n_i} \cdot \frac{1}{(kP_H+1)}. \qquad \cdots\cdots(6)$$

On the other hand, we assume the shape of pore as ellipsoid rotated around the minor axis, then the volume is

$$v_i = \frac{4\pi c_i^2 b_i}{3} \qquad \cdots\cdots(7)$$

where c_i and b_i are the major and minor radius respectively.

Equating formula (6) and (7), and assumeing that c_i does not vary with pressure, then the relation of the length of b_i with pressure is given by

$$b_i = \frac{3}{4\pi c_i^2} \cdot \frac{V}{m_i n_i} \cdot \frac{1}{(kP_H+1)} \qquad \cdots\cdots(8)$$

Next, we try to obtain the critical stress p_i, according to Griffith's theory (1921), at which the elliptic pore or crack begin to elongate by the applied compressional stress P along major axis, as is shown in Fig. 7. We take elliptic co-ordinates α, β and put $\alpha = \alpha_{0i}$ at the boundary of the i-th crack. The major and minor radius is given by c_i and $b_i = \alpha_{0i} c_i$, putting c_i the half length of focal line, as α_{0i} is very small.

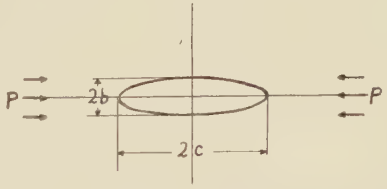

Fig. 7. Elliptic Pore Exposed under Axial Compressional Stress P along the Major Axis.

Then the increase of strain energy W_i by such crack is given by

$$W_i = \alpha_{0i} \frac{\pi P^2 c_i^2}{4E}(1-\sigma), \qquad \cdots\cdots(9)$$

where E, σ are the Young's modulus and Poisson's ratio of this material respectively. On the other hand, the surface energy of this crack is

$$U_i = 4c_i T, \qquad \cdots\cdots(10)$$

where T is the surface energy per unit area. From the condition that the crack may extend

$$\frac{d}{dc_1}(W_i - U_i) = 0, \qquad \cdots\cdots(11)$$

the strength of this crack can be expressed as

$$p_i^* = a\left(\frac{ET}{\pi(1-\sigma)}\right)^{1/2} \cdot b^{-1/2}, \qquad \cdots\cdots(12)$$

where a is the numerical constant (Ono, 1949).

Substituting (8) into (12), the relation of confining pressure and the strength of the crack oriented to the direction of compressional stress is given by

$$p_i^* = \frac{2}{\sqrt{3}} a c_i \left(\frac{ET}{(1-\sigma)} \cdot \frac{m_i n_i}{V}\right)^{1/2} (kP_H + 1)^{1/2}$$
$$= p_{i0}^* (kP_H + 1)^{1/2}, \qquad \cdots\cdots(13)$$

where p_{i0}^* is the strength of this crack at $P_H = 0$.

The value of k obtained from the above stated empirical equation is

$$k = 2.49\ 10^{-2} \times (\mathrm{kg/cm^2})^{-1}.$$

Though the value of k for Kitashirakawa granite from the compressibility measurements has not been given, the values of k from Zisman's data are

$$k = 0.22\ 10^{-2} \times (\mathrm{kg/cm^2})^{-1}$$

for Quincy granite, and

$$k = 0.30\ 10^{-2} \times (\mathrm{kg/cm^2})^{-1}$$

for Rockport granite.

5. The mechanism of deformation and fracture of granite becomes much simpler at high confining pressure, as seen in the case of quartz and so on, than at lower pressure, by the action of hydrostatic compression which decreases the porosity of porous media, while such rocks show a very complicated behavior under low pressure. This tendency may be kept at high temperature and high pressure. Therefore, in the deeper part of the crust where rocks are confined with enough high pressure, the feature of mechanical behavior of rocks seems to have lost their complicacy such as seen at the earth's surface, and may behave as a simple aggregate of constituent minerals.

So far as it is concerned at room temperature, these sorts of rocks are

not so much plastic even under high pressure. On the contrary, the elastic range is extended strikingly with the increase of pressure as the results of the raise of strength. However, if the pressure increases highly enough, the increment of strength does not become so remarkable, then the elevation of temperature may become more strongly effective on the plasticity than the increase of pressure, in the earth's interior.

Acknowledgements

The author expresses his sincere thanks to Prof. K. Sassa for his instructions and encouragements.

Referenees

1) Adams, L. H. : "Elastic properties of materials of the earth's crust." Internal Constitution of the Earth. Edited By Gutenberg B., New York, 1951.

2 Bridgman, P. W. : "Volume change in the plastic stages of simple compression" J. App. Phys., **20**, 1241, 1949.

3) Bridgman, P. W. : "Studies in Large Plastic Flow and Fracture." New York, 1952.

4) Griffith, A. A. : "The phenomena of rupture and flow in solids." Phil. Trans. Royal Soc. London, scr. A, **221**, 163, 1921.

5) Griffith, A. A. : "The theory of rupture." Proc. 1st Inter. Cong. App. Mech., Delft, 55, 1924.

6) Griggs, D. T., and Miller, W. B. : "Deformation of Yule marble : Part I, Compression and extension experiments on dry Yule marble at 10,000 atmospheres confining pressure, room temperature." Bull. Geol. Soc. Amer., **62**, 853, 1951.

7) Matsushima, S. : "On the flow and fracture of igneous rocks." Disater Prevention Res. Inst. Kyoto Univ. Bull., No. 36 (1960).

8) Ono, A. : "On fracture of materials taking place on a plane parallel to the direction of thrust." Memoirs Tech. Kyushu Univ., **11**, 189. 1949.

9) Paterson, M. S. : "Experimental deformation and faulting in Wombeyan marble." Bull. Geol. Soc. Amer., **69**, 465, 1958.

10) Robertson, E. C. : "Experimental study of the strength of rocks." Bull. Geol. Soc. Amer., **66**, 1275, 1955.

11) Turner, F. J., Griggs, D. T., and Heard, H. : "Experimental deformation of calcite crystals." Bull. Geol. Soc. Amer., **65**, 883, 1954.

12) Zisman, W. A. : "Compressibility and anisotropy of rocks at and near the earth's surface." Proc. Nat. Acad. Sci., **19**, 666, 1933.

DIASTER PREVENTION RESEARCH INSTITUTE
KYOTO UNIVERSITY
BULLETINS

Bulletin No. 37 August, 1960

On the physical properties within the B-layer deduced from olivine-model and on the possibility of polymorphic transition from olivine to spinel at the 20° Discontinuity

By

Tatsuhiko WADA

Abuyama Seismological Observatory, Faculty of Science, Kyoto University

(Commnicated by Prof. K. Sassa)

On the physical properties within the B-layer deduced from olivine-model and on the possiblity of polymorphic transition from olivine to spinel at the 20° discontinuity

By

Tatsuhiko WADA

Abuyuma Seismological Observatory, Faculty of Science, Kyoto University
(Communicated by Prof. K. Sassa)

ABSTRACT

An equation of state of forsterite is deduced theoretically based upon ionic model. The calculated variations of the density and incompressibility with pressure agree with those obtained by Bullen for the B-layer. Moreover, the activation energy of forsterite having Schottky defects is evaluted to be 3.29 *e.v.*, which is compatible with the experimental value of 3.0 *e.v.* measured by Hughes. The variation of the activation energy with pressure is investigated, and it is resulted that the extraporation from the experimental values obtained within 10,000 *bars* is not reliable and the second derivative of activation energy concerned with pressure is not meaningless. The tempeature distribution thus obtained within the B-layer is well in accordance with Gutenberg's one. By comparing the lattice energies of olivine and spinel (normal and inverse), which is evaluated theoretically, we find that the polymorphic transition from olivine to spinel is imposssible.

1. Introduction

The opinion that the B-layer is composed of dunite is supported widely with geophysical, geochemical and petrological evidences. But many problms are yet open to disccussion, for example, to investgated whether the variations of physical properties of dunite with pressure agree or not with those within the B-layer, is one of these problems.

We have only two observed quantities on the physical states of materials

composing the earth's interior: the distributions of seismic wave velocities and electric conductivities. Dunite is expected to have the physical properties deduced from those geophysical data.

Olivine, main constituent of dunite, contains usually 90 per cent forsterite (Mg_2SiO_4) and 10 per cent fayalite (Fe_2SiO_4). Thereupon the physical properties of forsterite should play most weighty part in those of the B-layer. We will estimate the physical properties of forsterite based upon solid-state physics, especially from microscopic point of view, since this kind of investigation for minerals has been little developed due to difficulties arised from complicated structure of minerals.

Another problem of olivine-model for the B-layer is concerned with the origin of the C-layer, which has peculiar physical properties. They are an abnormal increase of seismic wave-velocities and an abrupt anormaly of electric conductivity. Such an extraordinary behavior of the C-layer yields an attraction of many geophysists and enormous numbers of papers have been published on the origin of the C-layer. At present the following two types of hypothesis are current: a polymophic phase-transition hypothesis which is realized by a change in physical states of silcate, and a chemical transition hypothesis which is realized by a chemical inhomogeneity there. We will discuss in this paper a possibility of polymophic transition of forsterite from olivine-structure to sninel structure.

2. An equation of state of forsterite and its elastic properties

According to Bragg's result (1937), Mg_2SiO_4 crystal is orthorombic and has the three axes of the following length:

$$a=4.755\,A \qquad b=10.21\,A \qquad c=5.985\,A.$$

In Fig.1 the structure of Mg_2SiO_4 (olivine-structure) is shown. The cohesive property of Mg_2SiO_4 seems to be of both ionic and covalent, and hence is considerably complicated. As the first approximation, the assumption that Mg_2SiO_4 is an ionic crystal containing Mg^{2+}, Si^{4+} and O^{2-} may be acceptable, although the exact evaluation needs quantam mechanical treatment. As an expression for lattice energy of ionic crystal, Born and Mayer (1932) gave the following,

$$u(v)=-A/(v/v_0)^{1/3}+B\exp\{-(v/v_0)^{1/3}/\rho\}, \qquad (1)$$

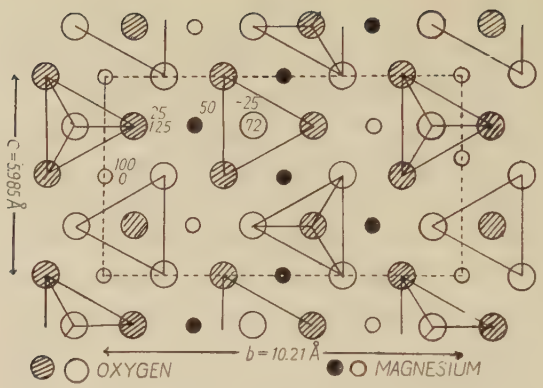

Fig. 1. Olivine structure of Mg_2SiO_4. Si atom of which position is the center of O-tetrahedral, is not shown in the figure.

where v shows volume per molecule, and A,B and ρ are constants but depend upon the crystal structure and the constituent ions, and the suffix 0 refers to zero pressure. We should prefer the expression (1) to another expression

$$u(v) = -A/(v/v_0)^{1/3} + B/(v/v_0)^{n/3}$$

which are also frequently used, since (1) has been shown by Pauling being able to be deduced from quantam theory, and our problem concerned with high pressure demandes such a formula that is applicable to wide range of the variation of v/v_0. The first term in (1) shows electrostatic potential energy, and A is called Madelung constant, as known for such simple crystals as NaCl, CsCl, rutile etc., but not for olivine structure. In the first place, we must evaluate the Madelung constant for olivine structure. This evaluation is carried out through summing up $e_i\, e_j/r_{ij} (i \neq j)$, where e_i is the charge of the ith-ion and r_{ij} the distance between the ith-and jth ions. Among several practical methods for this summing up, the method deviced recently by Bertaut (1952) is most suitable to be applied for such a complicated crystal as olivine. This method is as follows: a spherically symmetric charge-distribution $\sigma(\vec{r})$ having the center at the center of each ion is replaced for the actual ionic charge, where $\vec{r}$ is a vector showing the position from the center of the ion and, for convenience, we impose on $\sigma(\vec{r})$ the restriction that each $\sigma(\vec{r})$ may contact, but must not overlap each other, that is,

$$\sigma(\vec{r})\cdots\cdots\begin{cases}=C & |\vec{r}|\leq R\\ =0 & |\vec{r}|>R\end{cases}\qquad C=3/4\pi R^3, \tag{2}$$

where we adopt a half of the minimum distance between Si^{4+} and O^{2-} as R of (2), which is the maximum value permitted without violating above restriction (2). Expanding the crystal charge density-distribution $\rho(\vec{r})$ deduced from these $\sigma(\vec{r})$ to a three-fold Fourier series, we obtain the potential φ satisfying Poisson's equation

$$\Delta\varphi=-4\pi\rho(\vec{r}). \tag{3}$$

The φ corresponds to the first term of (1), namely the electrostatic potential energy. In practical calculation, we adopt the center of Mg^{2+} as origin and rectangular coordinates parallel to the three axes of olivine crystal lattice and then summation is over all ions within the sphere having the sufficient radius to contain the twelfth cell (the unit cell is composed of $8Mg^{2+}$, $4Si^{4+}$ and $16O^{2-}$) along a-axes from the cell containing the origin. Then we obtain

$$Ae^2/(v/v_0)^{1/3}=155.22e^2/b \tag{4}$$

for a molecule, where b is the length of b-axes.

The second term of (1), expressing the repulsive potential energy due to the overlapping between each electron-cloud, has two unknown paramenters B and ρ. To determine these, we differentiate (1) with v once and twice, and then the expressions for pressure p and imcompressibility K,

$$p=-du(v)/dv=(1/3v)[-A/(v/v_0)^{1/3}+B\{(v/v_0)^{1/3}/\rho\}\exp\{-(v/v_0)^{1/3}/\rho\}] \tag{5}$$

$$K=-vdp/dv=(1/9v)[-A/(v/v_0)^{1/3}+B\{(v/v_0)^{1/3}/\rho\}\exp\{-(v/v_0)^{1/3}+B\{(v/v_0)^{2/3}/\rho^2\}\exp\{-(v/v_0)^{1/3}/\rho\}]+p, \tag{6}$$

are obtained. For static equilibrium $p=0$, using the experimental value for the imcompressibility K of Mg_2SiO_4 at zero pressure, we can determine B and ρ. The explicit expression of (1) thus obtained is as follows :

$$u(v)=350.709185/(v/v_0)^{1/3}+5890.089736\exp\{-4.2735(v/v_0)^{1/3}\}. \tag{7}$$

From (5), (6) and (7), the variations of K, and the density d with $(v/v_0)^{1/3}$ are evaluated, where for $(v/v_0)^{1/3}=1$, $d=3.3\,gr/cm^3$ is adopted (the calculation by using atomic weights and lattice dimensions gives $3.216\,gr/cm^3$). These results are shown in Table 1. Comparing these values with those

obtained by Bullen (1943) for the B-layer, we can find well accordance between both values (see Fig. 2). In fact, both values of d agree perfectly and even the maximum discrepancy between both of K amounts to only 8 per cent, which may be found to correspond to difference in the seismic velocities for a given depth of as much as 2 or 3 per sent, as pointed out by Birch (1939), since uncertainty in K/d is increased several times due to the fact that K/d is deduced from $V_p^2-(3/4)V_s^2$ (V_p and V_s are the velocities of compressional and shearing waves, respectively). In addition, considering that the calculated value denotes isothermal one and the "observed value" adiabatic, the discrepancy as above cited should be regarded as a slight one.

Table 1. Variation of density d, incompressibility k and pressure p of Mg_2SiO_4 versus change $(v/v_0)^{1/3}$.

$(v/v_0)^{1/3}$	p (10^{12} *dynes/cm²*)	k (10^{12} *dynes/cm²*)	d (*gr/cm³*)
1	0	1.22	3.30
0.99	0.039	1.32	3.40
0.98	0.082	1.44	3.51
0.97	0.129	1.56	3.62
0.96	0.180	1.70	3.73

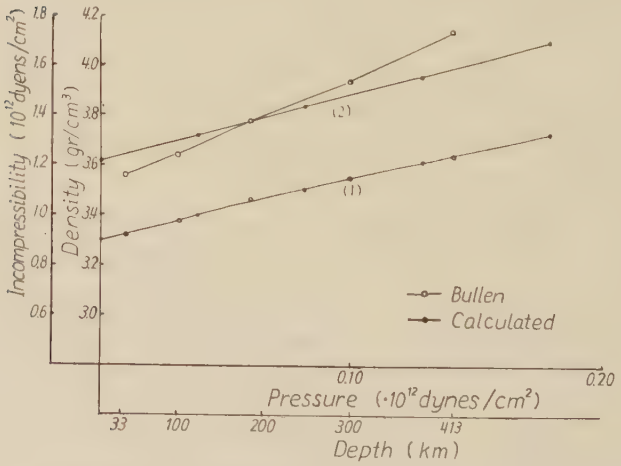

Fig. 2. Distribution of density (curve 1) and incompressibility (curve 2) within the B-layer.

3. Electric conductivity of Mg_2SiO_4

The electric conductivity of material within the Earth is deduced from geomagnetic data. On the other hand, Coster (1948) found that the electric conductivity σ of igneous rock is expressed by

$$\sigma = \sigma_0 \exp(-E_A/kT) \tag{8}$$

where E_A is called activation energy, k is Boltzman's constant and σ_0 is constant. This result means that the electric conductivity of igneous rock increases with temperature in a similar way to that of ionic and semiconductors. Coster, Hughes (1955) and Rikitake (1952) estimated the temperature within the Earth from formula (8) in connection with the distribution of the electric conductivities "observed" within the Earth. However, their treatments of the variation of E_A with pressure come into question, for example, Coster's treatment is restricted to the variation of the thermal-vibrational term of E_A, and Rikitake's contains an uncertainty in the estimation of the pressure-dependence of lattice energy and, in addition, disregards the variation of polarization energy with pressure (the details will be cited later: also see T. Wada, (1958)). At any rate, this problem is desired to be studied further.

Hughes has shown that olivine exhibits three types of conductions. Above 1,000°C the conduction becomes primarily ionic (see Runcorn and Tozer, (1955)). In present section, we may consider only ionic type of conduction, since ionic type prevails the other types within the B-layer, where the temperature is anticipated above 1,000°C. Ionic conductors are insulators in which certain mobile ions may move through the crystal lattice as result of defects in it. Assuming a Schottky defect, for Mg_2SiO_4 (in most of ionic crystals Schottky type is more advantageous than Frenkel type) (see Mott and Gurney (1948)), the activation energy E is represented with

$$E_A = (1/2)(W_L + W_+ + W_-) + U \tag{9}$$

where W_+ is the work required to remove a positive ion out of crystal, W_- the work required to remove negative ion, W_L the lattice energy of the crystal per ion-pair, and U is the work required to move the ion or hole half way to its next metastable position. We may consider Mg^{2+} and O^{2-} as the mobile ions, since Si^{4+}, having higher charge than Mg^{2+}, requires

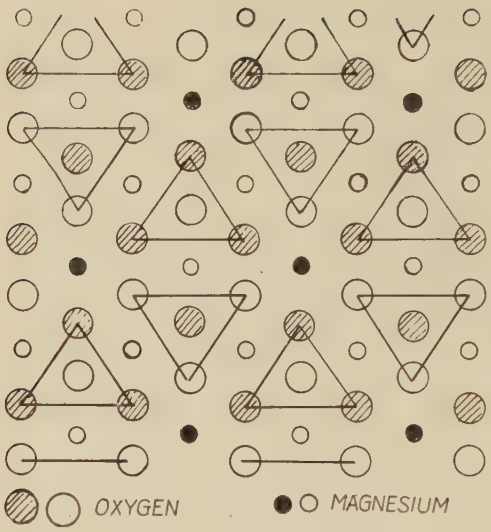

Fig. 3. Spinel structure of Mg_2Sio_4, of which a section most similar to Fig. 1 is shown.

higher energy to be removed than Mg^{2+}.

(a) We can not directly estimate W_L, since the lattice energy of olivine obtained in the previous section can not be shared to the three kinds of ions. Fortunately, the electrostatic potential energy of spinel structure, which is very similar to olivine structure (Fig. 3 and Fig. 6; see also section 4), has been evaluated by Verway, de Boer and van Santen (1948), whose result carried out with Ewald's method is separable for the three kinds of ions. Thereupon we assuem that $l_{0a}/L_0 = l_{sa}/L_s$, where

L_0 : lattice ennergy of olivine structure per molecule

L_s : electrostatic energy of spinel structure per molecule

l_{0a} : lattice energy per a-ion in olivine structure

l_{sa} : electrostatic energy per a-ion in spinel structure.

($a = Mg^{2+}$, Si^{4+} and O^{2-})

Finally we get

$$W_L = 35.84 \ e.v., \qquad (10)$$

from above assumption and (7).

(b) W_+ and W_- are calculated through the method deviced by Mott and Littleton (1937). When an ion is removed, the medium surrounding the vacant lattice point will find itslf in an electric field. It therefore become polarized, and in calculating W_+ or W_- the energy of this polarization must be taken into account. The polarization of the surrounding medium will set up at the vacant lattice point an electrostatic potential, which we denote by ϕ_+ or ϕ_-. Then the work necessary to remove an ion will be, instead of W_L,

$$W_+ = W_L - (1/2)Z_+e\phi_+ \quad \text{or} \quad W_- = W_L - (1/2)Z_-e\phi_-. \qquad (11)$$

Our problem is to calculate ϕ_+ and ϕ_-. We discuss first the problem of a rigid lattice, in which the ions are not allowed to move away from their mean positions, but in which they have polarizabilities

$$\alpha_{Mg}=0.094, \quad \alpha_{Si}=0.0165 \quad \text{and} \quad \alpha_{\cdot}=2.4. \quad (10^{-24}\,cm^3)$$

Suppose a charge e is placed at a definite point of the lattice, refered to as the point Q. Then dipoles are induced on all other ions. If r is the distance from Q, the center of the hole, we have for the polarization P

$$P=(1/4\pi)\{1-(1/\varepsilon_0)\}\ (e/r^2) \qquad (12)$$

where ε_0 is the dielectric constant for alternating fields, that is obtained from the polarizabilities of ions in connecton with Clausius-Mossotti's formula. The dipoles on the three kinds of ions are respectively

$$\mu_i=\{\alpha_i/(2\alpha_{Mg}+4\alpha_0+\alpha_{Si})(1/4\pi)(1-(1/\varepsilon_0))(ve/2r^2) \qquad (13)$$
$$(i=\text{Mg, Si and 0})$$

where v is volume per an ion-pair of Mg^{2+} and 0^{2-}. Since a dipole μ_i at a given lattice point gives a potential μ_i/r^2 at Q, we obtain the potential by summation:

$$\phi=\sum_{Mg}\mu_{Mg}/r^2+\sum_{Si}\mu_{Si}/r^2+\sum_{0}\mu_0/r^2, \qquad (14)$$

where the summations are over the lattice points of type Mg, Si and 0. Summations of these type have carried out with Misra's method. We pass on to the case of an actual crystal in equilibrium in a static field, so that the ions are displaced into new positions. Let $-cx$ be the restoring force, due to overlop forces, on any ion in a uniformly polarized medium where each ion is displaced by a distance $\pm x$. Then dipoles μ_i induced at the lattice points of types Mg^{2-}, Si^{4+} and 0^{2-} are

$$\bar{\mu}_i=\alpha_i\{E+(4\pi/3)(P_0+P_1)+(Z_ie/2c)^2\}\{E+(4\pi/3)(P_0+P_1)\} \qquad (15)$$
$$(i=\text{Mg, Si and 0})$$

where E is the electric field due to absence of ion, that is, $E=Ze/\varepsilon r^2$, ε is the dielectric constant for static field, P_0 is the polarization due to the induced dipoles on the ions and P_1 is the polarization due to the displacement of the ions. E, ε, P_0 and P_1 is deduced from α_i and c. To obtain directly the c for Mg_2SiO_4 is very difficult. But we can find the c for MgO, which contains Mg^{2+} and 0^{2-} and has similar elastic properties to Mg_2SiO_4. (According to Szigetti (1950), we must consider the difference

between the c duduced from the experiment of elasticity and the c calculated from the dispersion frequency.) From these valuses and (13), we get

$$(1/2)Z_+e\bar{\phi}_+=18.63\ e.v.,\ \text{and}\ (1/2)Z_-e\bar{\phi}_-=12.36\ e.v.,$$

whre the $\bar{\phi}_+$ and $\bar{\phi}_-$ are the potentials in the case of a deformable lattice corresponding to the ϕ_+ and ϕ_- in the case of a rigid lattice.

(c) U in (9) is interpretated by Koch and Wagner as the activation energy of "structure-sensitive" ionic conduction, that is due to a trace of impurity in the crystal, acting in a way similar to the Cd ions in the silver salts. According to Hughes' experiment, the conduction of olivine under low temperature ($<600°C$) is of "impurity" type, the activation energy of that is 1 $e.v.$, compatible with those of common "structure sensitive" conductions. Moreover, the value of σ_0, $10^{-4}\ ohm^{-1}\ cm^{-1}$, is acceptable in the case of "structure sensitive" conduction. The assumption that 1 $e.v.$ is adopted as U may be reasonable.

From (a), (b) and (c), the activation energy E_A becomes

$$E_A=3.29\ e.v.,$$

which agrees well with the experimental value of olivine, 3.0 $e.v.$.

By estimating the variations of W_L, W_+, W_- and U with pressure, we can find the variation of the activation energy E_A of Mg_2SiO_4 with pressure. (i) The variation of W_L is easily estimated, since this follows that of the lattice energy, given in section 2. (ii) The variation of W_+ and W_- can not be exactly expressed, since a_i and c also depend on pressure in unknown connection. We consider three cases of the variation of W_+ or W_- with pressure: (case 1) independent of pressure, (case 2) varies with $v^{-1/6}$ and (case 3) varies with $v^{-1/6}$. (iii) The variation of U also can not be exaxtly estimated, since we cannot find the repulsive potential in the neibourhood of the center of ion. We assume that U varies with $v^{-12/3}$. (iv) temperature also affects E_A, since ionic conduction predominates avove 1,000°C. The influence of temperature upon E_A is estimated by using the equation of state of Mie-Grüneisen:

$$p+du(v)/dv=\gamma E_{vib}/v, \qquad (16)$$

where γ is Grüneisen constat, $\gamma=1.2$ for Mg_2SiO_4, and E_{vib} is as follows:

$$E_{vib}=(9/8)\Theta\cdot k+3k\cdot T\cdot D(\Theta/T), \qquad (17)$$

which shows the vibration-term of the lattice energy, where Θ is Debye tem-

perature, and $D(\Theta/T)$ is Debye function. The variation of Θ with pressure is given by $\Theta = \Theta_0(v/v_0)^{-\gamma}$ ($\Theta_0 = 726°K$ for Mg_2SiO_4). The temperature effect thus estimated is shown in Fig. 4, where we find, at $T = 500$, 1,000 and 1,500°K, the thermal expansions of Mg_2SiO_4 are 0.3, 0.6 and 1.0 per cent, corcesponding to decreases of pressure of 3,000, 6,900 and 10,300 *bars*, respectively.

From (i), (ii), (iii) and (iv), in the case of $T = 1{,}500°K$, the variation of E_A with pressure is evaluated. The results are shown

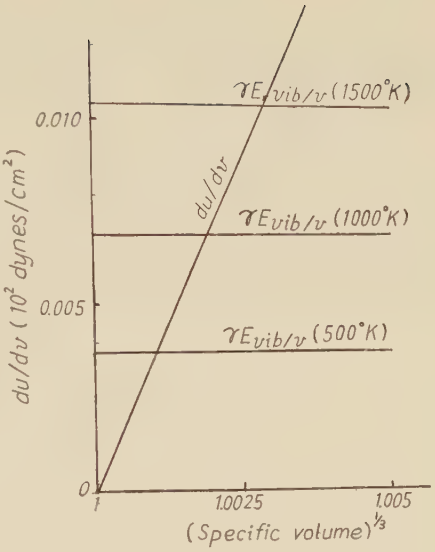

Fig. 4. Graphical solution of the equation of state of Mie-Grüneisen.

Table 2. Pressure dependence of activation energy at 1500°K.

p (10^{12} *dynes/cm²*)	E_A (e.v.)		
	(case 1)	(case 2)	(case 3)
0	3.250	3.265	3.296
0.010	3.290	3.290	3.290
0.019	3.405	3.370	3.260
0.092	3.515	3.420	3.210
0.137	3.620	3.480	3.150
0.187	3.720	3.570	3.100

(case 1) $(1/2)Z_{Mg}e\bar{\phi}_{Hg} + (1/2)Z_0e\bar{\phi}_0 = \text{const}$
(case 2) 〃 $\propto (v)^{-1/6}$
(case 3) 〃 $\propto (v)^{-1/3}$

in Table 2., from which we can find the following: d^2E/dR^2 (R denotes the distance from the center of the Earth) is not zero, as mentioned by Verbogen (1956), even in the B-layer. In fact, $dE_A/dp = 4.0 \cdot 10^{-6}$ *e.v./bar* at $p = 0 \sim 10{,}000$ *bars*, and $dE_A/dp = 2.0 \cdot 10^{-6}$ *e.v./bar* at about 150,000 *bars*.

Therefore, the extrapolation of dE_A/dp derived by any experiment under low pressure ($p<10{,}000$ *bars*) will result in overestimating the temperature within the Earth's interior, as mentioned by Hughes.

Considering the Hughes's value of $dE_A/dp=4.3\cdot10^{-6}$ *e.v./bar* for peridot, we should take (case 1). When we adopt 10 $ohm^{-1}\ cm^{-1}$ as σ_0 and the *d*-curve given by Lahiri and Price (1939) (1) and the distribution given by Rikitake (1950, 1951) (2) are adopted as the distribution of the electric conductivities within the B-layer, the temperature distribution, is obtained, as given in Table 3 and shown in Fig. 4. For comparison, the temperature

Table 3. Temperature distribution within the B-layer.

depth (*km*)	Temperature °*K*	
	(1)	(2)
100	1,820	1,500
200	1,920	1,540
300	2,010	1,580
400	2,100	1,600
Mean of dT/dR	1°/*km*	0.4°/*km*

(1) calculate d value based upon Lahiri and Price's d-curve.
(2) calculated value based upon Rikitake's model.

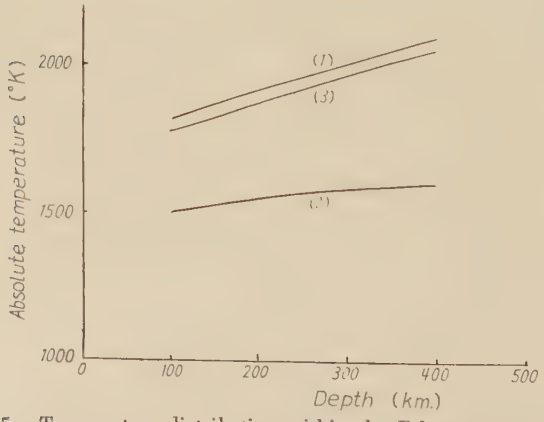

Fig. 5. Temperature distribution within the B-layer.
(1) calculated value based upon Lahiri and Price's d-curve.
(2) calculated value based upon Rikitake's model.
(3) gutenberg's result.

distribution given by Gutenberg is also shown in Fig. 4.

4. Possibility of the polymorphic transision of Mg_2SiO_4

Bernal suggested first the possibility of polymorphic transition of olivine at meeting when Jeffreys reported the existence of the *C*-layer. The magnesium germanate (Mg_2GeO_4) has a similar chemical formula to Mg_2SiO_4 and shows a polymorphic transision. Thus he infered that the same kind of polymorphic transition might take place for Mg_2SiO_4. Goldschmidt reported that Mg_2GeO_4 has two types of possible crystal structures, viz. olivine type (orthorombic) and spinel type (cubic). Many other experimental works have been carried out to confirm the above report. Romeijin and Ringwood found that Mg_2GeO_4 changes its structure from spinel to olivine at about 600°*C*. On the other hand, Bridgeman found by high pressure experiments that the olivine shows a discontinuous jump of shearing strength at 84 *kbars*. He suggested that this discontinuous jump may be related to its polymorphic transition of crystal structure.

A theoretical study of the polymorphic transition of crystal has been carried out on ionic crystals, especially on a simple crystale such as alkali halides. One way of attack is to calculate the lattice energy based upon a classical treatments. Though the results thus obtained give transition-pressures, the values are so unreliable that only the possibilities of transitions are confirmed, even if higher terms of energies are considered and the dependence on pressure is estimated as exactly as possible. (see, for instance, Jacobs (1938), and Born and Hung (1954)).

A stability condition of crystal at high pressure and at absolute zero temperature is given by examining the Gibbs free energy (or enthalpy) $U+PV$. U, P and V denote lattice energy, pressure and volume. When the transition takes place at the pressure P, the stability condition gives

$$U_A+PV_A=U_B+PV_B \tag{18}$$

or

$$P=(U_B-U_A)/(V_A-V_B) \tag{19}$$

Neglecting the effect of pressure upon U and V for the first approximation (as above mentioned, we should be concerned with the possibility of transition only), we get

$$P \simeq (U_{B,0} - U_{A,0})/(V_{A,0} - V_{B,0}) \qquad (19')$$

where the suffix 0 denotes the value at $P=0$.

The repulsive energy represented by exponential type in (1) is a rigorous expression. However the inverse power type is frequencly used for many practical problem owing to its simple expression. In the following we use the lattice energy as

$$U = -(A/r) + (B/r^n) \qquad (20)$$

From the equilibrium condition $(dU/dr)=0$, the value r_0 and U_0 at $P=0$ are given by

$$r_0 = (nB/A)^{1/(n-1)}, \quad U_0 = -(A/r_0)/\{(n-1)/n\} \qquad (21)$$

From (19′) and (21), we get

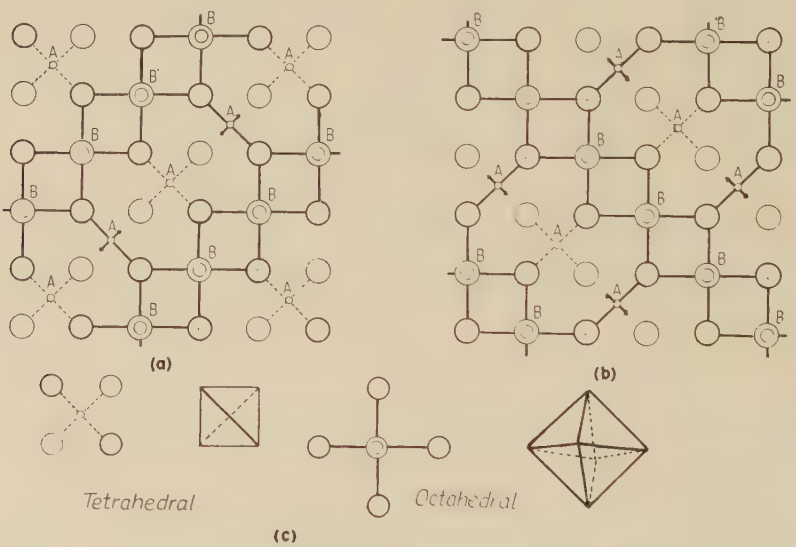

Fig. 6. The structure of spinel.

The structure in idealized form. The oxygen atoms (shown by large circles) are approximately in cubic closed packing. (a) and (b) show two close-packed layers projected upon the cubic face. One set of silicon atoms (shown by small circles A) is in positions of four-coordination between a tetrahedral group of oxygen atoms and the other set of magnesium atoms (shown by small circles B) in six coordination between an octahedral group. (shown in (c)) We may picture as a series of layers as above shown. The bottom layer of (a) has diagonal chains of magnesium-octahedra, which are linked laterally by silicon-tetrahedra lying alternately above and below heavily outlined oxygen atoms. In the next layer (b), the slant of the chains is reversed. Four such layers makes up the complete unit cell.

$$P=(A/sr_0^4)F_n \qquad (22)$$

$$F_n=\{(n-1)/n\}\{1-(A_B/A_A)^{n/(n-1)}(B_A/B_B)\}/\{1-(s_B/s_A)(B_B/B_A)^{3/(n-1)}(A_A-A_B)^{3/(n-1)}\}$$

where $V_A=s_A r_A^3$, $V_B=s_B r_B^3$.

The spinel XY_2O_4 has generally the spinel structure which is shown in Fig. 3 or Fig. 6 for the normal spinel structure. We notice that the Fig. 3 is quite similar to the olivine structure of XY_2O_4 shown in Fig. 1. In the normal spinel X-ions occupy the center of the O-tetrahedra (half of Y-ion in the inverse case). According to Verwey et al. the electrostatic potential energy of the spinel expressed by

$$U_{sp}=-(1/2)(e^2/a)(p\,M_{tetra}+2qM_{oct}+8M_0)=-M(e^2/a) \qquad (24)$$

where

a : length of the cube edge of the cubic lattice
M_{tetra} : contribution from tetrahedral interstices
M_{octa} : contribution from octahedral interstices
M_0 : contribution from O lattice points
p : ionic charge number of the tetrahedral interstices
q : ionic charge number of the octahedral interstices

For the normal and inverse spinels $p=4$, $q=2$, and 2, $(1/2/)(4+2)=3$, respectively. Table 4 is the numerical table for M. According to Bron and Mayer's expression, a repulsive potential R between two kinds fo ions, α and β,

Table 4. Electrostatic energy of normal and inverse spinel for several values of oxygen parameter (unit : (e^2/a) 10^{-12} *erg*) (after Verwey et al.)

Parameter u	Charge p q	M_{tetr}	M_{oct}	M_0	M
0.375	4 2	24.94	15.00	14.55	138.1
	2 3	17.53	17.99	14.27	138.6
0.380	4 2	23.63	16.23	14.00	135.8
	2 3	16.25	19.23	14.35	131.4
0.385	4 2	22.50	17.47	13.42	133.6
	2 3	15.10	20.47	14.37	134.0
0.390	4 2	21.41	18.71	12.82	131.5
	2 3	14.01	21.70	14.35	136.5

(For explanation see (24))

$$R=C\lambda_{\alpha,\beta}\bar{b}\exp\{(r_\alpha+r_\beta-r_{\alpha,\beta})/\rho\} \tag{25}$$

where C and $\bar{b}$ are the coordination number and a constant, respectively, and $\lambda_{\alpha,\beta}$ is expressed by

$$\lambda_{\alpha,\beta}=1+Z_\alpha/N_\alpha+Z_\beta/N_\beta \tag{26}$$

where Z is the charge of ion, N is the number of electron in the outer-shell of ion, and the suffix α or β denotes α- or β-ion, r_α, r_β and $r_{\alpha,\beta}$ in (25) are basic radii of α- and β- ions and the nearest distance between both ions, respectively. Refering to (25) and (26) we obtain the repulsive potential R per molecule as follows:

for olivine-structure

$$\begin{aligned}R_{oe}=&4\lambda_{Si,O}\bar{b}\exp\{(r_{Si}+r_O-0.1777b)/\rho\}\\&+12\lambda_{Mg,O}\bar{b}\exp\{(r_{Mh}+r_O-0.2044b)/\rho\},\end{aligned} \tag{27}$$

for normal spinel-structure,

$$\begin{aligned}R_{ns}=&4\lambda_{Si,O}\bar{b}\exp\{(r_{Si}+r_O-\sqrt{3}\,a/8)/\rho\}\\&+12\lambda_{Mg,O}\bar{b}\exp\{(r_{Mg}+r_O-a/4)/\rho\},\end{aligned} \tag{28}$$

and for inverse spinel-atructure,

$$\begin{aligned}R_{is}=&4\lambda_{Mg,O}\bar{b}\exp\{(r_{Mg}+r_O-\sqrt{3}\,a/8)/\rho\}+6\lambda_{Mg,O}\bar{b}\exp\{(r_{Mg}+r_O-a/4)/\rho\}\\&+6\lambda_{Si,O}\bar{b}\exp\{(r_{Si}+r_O-a/4)/\rho\},\end{aligned} \tag{29}$$

where the constants ρ and $\bar{b}$ are $0.345A$ and 10^{-12} erg, respectively.

To compare the energies of the three types of structures, viz. olivine, normal spinel and inverse spinel, it is convenient to transform the unit of length from a (cubic edge length of spinel) to b (b-axes length of olivine), By using this transformation, we set up approximately

$$\begin{aligned}&\exp(-0.1777b/\rho)/\exp(-0.2044b/\rho)\\&\quad\cong\exp(-0.1770b/\rho)/\exp(-0.20434b/\rho)\equiv G\end{aligned} \tag{30}$$

Then, referring to (22) and (30), B_A/B_B is expressed approximately by R_{oe}, R_{ns} and R_{is}.

We must consider the effect of oxygen parameter, as previously mentioned. It is well known that the actual spinel has u greater than 0.375. In the present section, the effect of oxygen parameter greater than $u=0.375$ is discuussed. Putting $u=0.375+\delta$, then we replace $\sqrt{3}\,a/8$ and $a/4$ in (26) and (27) with $\sqrt{3}\,a\{(1/8)-\delta\}$ and $a\{(1/4)-\delta\}$, respectively.

In conclusion we have F_n and P in (23) as shown in Table 5, where $3\leqq n\leqq 7$. The condition of transition from A to B is given by $F_n>0$, and

Table 5. Signs of F_n and V_{ol}/V_{sp} for several values of n and u. The sufficient condition for a polymorphic transition is $F_n>0$ and $V_{ol}/V_{sp}>1$.

n	$u=0.375$		$u=3.80$	
	normal spinel	inverse spinel	normal spinel	inverse spinel
3	negative	negative	negative	negative
4	negative	positive <1	negative	negative
5	negative	positive <1	negative	negative
6	negative	positive <1	negative	negative
7	negative	positive <1	negative	negative

$V_A/V_B\geq 1$. In table 5 V_A/V_B is shown only for $F_n>0$. The results thus obtained mean that the polymorphic transition from olivine to spinel (normal or inverse) is impossible.

5. Conclusion

The variations of the elastic and electrical properties of Mg_2SiO_4 with pressure agree well with those deduced from seismic data and geomagnetic data within the B-layer. It seems true that the B-layer is composed of dunite.

On the other hand, the possibility of polymorphic transition from olivine to spinel is denied at any rate. However to confirm the possibility of phase-transition theoretically, generally speaking, is a difficult problem, since whether the transisition is possible or not, depends upon the difference between the lattice energies of both phases. Even if the lattice energies of both phases is considerably well evaluated, the difference may be not reliable, though the unknown errors in both lattice energies are somewhat cancelled. Thereupon we should say that this problem is yet open to discussion.

Acknowledgements

The writer wishes to thank Prof. K. Sassa of the Geophysical Institute, Kyoto University, and Prof. H. Miki of Abuyama Seismological Institute, Kyoto University, for their continuous encouragements. The present study has been suggested by Dr. Y. Shimazu of the Institute of Earth Sciences,

Nagoya University, to whom the writer's thanks are due.

References :

1) Bertaut, F., "L énergie electrostatique de resaux ioniques". J. Phys. Radium, 12, 499–505, 1952.

2) Birch, F., "The variation of seismic velocities within a simplified earth model, in accordance with the theory of finite strain". Bull. Seis. Soc. Amer., 29, 463–479, 1939.

3) Born, M., and Mayer, M., "Lattice theory of ionic crystals". Z. f. Phys., 75, 1–18, 1932.

4) Born, M., and Hung, K., "Dynamical theory of crystal lattices". Clarendon Press, Oxford, 1954.

5) Bragg, W. L., "Atomic structure of minerals". Cornell Univ. Press, Ithaca. 1937.

6) Bullen, K. E., "An introduction to the theory of seismology". Cabridge Univ. Press, 1953.

7) Coster, H. P., "The electrical conductivity of rocks at high temperature". M. N. R. A. S., Geophys. Suppl, 5, 193–199, 1948.

8) Hughes, H., "The pressure effect on the electrical conductivity of peridot". J. Geophys. Res., 60, 187–191, 1955.

9) Jacobs, R. B., "Polymorphic transition in metallic halides". Phys, Rev., 54, 468–474, 1938.

10) Lahiri, B. N., and Price, A. T., "Electromagnetic conduction in non-uniform conductivity of the earth from terrestrial magnetic variations". Phil. Trans. Roy. Soc., A 237, 509–540, 1939.

11) Mott, N. F., and Gurney, P. W., "Electronic processes in ionic crystals". Clarendon Press, Oxford, 1948.

12) Mott, N. F., and Littleton, M. J., "Conduction in polar crystals. I Electrolytic conduction in solid salts". Trans. Faraday Soc., 34, 485–499, 1938.

13) Rikitake, T., "Electrical conductivity and temperature in the Earth". B. E. R. I., 30, 13–24, 1952.
Rikitake, T., "Electromagnetic induction within the Earth and its relation to the electrical states of the Earth's interior". B. E. R. I., 28, 45–100, 1950; ibid, 29, 219–262 ; 263–283, 1951.

14) Runcorn, S. K., and Tozer, D. C., "The electrical conductivity of olivine at high temperature and pressure". Ann. Geophys., 11, 98–102, 1955.

15) Szigetti, B., "Compressibility and and absorption frequency of ionic crystals". Proc. Roy. Soc., A 204, 51–62, 1950.

16) Verhoogen, J., "Temperature within the Earth". Physics and Chemistry of the Earth, 1, 17–43, 1956.

17) Verwey, E. J. W., de Boer, F., and van Santen, J. H., "Cation arrangement in spinels". J. Chem. Phys., 16, 1091–1092, 1948.

18) Wada, T., "An equation of state of forsterite (Mg_2SiO_4) and the uppre part of the earth's mantle". Zisin, Ser. 2, 11, 55–67, 1958.